

Petrophysical Rock Classification: Pitfalls, Practices, New Concepts, and Field Applications

SPWLA 2013 Convention Workshop:
New Concepts in Petrophysics
New Orleans, LA, June 23



Carlos Torres-Verdín
The University of Texas at Austin

Contributors

- Chicheng Xu
- Tatyana Torskaya
- Vahid Shabro
- Qinshan Yang
- Ben Voss
- Elton Diniz-Ferreira

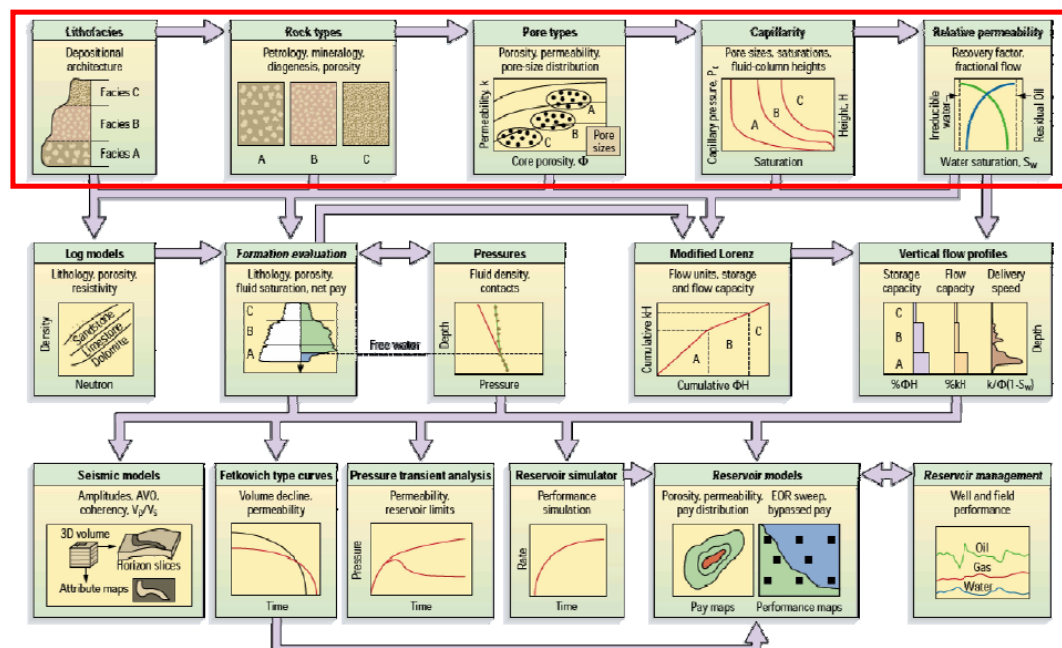
Outline

- Motivation and Background
- Geology: Bedding and Grain Size
- Petrophysics: Pore Geometry
- Core-Based Rock Typing
- Rock Typing Gaps: from Core to Logs
- Log-Based Rock Typing
- Field Applications
- Summary of Best Practices

3

Motivation: Reservoir Description

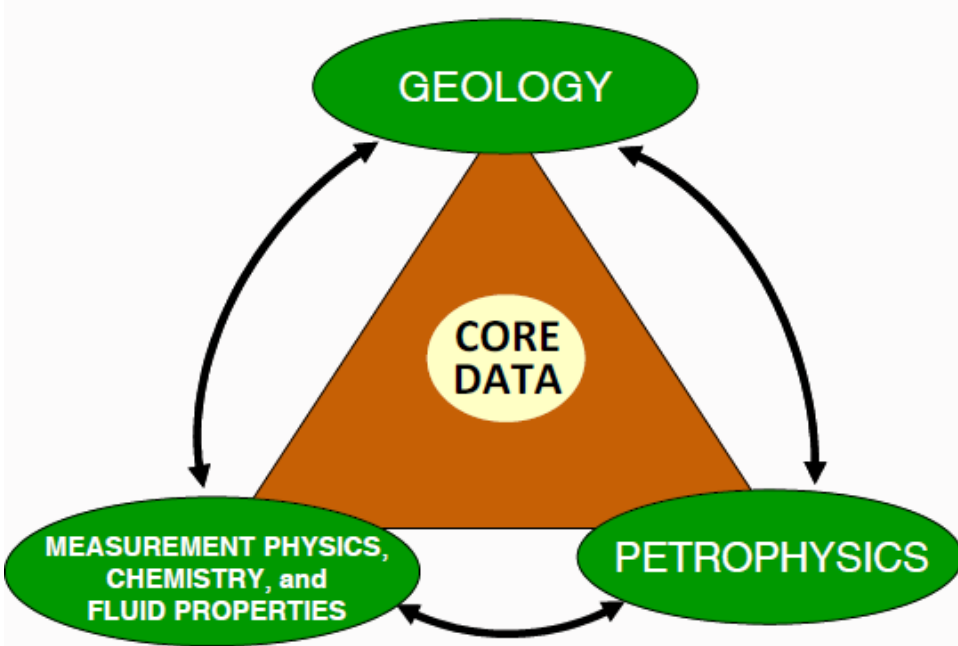
Petrophysical Integration Process Model



4

Gunter et al. (SPE 38748, 1997)

Approach: Discipline Integration



5

Objectives

- Enhance reservoir description by integrating core and logs to achieve:
 - Facies interpretation,
 - Permeability prediction,
 - Saturation-height analysis,
 - Dynamic petrophysical modeling,
 - Uncertainty quantification,
 - Petrophysical upscaling, and
 - Production forecasting.

6

Geology: Clastic Rocks - Bedding



Fluvial/Lacustrine
Eocene
Wasatch Formation
Canon Pintado, Colorado

Photo by Kevin Bohacs

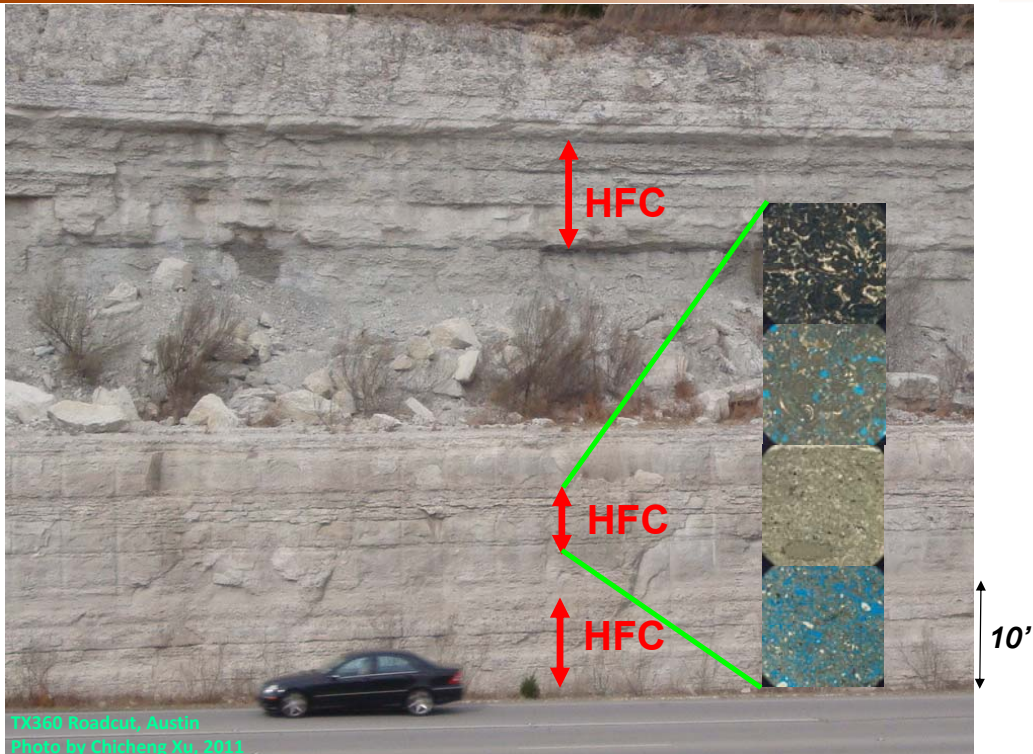
7

Geology: Clastic Rocks - Bedding



8

Geology: Carbonate Rocks - Bedding



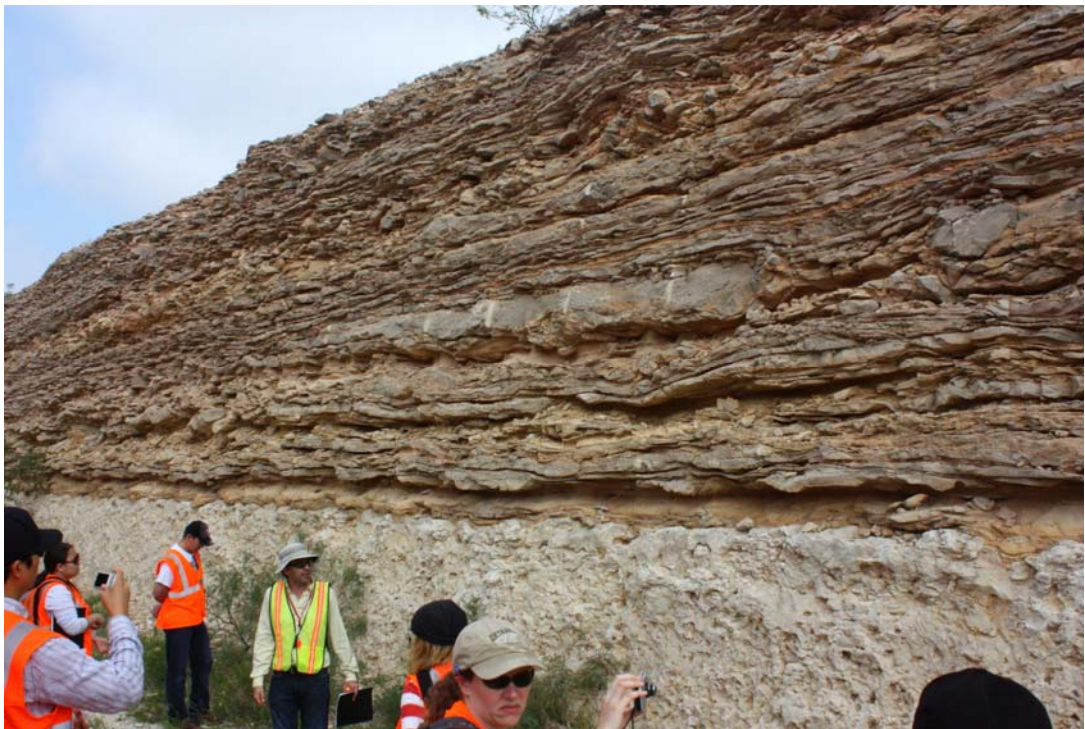
9

Geology: Carbonate Stromatolite Structure



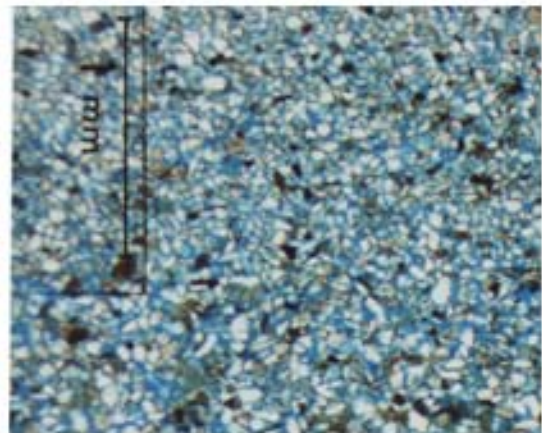
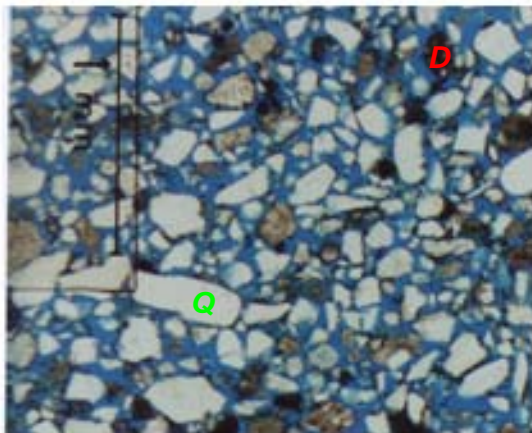
10

Geology: Organic Mud Rock



11

Geology: Grain Size, Shape, and Type

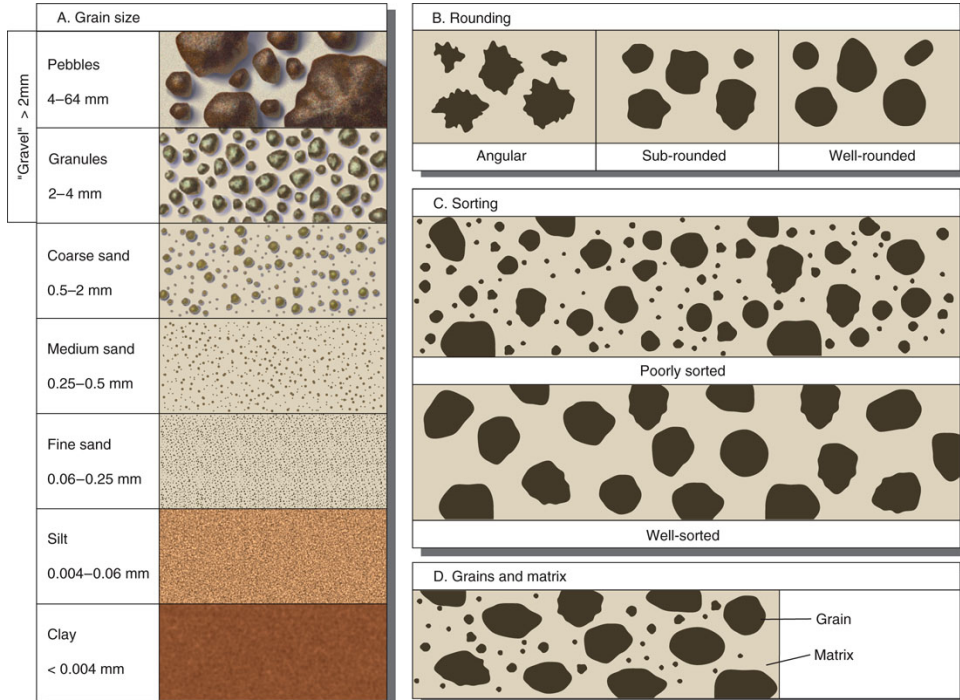


Q: Quartz

D: Ductiles

12

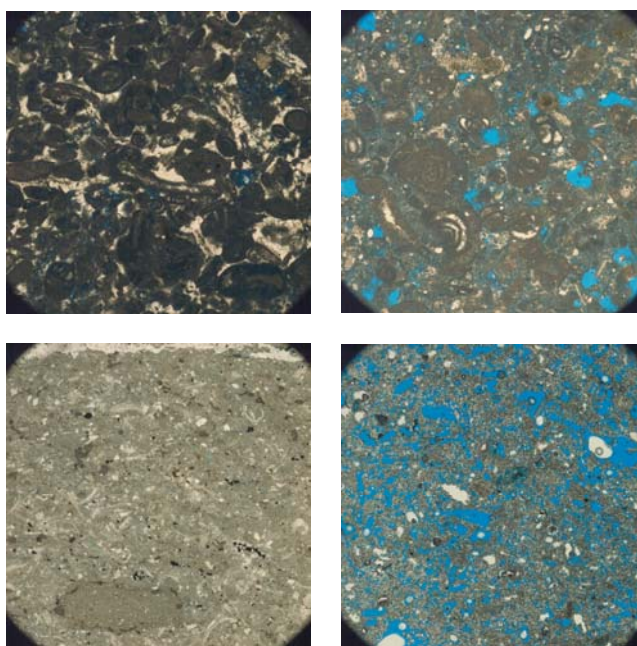
Rock Classification: Clastic Rocks



(From Jones & Jones, 2003)

13

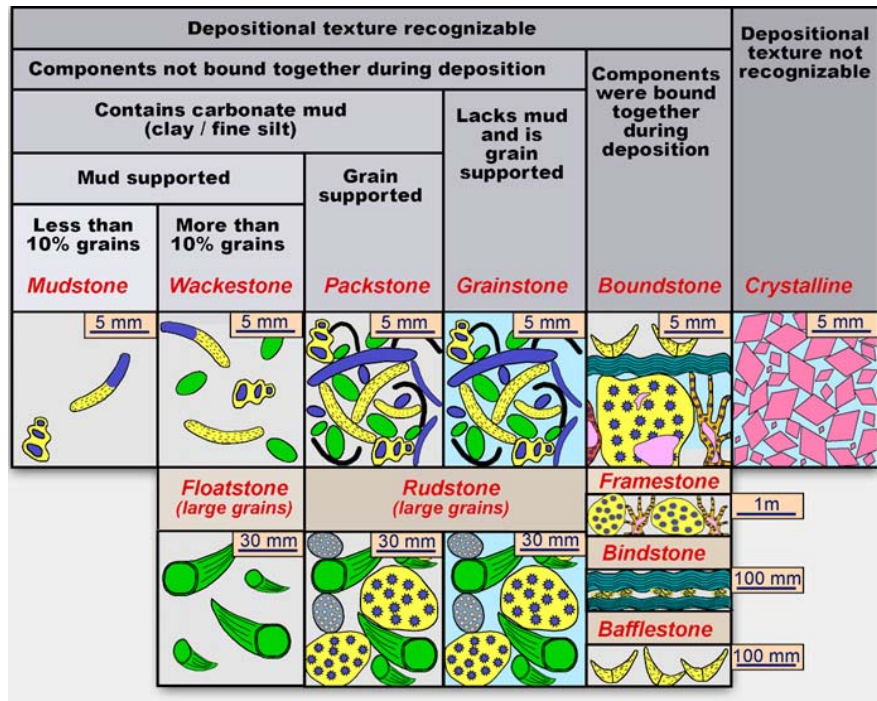
Geology: Grain Size, Shape, and Type



Courtesy of Kerans

14

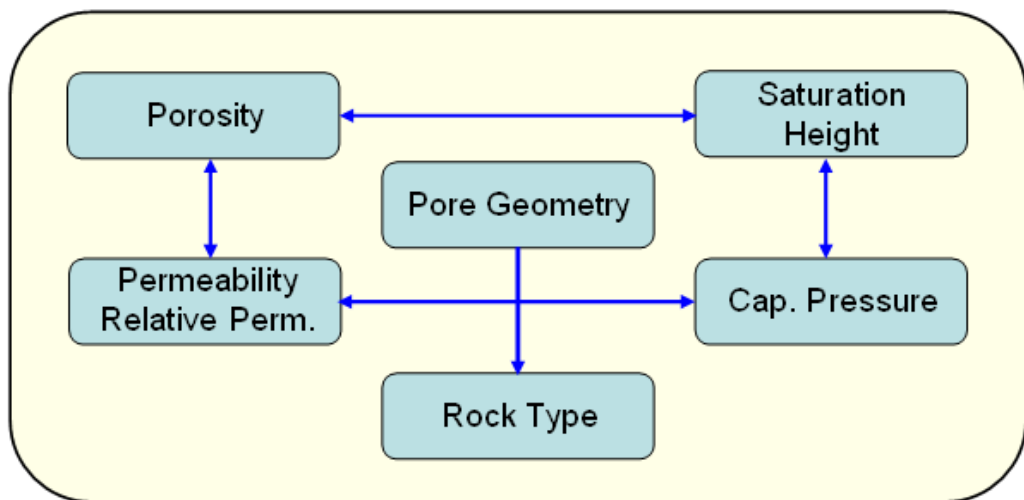
Rock Classification: Carbonate Rocks



Dunham's Carbonate Rock Texture Classification
with modifications by Embry and Klovan

15

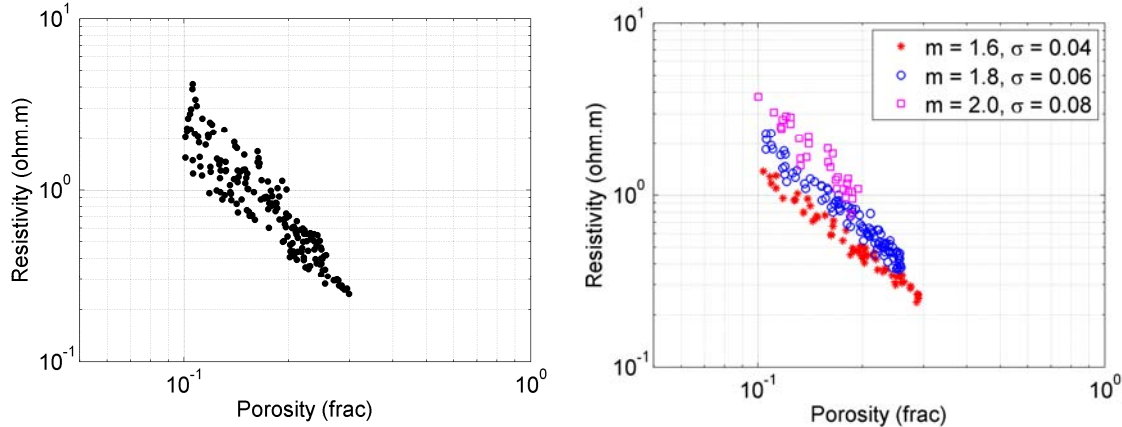
Petrophysical Rock Type Definition



Archie (1950)

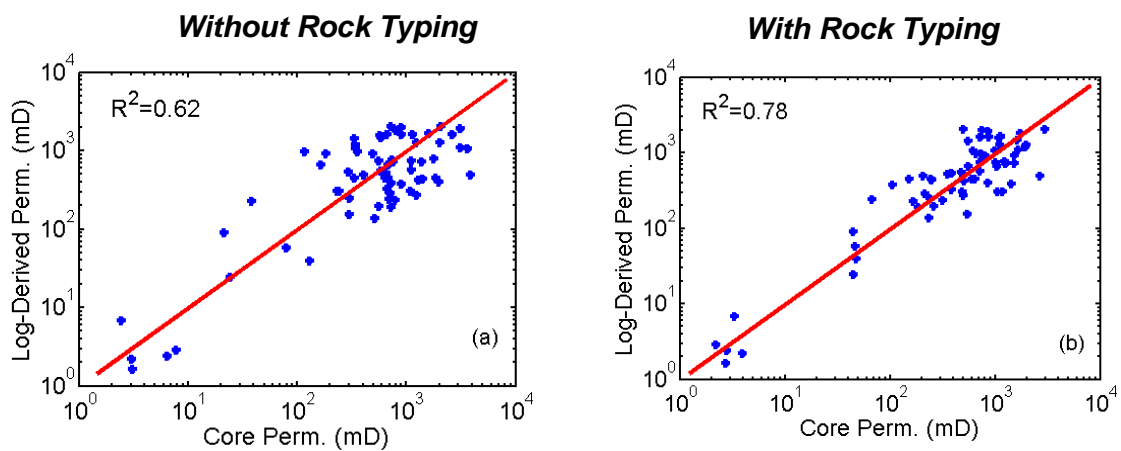
16

Example of “Scattering” due to Mixing of Rock Classes



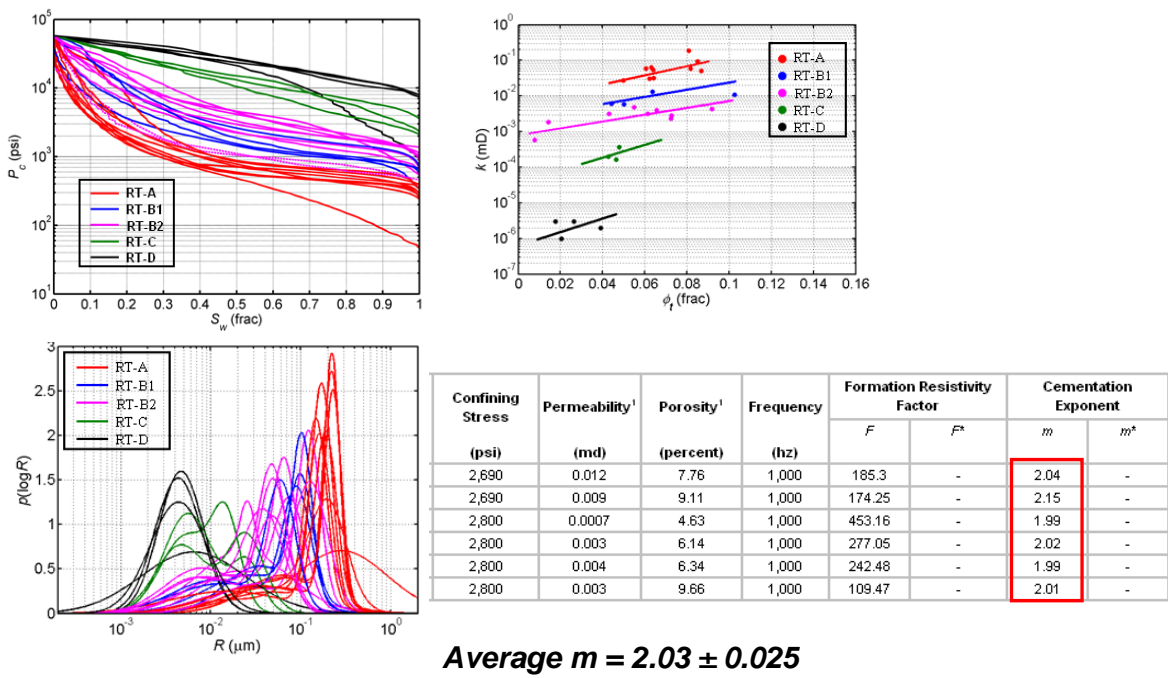
17

Rock Typing and Permeability “Scattering”



18

Tight-Gas Sandstone Case



19

Core Data for Rock Typing

- Mineralogy (XRD),
- Grain-size distribution (LPSA),
- Routine porosity/permeability,
- Dean-Stark water saturation (BVW),
- Capillary pressure (MICP),
- NMR spectroscopy,
- Relative permeability,
- Core petrography (Semi-quantitative), and
- Core facies description (Qualitative).

20

Existing Quantitative Classification Schemes

- Core-Based

- Winland's: r_{35}
- Leverett's RQI: $\sqrt{k / \phi}$
- Flow Zone Index (FZI)

$$RQI = 0.034 \sqrt{k / \phi_e}$$

$$FZI = RQI \times \frac{1 - \phi_e}{\phi_e}$$

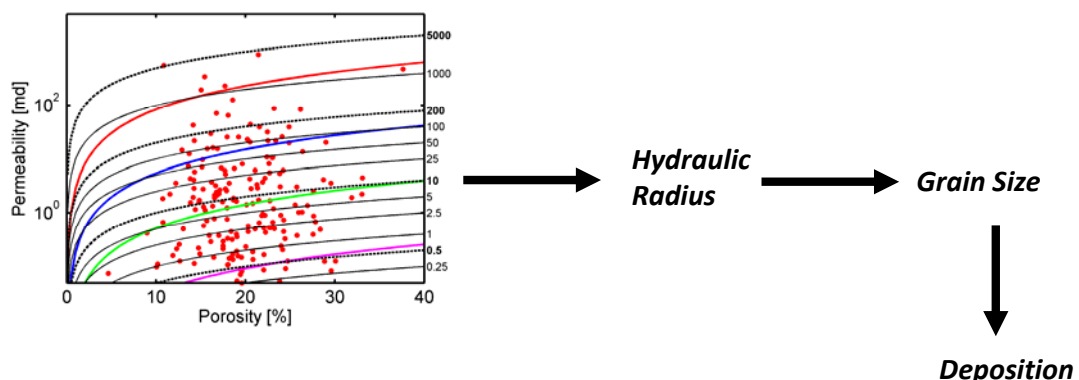
- Lucia's Rock Fabric Number (RFN)

- Well-Log Based

- Electro-facies
- BVW (Buckle's Number = $\Phi_t * S_w$)

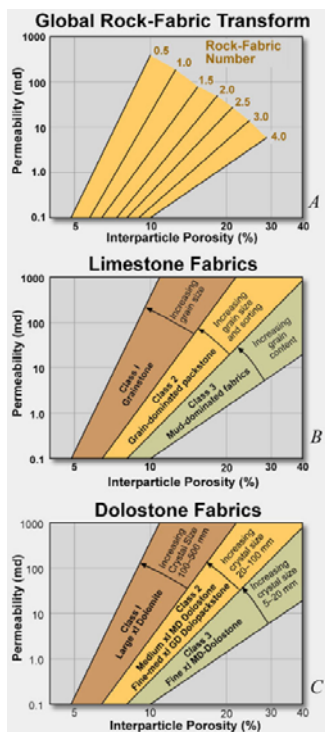
21

Clastic Rocks: R35/RQI/FZI



22

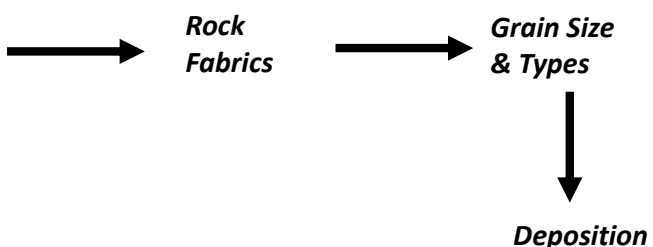
Carbonate Rocks: Rock-Fabric Number (RFN)



$$\log k = (A - B \log RFN) + (c - D \log RFN) \log \phi_{ip}$$

$$A = 9.7982, B = 12.0838, C = 8.6711, D = 8.2065$$

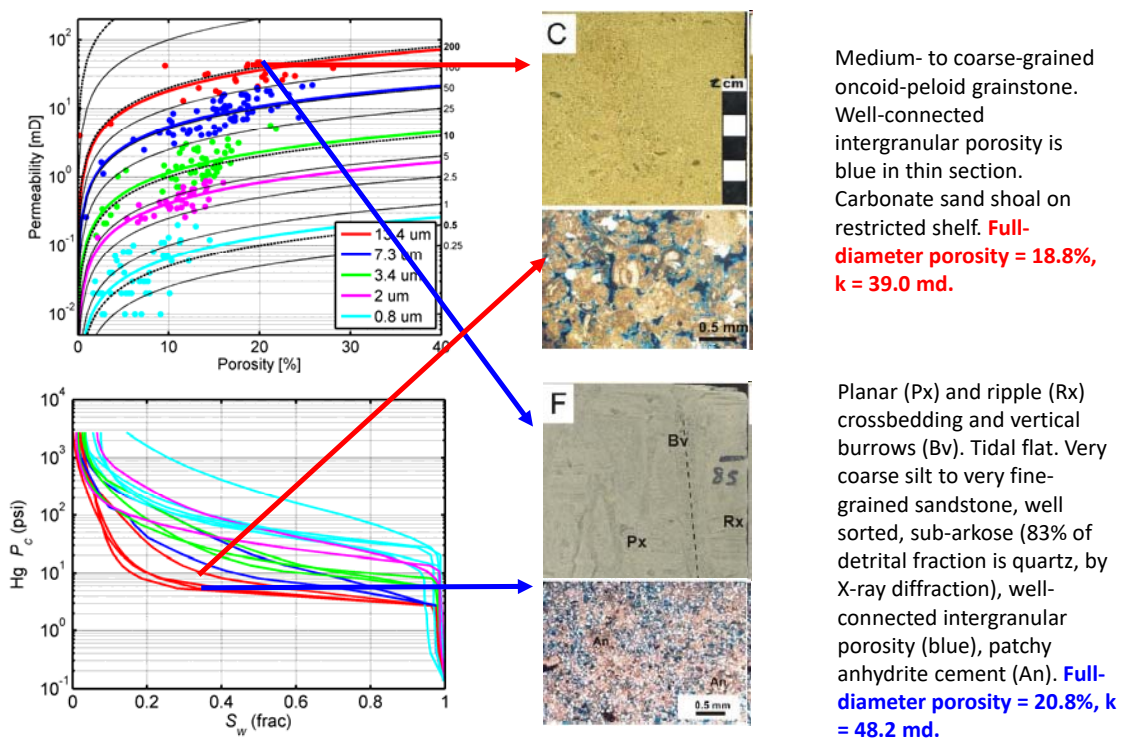
ϕ_{ip} is interparticle porosity from thin sections.



Lucia (1995)

23

Pitfall No.1: Cross-Lithofacies Rock Typing



24

Pitfall No.2: Selection of RQI/FZI/R35

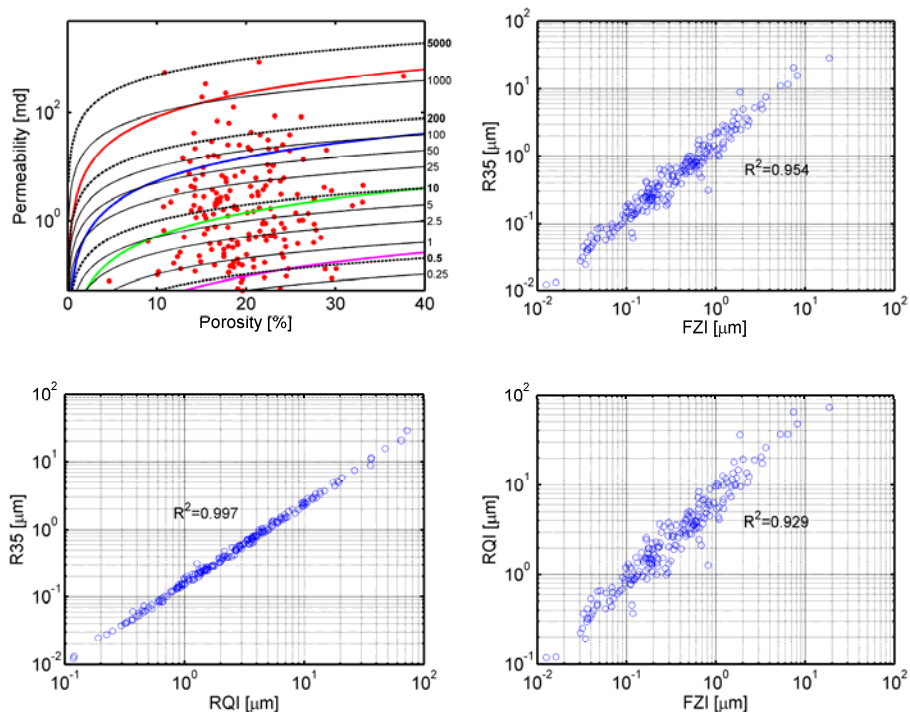
$$\log \Theta = x \log k + y \log \phi + z$$

	x	y	z
Leverett's RQI	0.5	-0.5	0.0
Winland's R35	0.588	-0.864	0.732
Amaefule's FZI	0.5	-0.5	Variable of porosity

Q: Which one is the best?

25

Pitfall No.2: Selection of RQI/FZI/R35



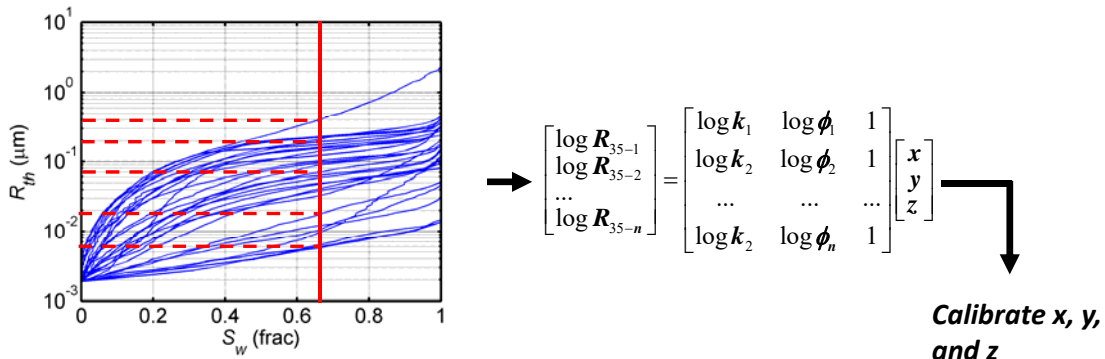
26

Pitfall No. 3: Uncalibrated R35 Formula

$$\log R_{35} = 0.588 \log k - 0.864 \log \phi + 0.732$$



$$\log R_{35} = \underline{x} \log k + \underline{y} \log \phi + \underline{z}$$



27

Pitfall No. 3: Uncalibrated R35 Formula

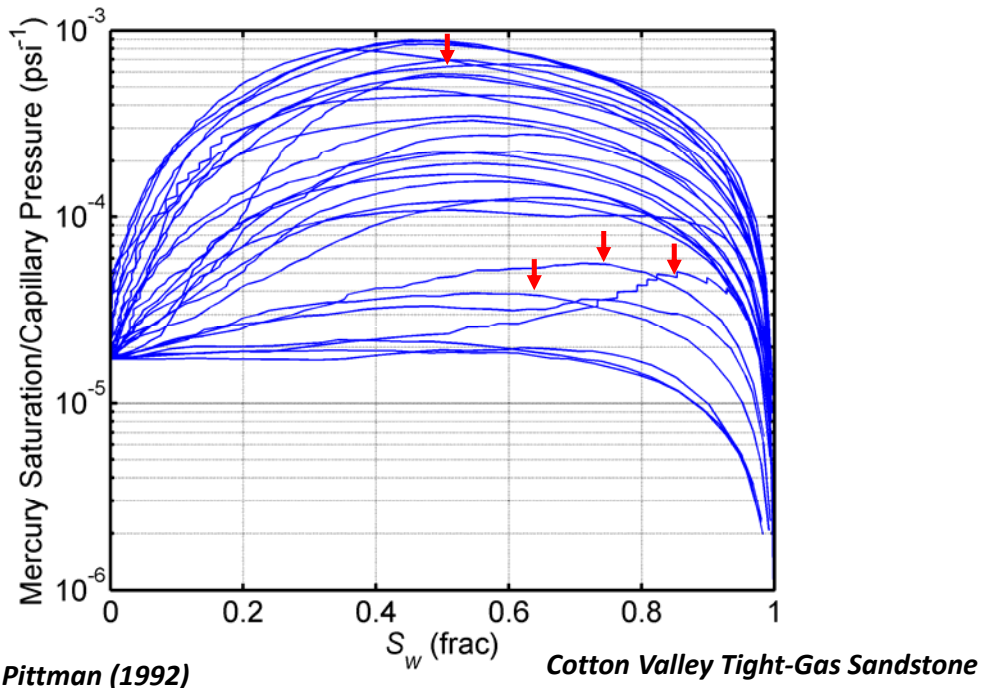
$$\log R_{35} = x \log k + y \log \phi + z$$

	x	y	z	R^2
Winland's R35	0.588	-0.864	0.732	--
Pittman's R35	0.565	-0.523	0.255	0.918
Kolodzie's R35	0.5547	-0.9033	0.9058	--
Cotton Valley Tight-Gas Sand	0.4348	-0.9263	0.2086	0.9388
Bossier Tight-Gas Sand	0.5855	-0.9022	0.5481	0.988
Hugoton Carbonate Gas Field	0.5215	-1.8203	1.6674	0.8631

28

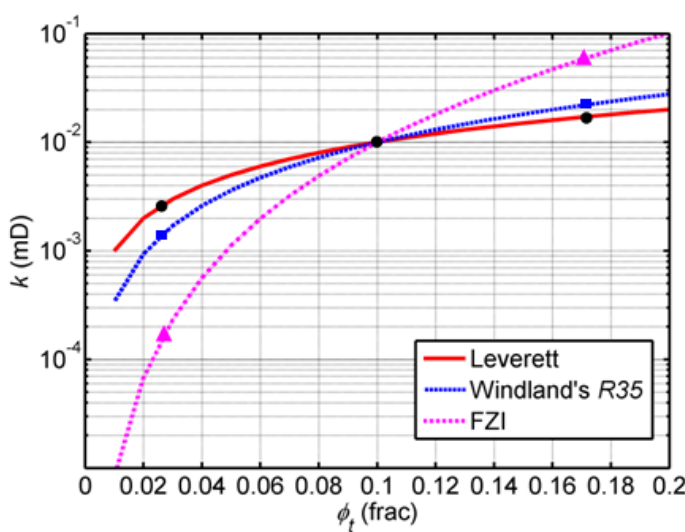
Pitfall No. 4: Dynamic and Flat “Apex”

- R20, R25, R30, R35, R40, or R50?



29

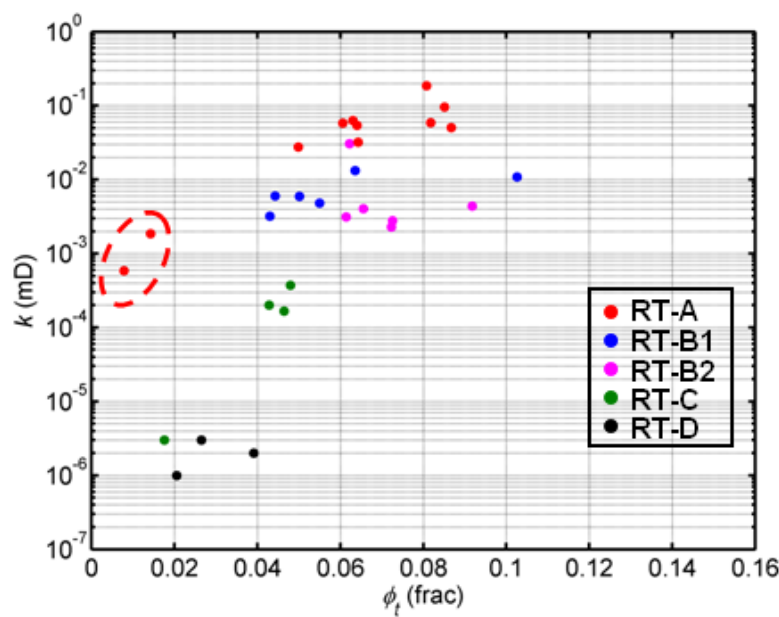
Pitfall No. 5: Inadequacy in Tight Rocks



Rely too much on TREND! None considers pore volume or storage capacity.

30

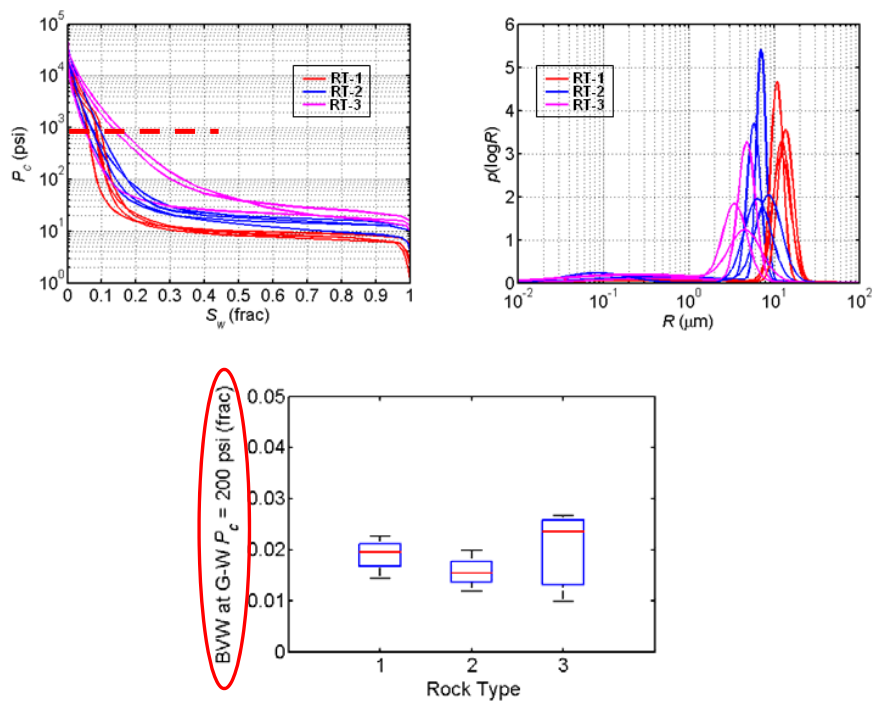
Pitfall No. 5: Inadequacy in Tight Rocks



Rock classification with MICP-derived R35 in Cotton-Valley tight-gas sandstone

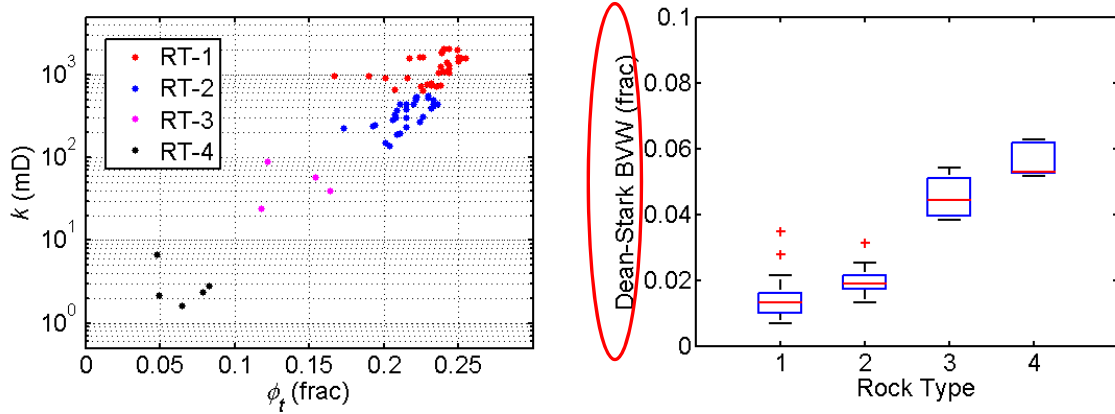
31

Pitfall No. 6: Swirr from MICP vs. BVW



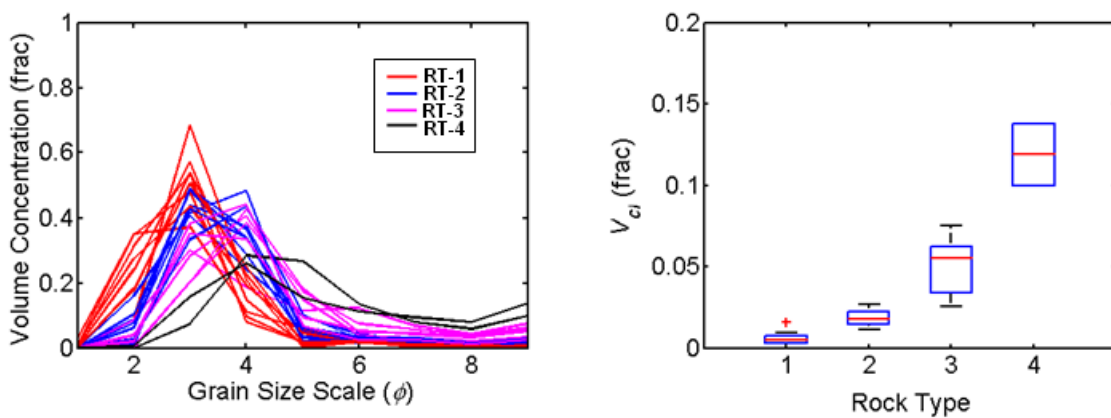
32

Pitfall No. 6: Swirr from MICP vs. BVW



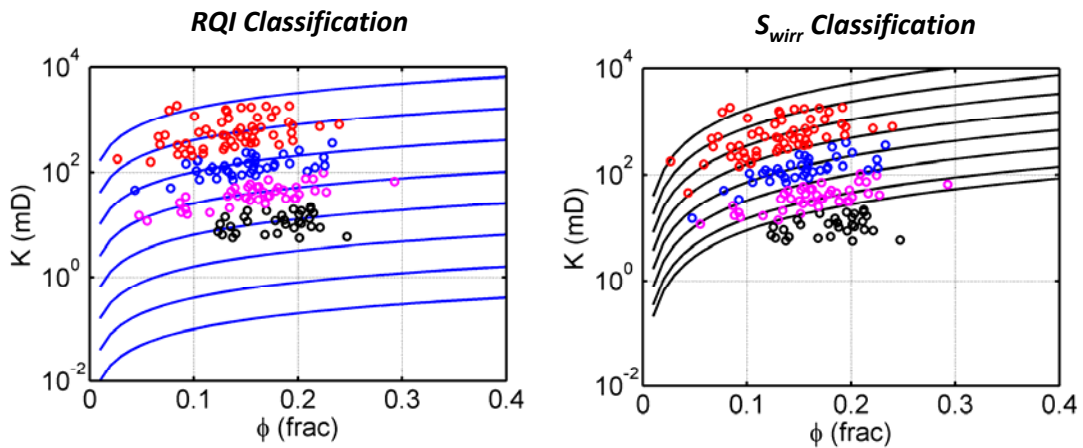
33

Pitfall No. 6: Swirr from MICP vs. BVW



34

Pitfall No. 6: S_{wirr} from MICP vs. BVW

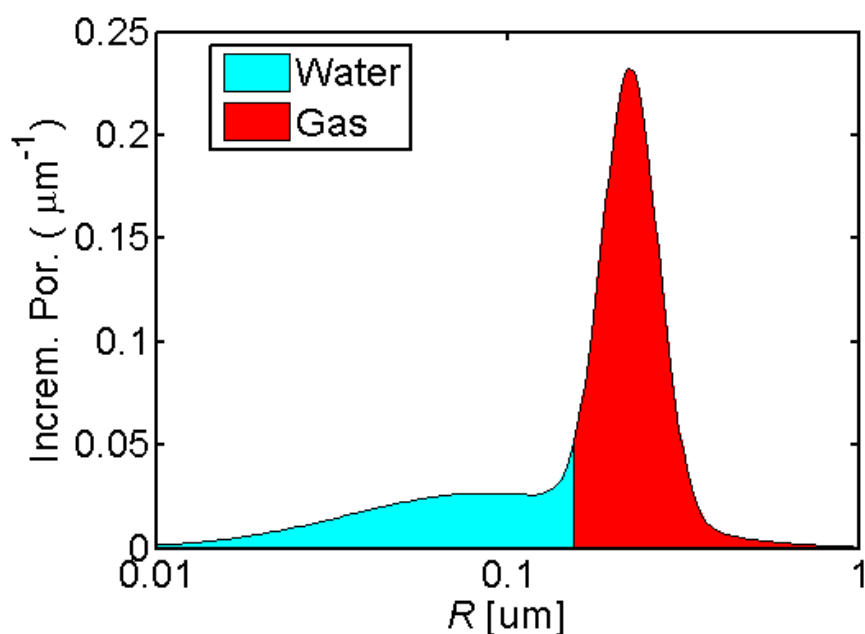


$$k = \alpha \frac{\phi^\beta}{S_{wirr}^\gamma} \quad \text{Timur-Tixier Model}$$

$$\log \Theta = x \log k + y \log \phi + z \quad \log S_{wirr} = -\frac{1}{\gamma} \log k + \frac{\beta}{\gamma} \log \phi + \frac{1}{\gamma} \log \alpha$$

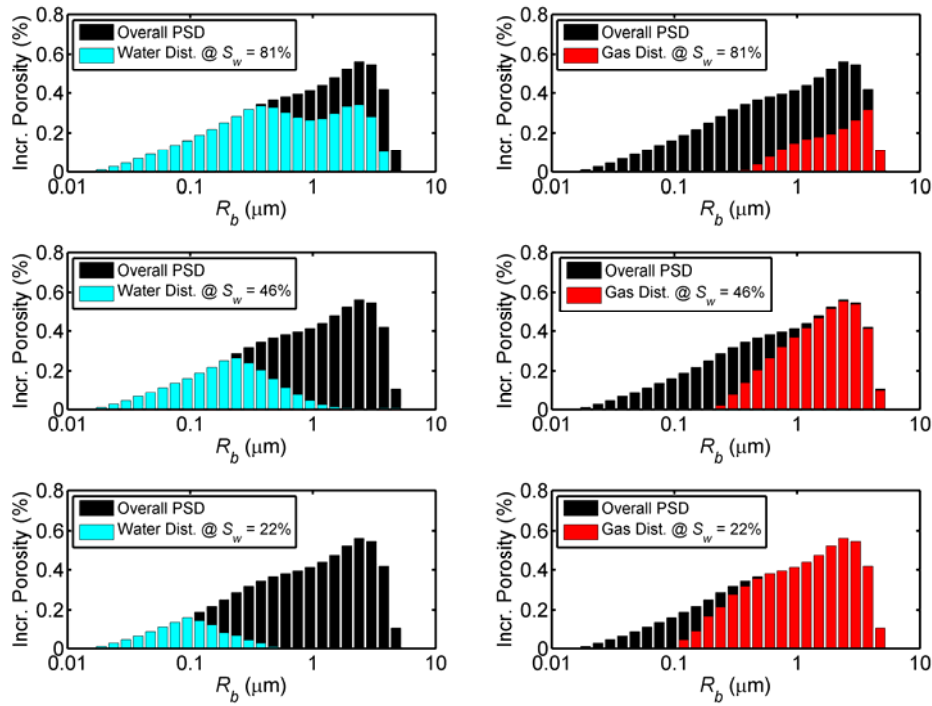
35

Pitfall No. 7: Bound Fluid from NMR



36

Pitfall No. 7: Bound Fluid from NMR



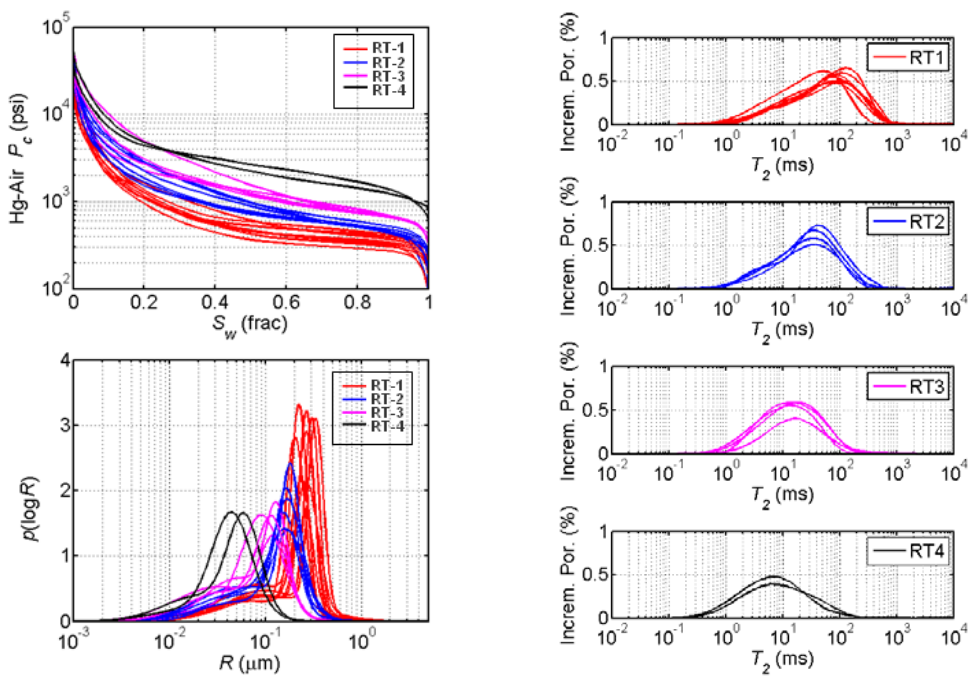
37

Pitfall No. 8: MICP vs. NMR

- Different measurement physics.
- Different petrophysical sensitivity.
- Pore throat vs. pore body.
- Partially correlated.

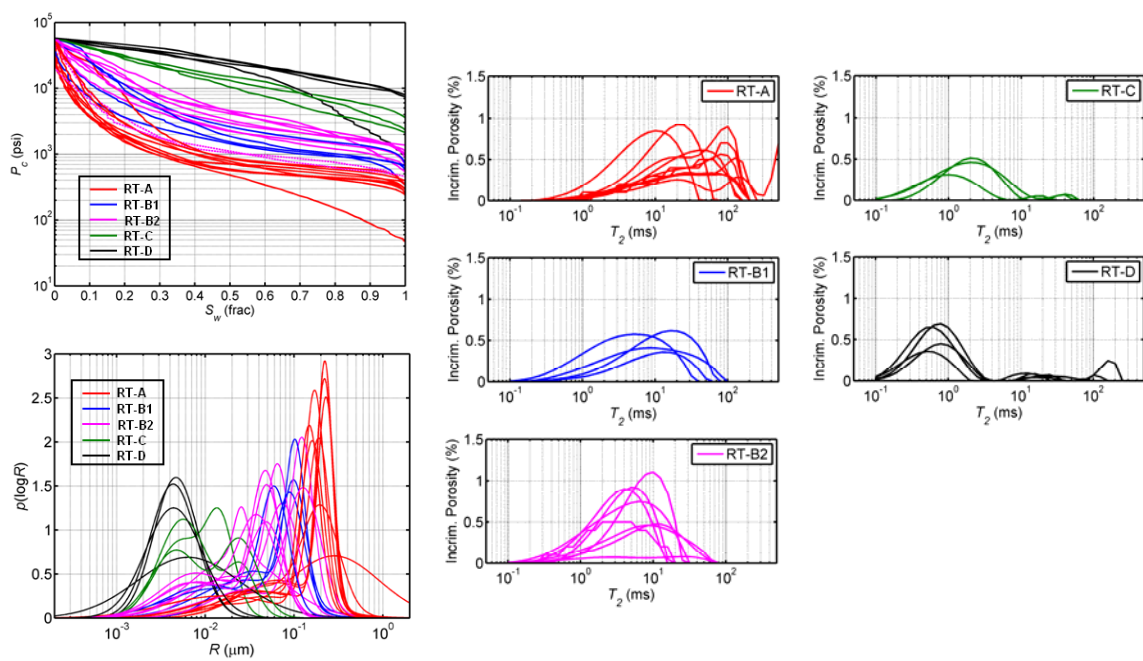
38

Pitfall No. 8: MICP vs. NMR



39

Pitfall No. 8: MICP vs. NMR



40

Quantifying Pore Geometry and Fluid Distribution

- Pore Geometry
 - Pore body size,
 - Pore throat size,
 - Pore volume,
 - Pore inter-connectivity,
 - Pore size uniformity,
 - Pore morphology,
 - ...
- Fluid distribution
 - Irreducible water (Drainage), and
 - Residual hydrocarbon (Imbibition).

41

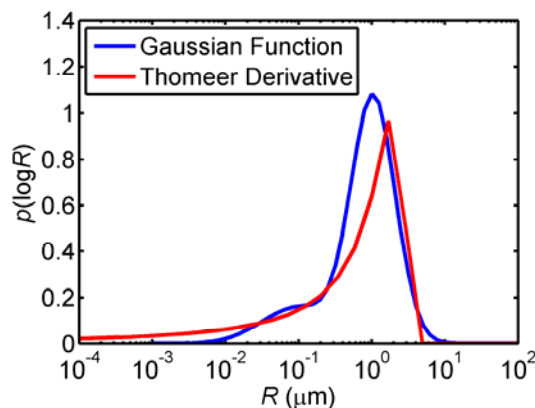
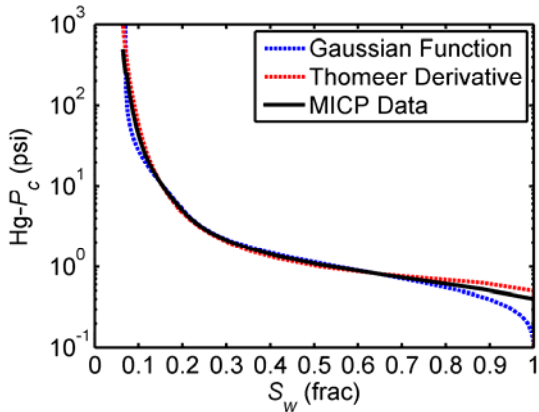
Quantifying Pore Geometry

- Pore body size,
- Pore throat size,
- Pore volume,
- Pore inter-connectivity,
- Pore size uniformity,
- Pore morphology,
- ...
- [Pd, G, BV]: Thomeer (1960); Clerk (2009)
- [Pd, λ , Swirr]: Brooks-Corey (1966); Peters (2010)
- [$w_1, \mu_1, \sigma_1; w_2, \mu_2, \sigma_2$]: Xu and Torres-Verdín (2013)

42

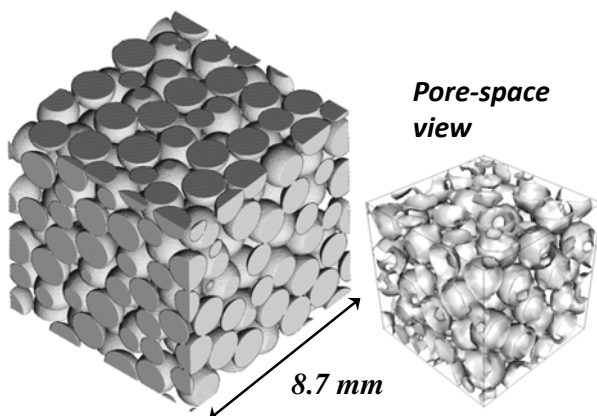
Quantifying Pore Geometry: Models

- [Pd, G, BV]: Thomeer (1960); Clerk (2009)
- [Pd, λ , Swirr]: Brooks-Corey (1966); Peters (2010)
- [$w_1, \mu_1, \sigma_1; w_2, \mu_2, \sigma_2$]: Xu and Torres-Verdín (2013)



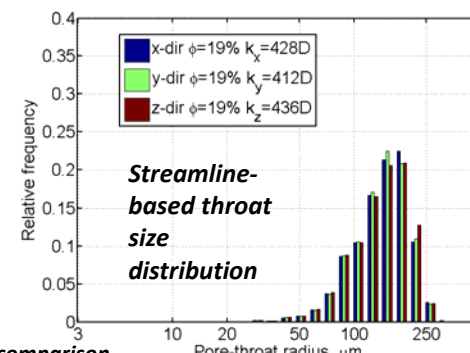
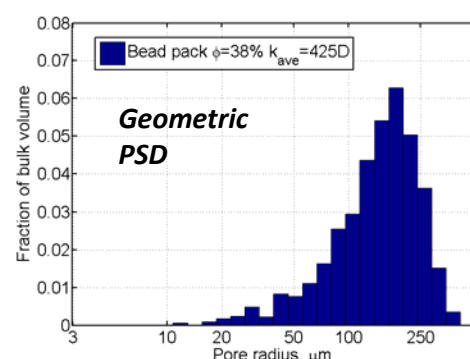
43

Silica Sphere Pack



A packing of silica spheres with a void volume fraction (porosity) of 37.9 %.

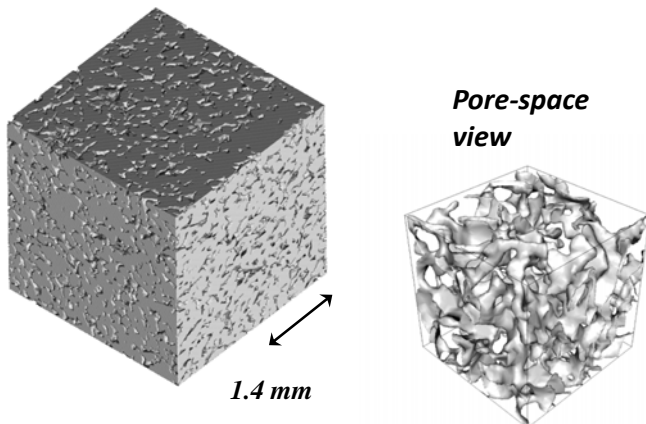
The diameter of the beads is 1.59mm (1/16 inch) and the voxel size is 17.5 um. Image dimensions are 500x500x500 voxels.*



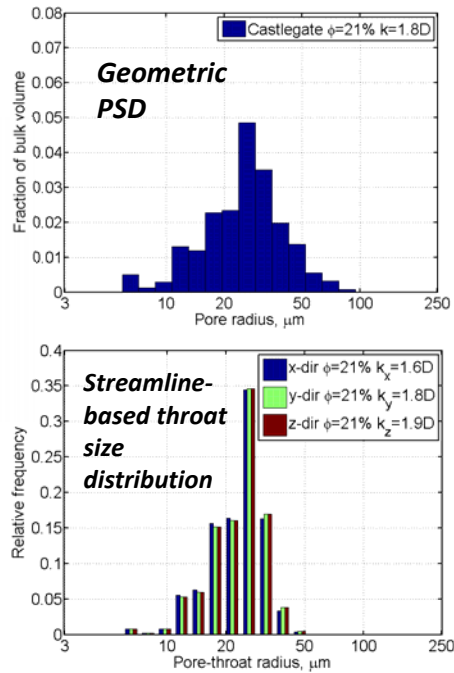
44

*Original image source: http://xct.anu.edu.au/network_comparison

Castlegate Sandstone



Castlegate outcrop sandstone segmented CT-scan, from southeastern Utah, USA.
Image with dimensions 500^3 voxels and original porosity of 20.6 %. Voxel resolution is $5.6 \mu\text{m}/\text{voxel}$.*



*Original image source: http://xct.anu.edu.au/network_comparison

45

Fountainbleau Sandstone

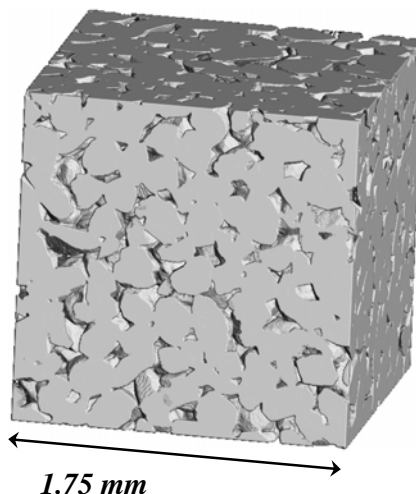
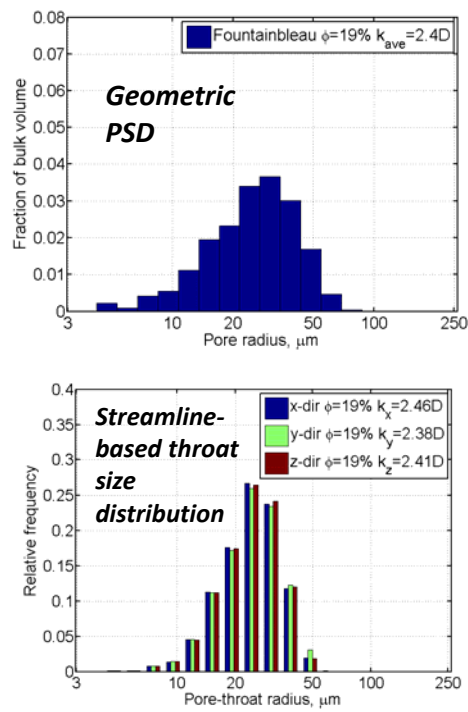
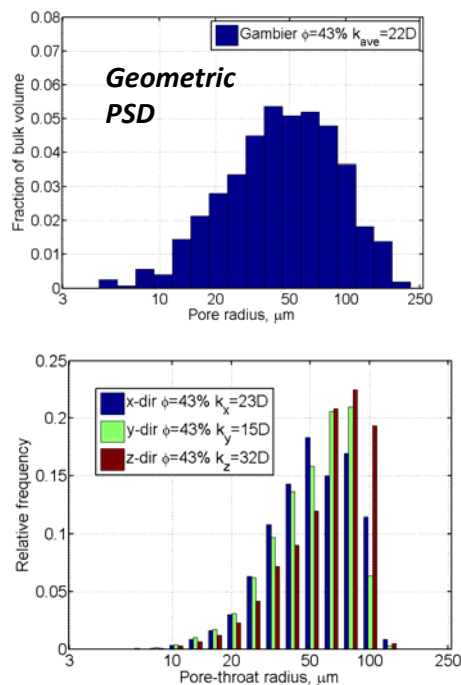
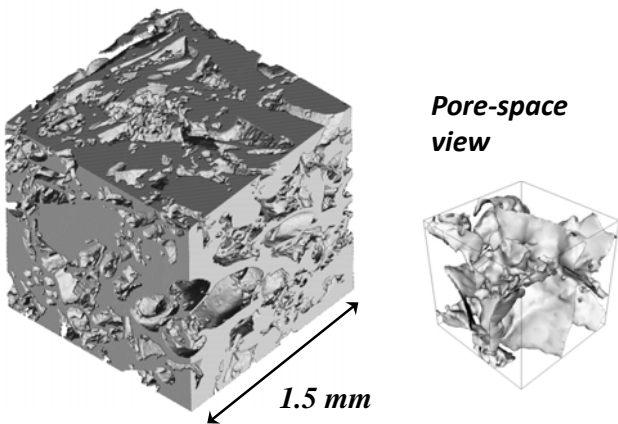


Image with dimensions 500^3 voxels and a voxel resolution of $3.5 \mu\text{m}/\text{voxel}$. Porosity is 19.3%.



46

Mt Gambier Limestone



47

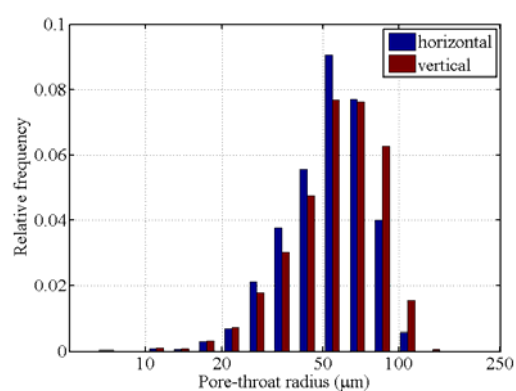
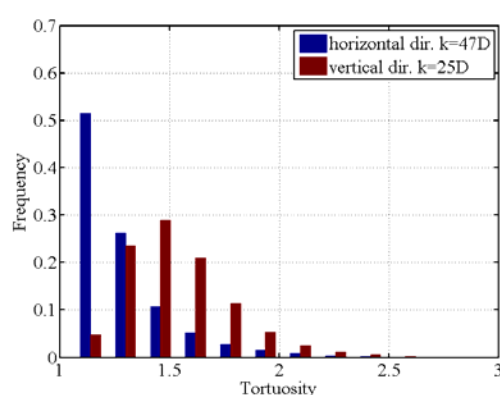
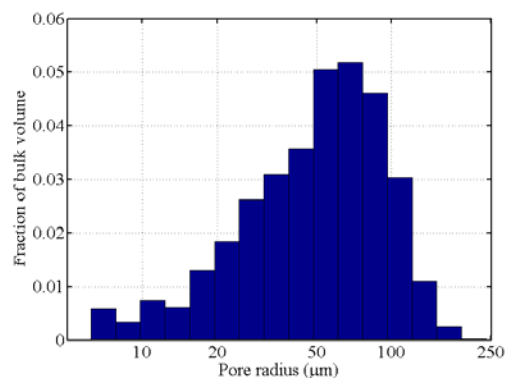
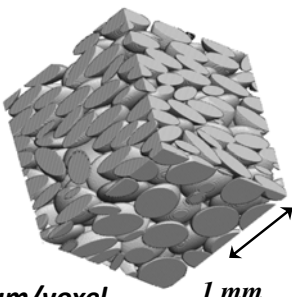
*Original image source: http://xct.anu.edu.au/network_comparison

Tortuosity distributions for anisotropic sample:
Porosity = 34%
Oblate ellipsoids:
Larger axis - 286 μm
Smaller axis – 95.3 μm

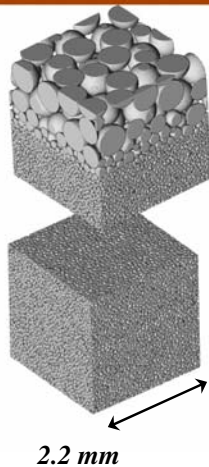
Image resolution: 4.77 $\mu\text{m}/\text{voxel}$

Horizontal direction: $k_h = 47\text{D}$, $F_h = 0.04$

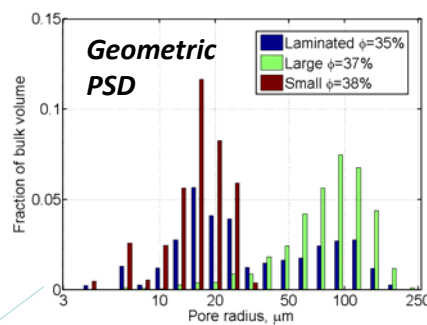
Vertical direction: $k_v = 25\text{D}$, $F_v = 0.09$



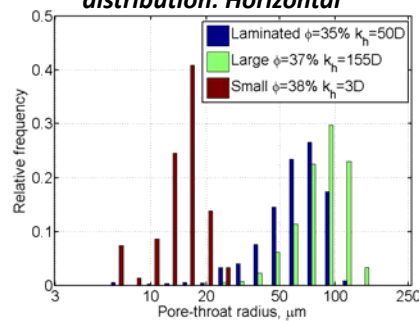
Laminations



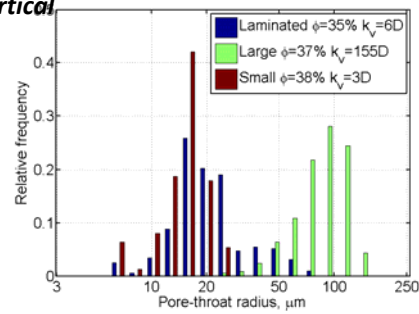
$R(\text{large}) = 250 \mu\text{m}$
 $R(\text{small}) = 31.25 \mu\text{m}$



Streamline-based throat size distribution: Horizontal

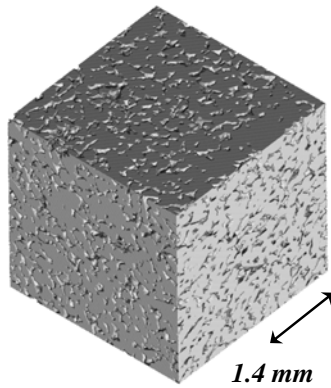


Streamline-based
throat size distribution:
Vertical



49

Cementation: Castlegate sandstone



Castlegate outcrop sandstone
segmented CT-scan*, from
southeastern Utah, USA.

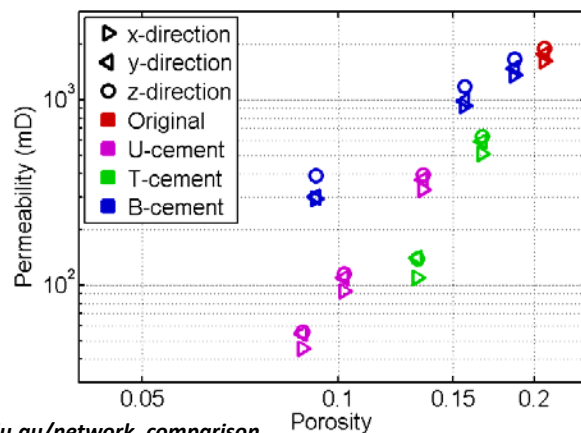
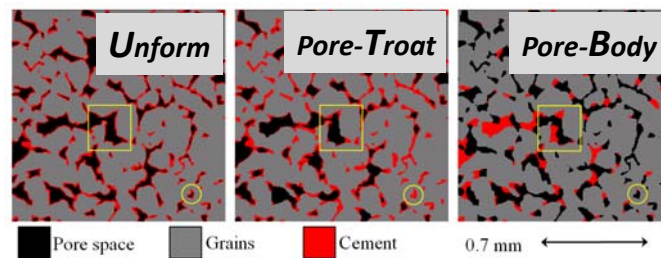


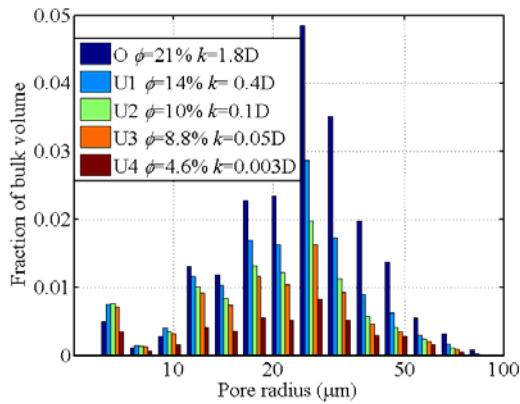
Image with dimensions 500^3
voxels and original porosity of
20.6 %. Voxel resolution is 5.6
 $\mu\text{m}/\text{voxel}$.

*Original image source: http://xct.anu.edu.au/network_comparison

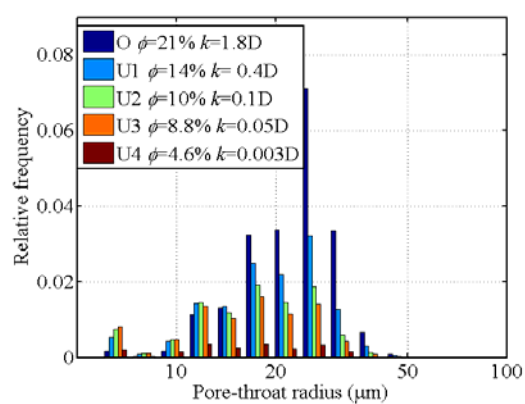
50

Castlegate Sandstone - Uniform Cement

Geometric PSD



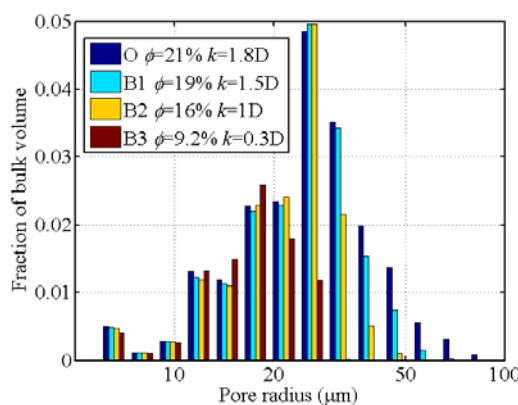
Streamline-based throat size distribution



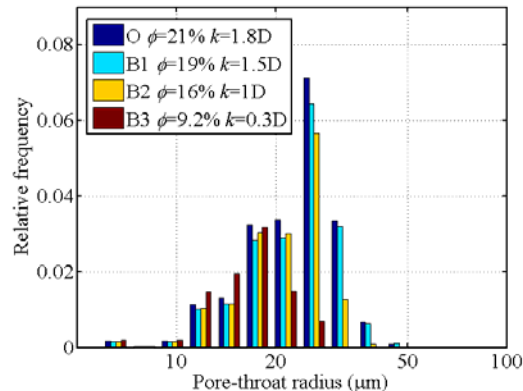
51

Castlegate Sandstone - Non-uniform Cement (Pore-Body Preferential)

Geometric PSD



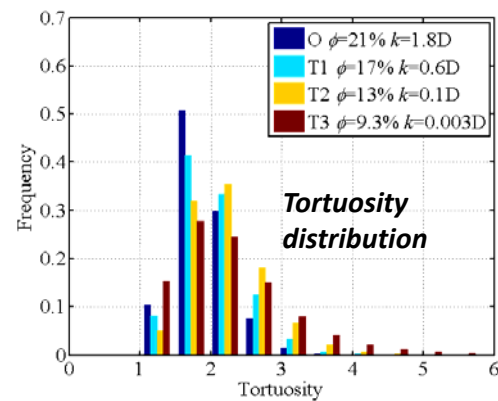
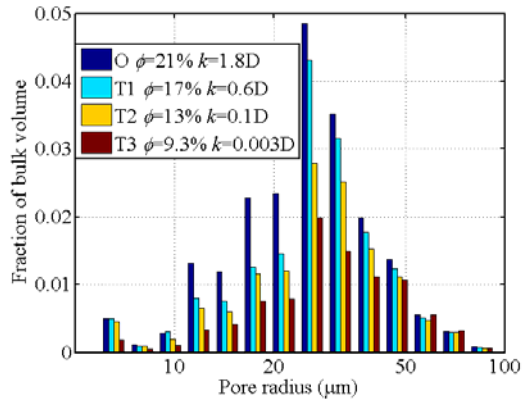
Streamline-based throat size distribution



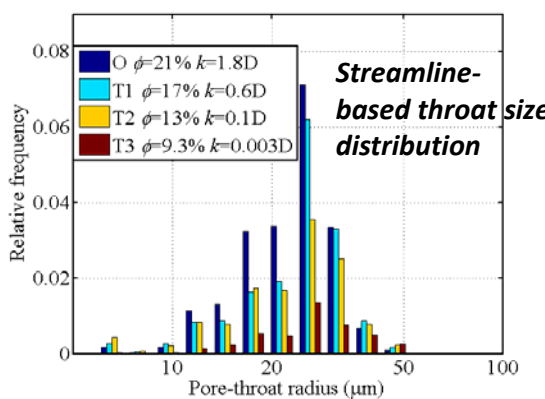
52

Castlegate Sandstone Throat-Cementation

Geometric PSD

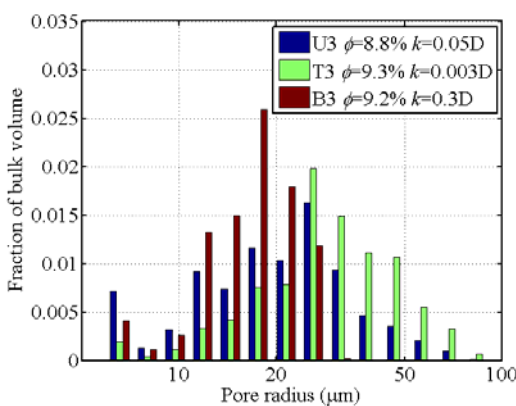


Streamline-based throat size distribution

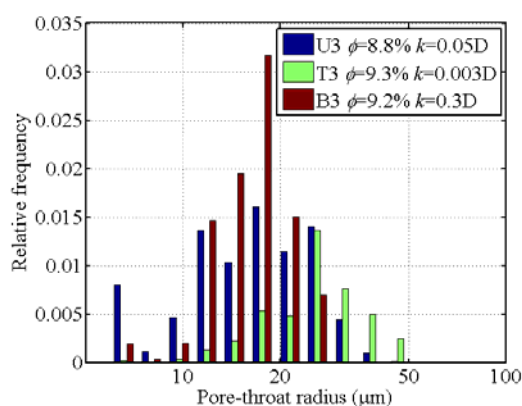


Cement Cases Comparison at Equivalent Porosities

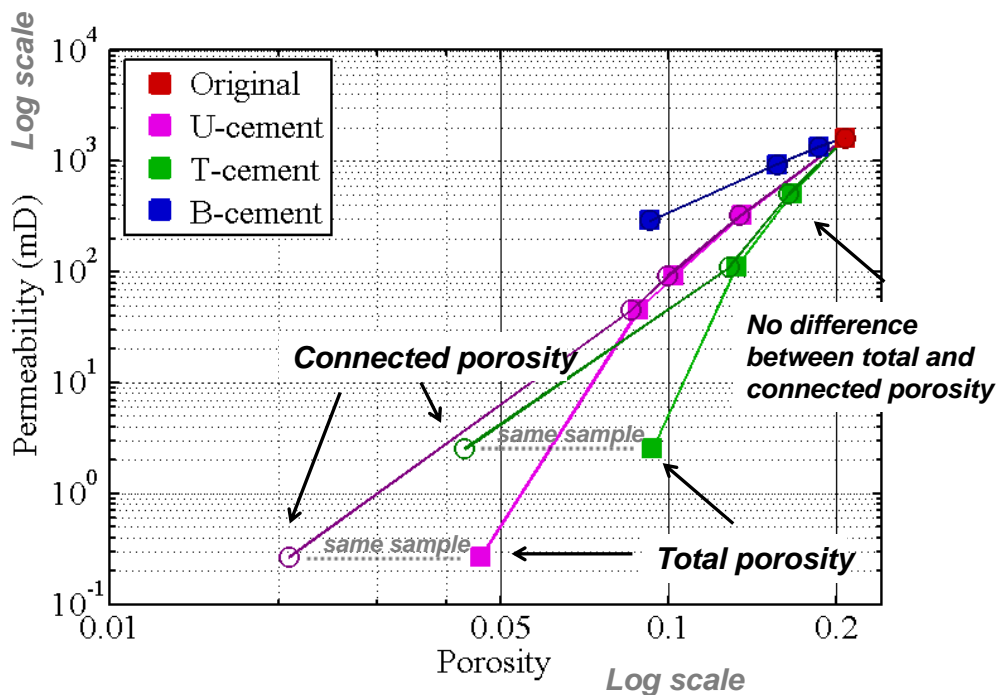
Geometric PSD



Streamline-based throat size distribution

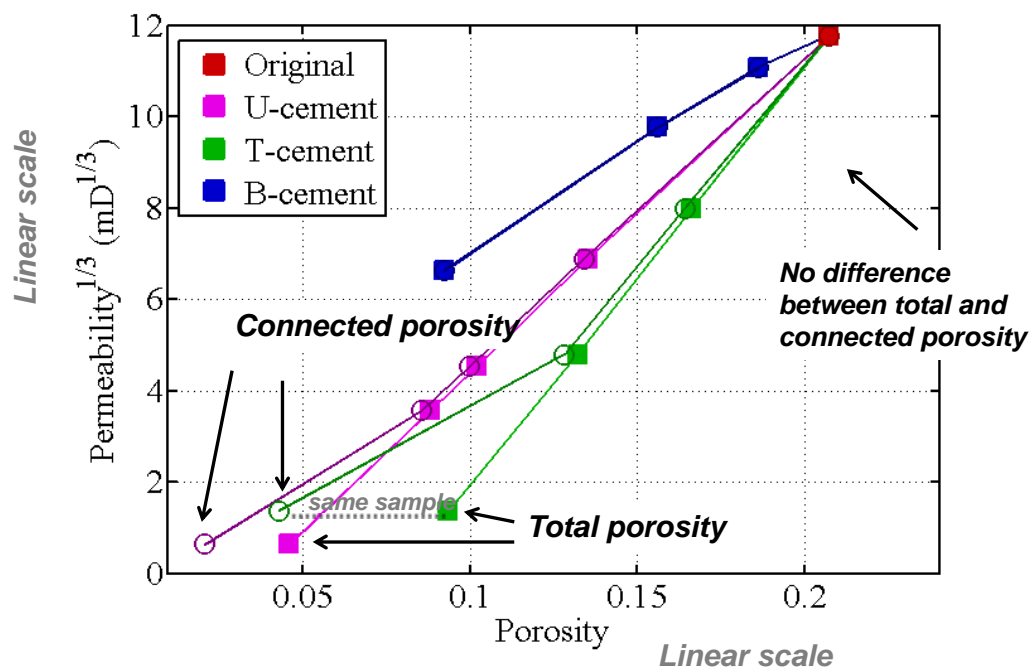


Connected vs. Total Porosity for Cemented Samples



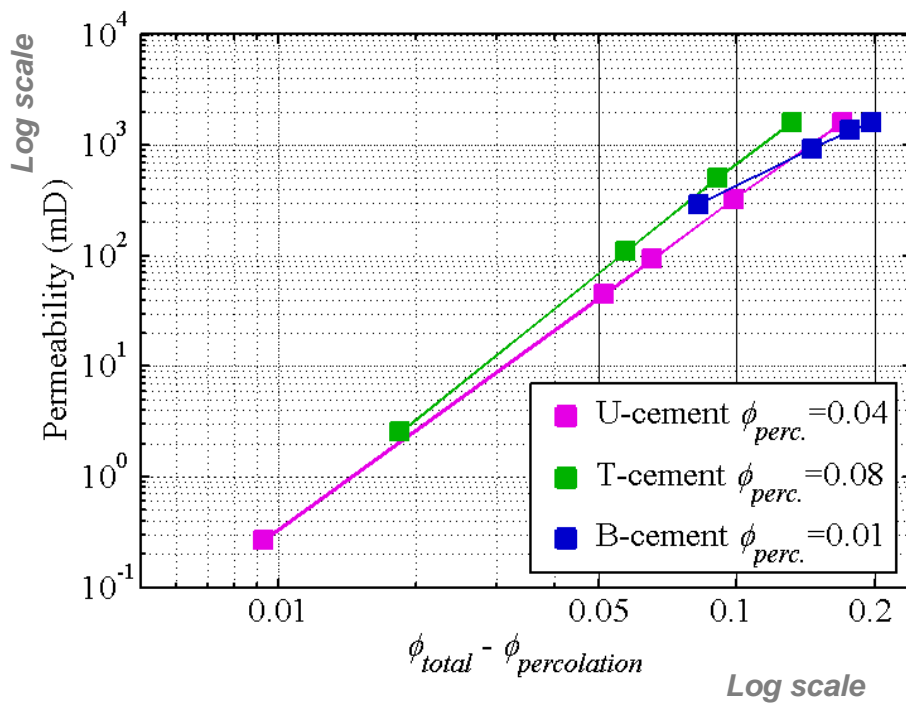
55

Connected vs. Total Porosity for Cemented Samples



56

Porosity Percolation Threshold for Cemented Samples



57

Question:

Is there a unified (or generalized!) and simple description of microscopic rock properties that can quasi-analytically predict all macroscopic rock properties (i.e. fluid transport, electrical conduction, proton diffusion, Fickian diffusion, elastic, etc.)?

58

58

Vuggy Carbonate

Porosity and Permeability are not everything!

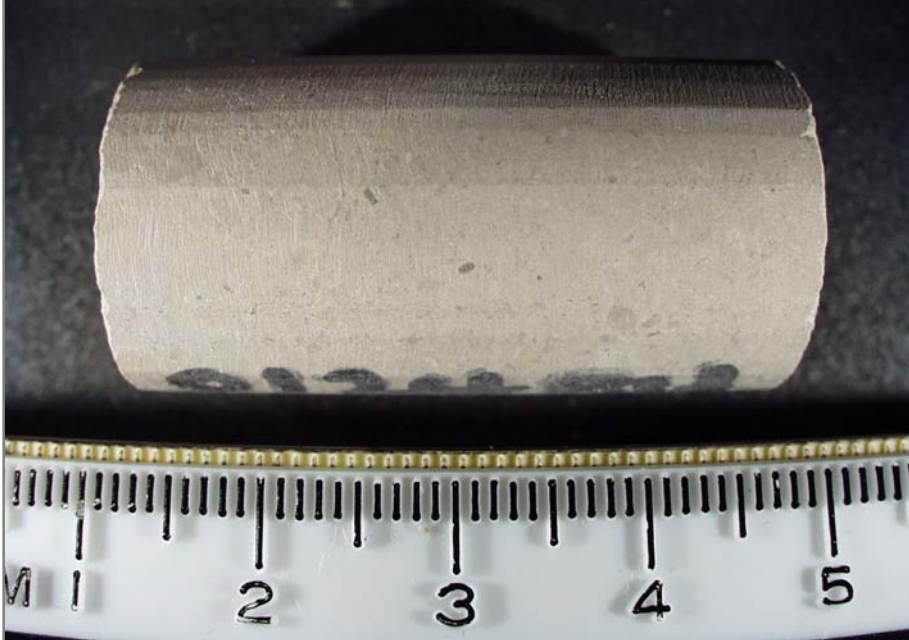


Photograph courtesy of Austin Boyd

59

Low Permeability Wackestone

Porosity and Permeability are not everything!

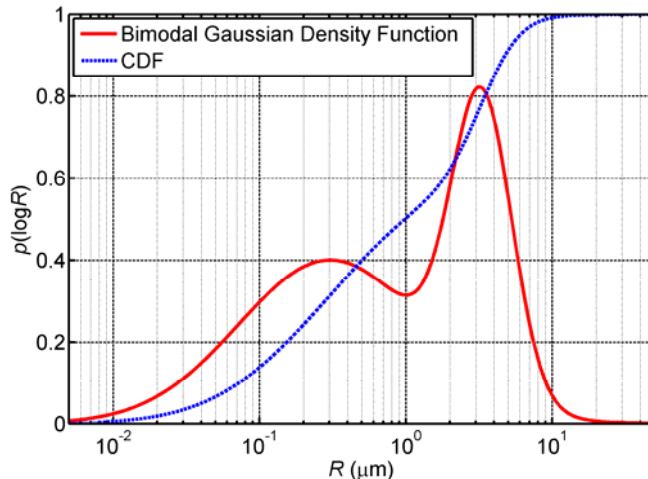


Photograph courtesy of Austin Boyd

60

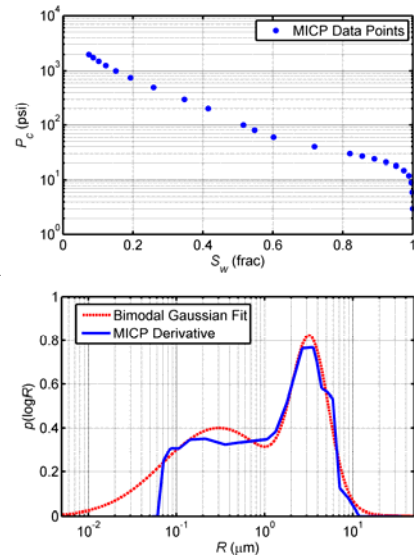
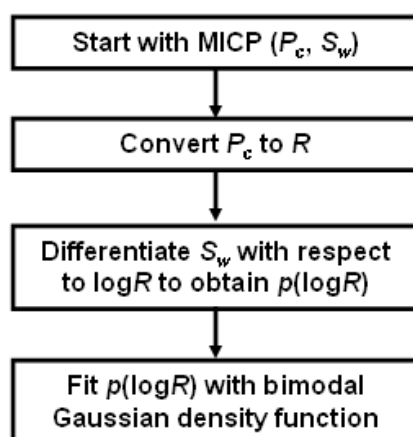
Quantifying Pore Geometry: Bimodal Lognormal Distribution

$$p(\log R; w_1, \log \mu_1, \log \sigma_1; w_2, \log \mu_2, \log \sigma_2) = \\ w_1 \frac{1}{\sqrt{2\pi} \log \sigma_1} e^{-\frac{(\log R - \log \mu_1)^2}{2(\log \sigma_1)^2}} + w_2 \frac{1}{\sqrt{2\pi} \log \sigma_2} e^{-\frac{(\log R - \log \mu_2)^2}{2(\log \sigma_2)^2}}$$



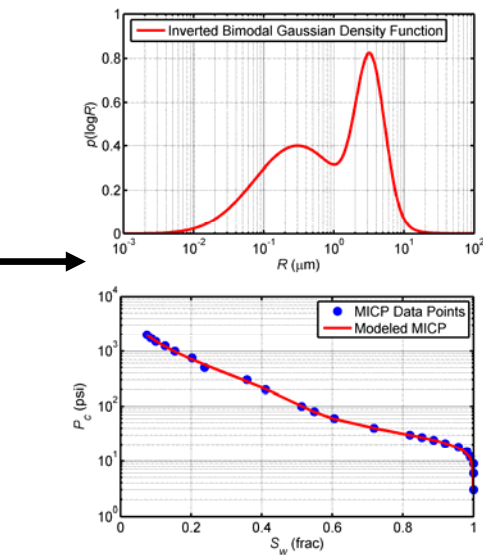
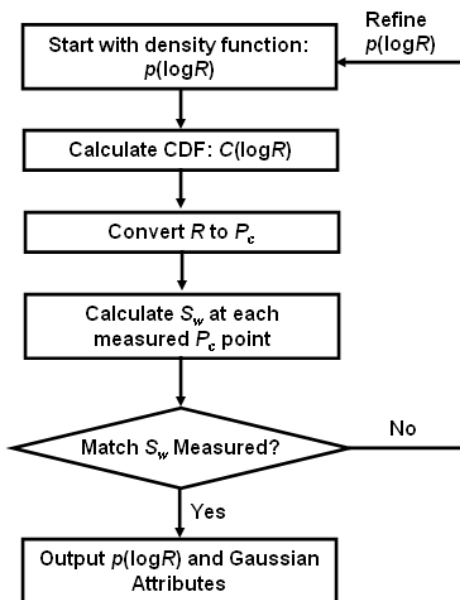
61

Quantifying Pore Geometry: Derivation Method



62

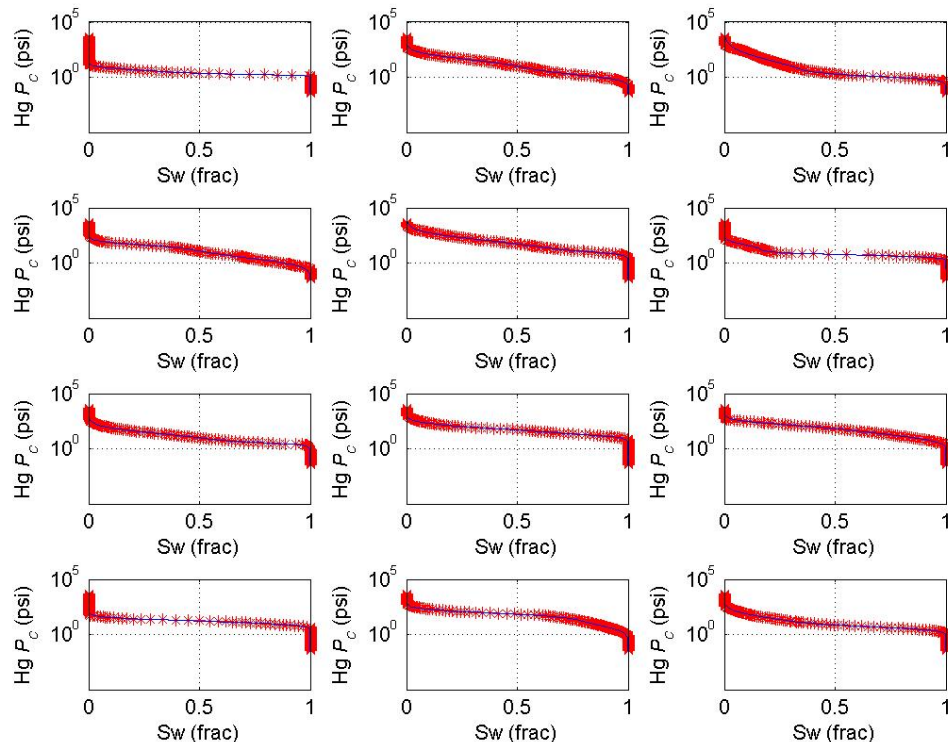
Quantifying Pore Geometry: Inversion Method



Xu and Torres-Verdín, 2013
Mathematical Geosciences

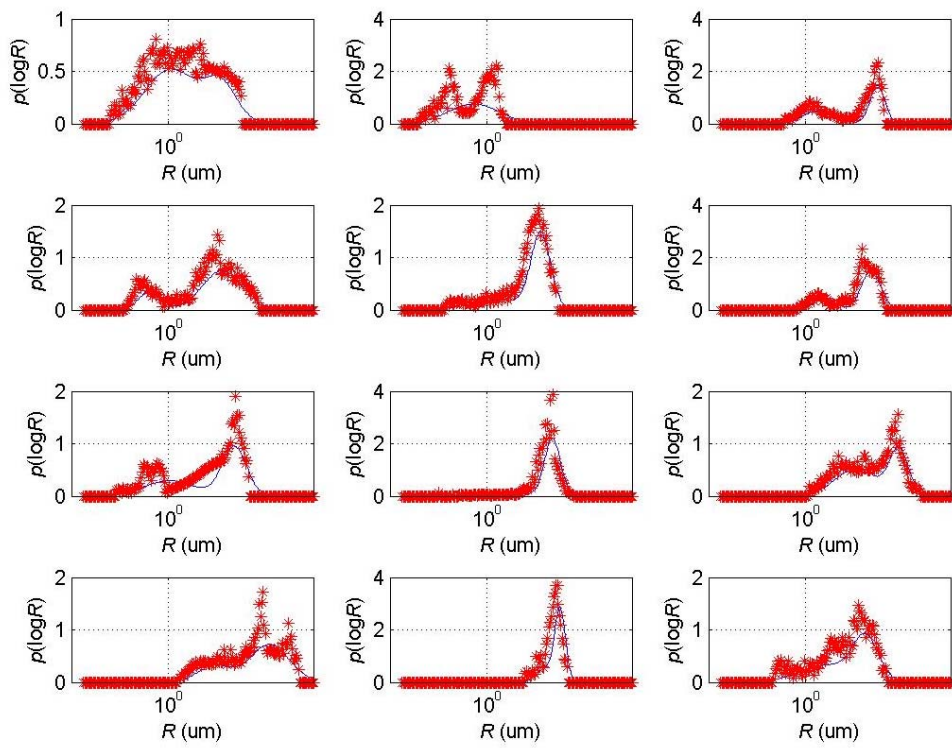
63

Example of P_c Curve Fitting in Carbonate Rocks



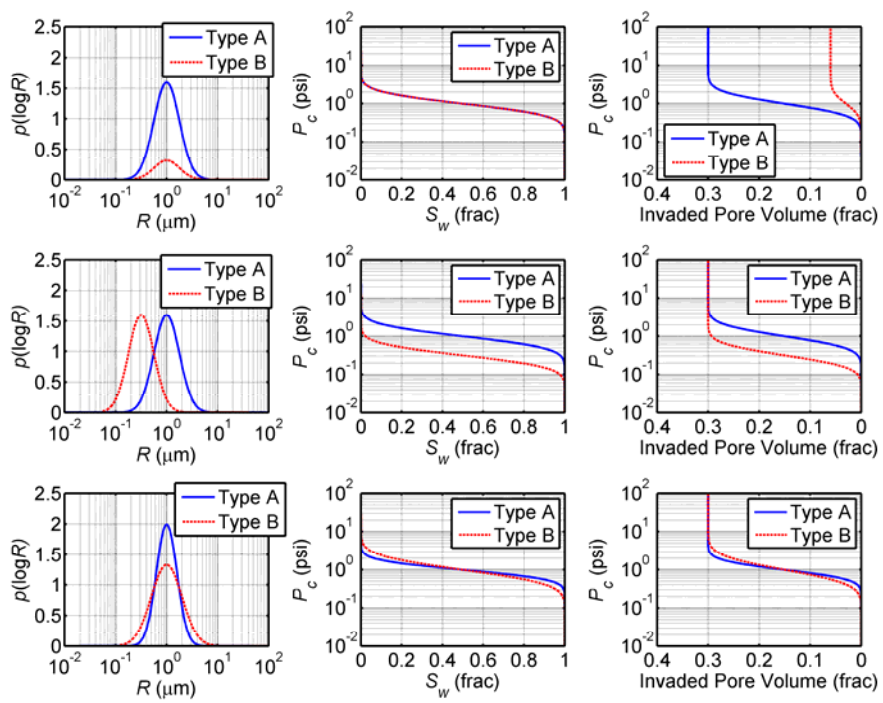
64

Corresponding Throat-Size Distributions



65

Pore Volume vs. Pore Connectivity vs. Pore Uniformity



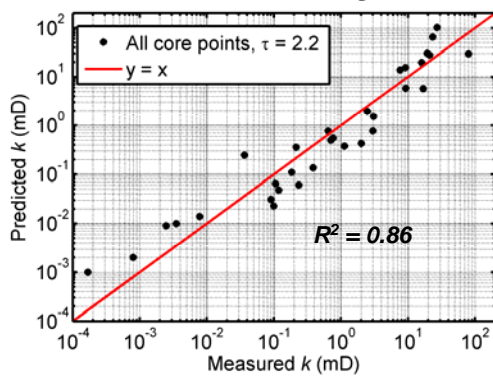
66

Quantifying Petrophysical Orthogonality or Dissimilarity

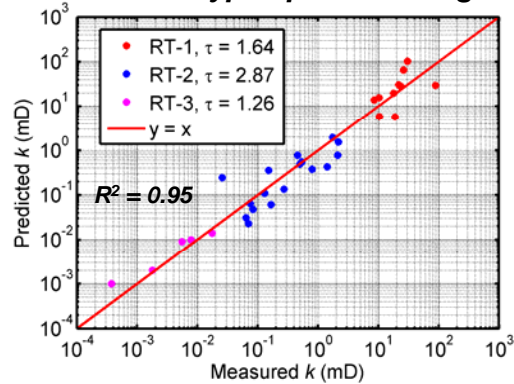
$$k = \frac{\phi}{32\sqrt{\tau}} \left[\frac{\int_0^\infty f(\delta) \delta^4 d\delta}{\int_0^\infty f(\delta) \delta^2 d\delta} \right] = \frac{\phi}{32\sqrt{\tau}} (\bar{R})^2$$

Peters (2012)

Overall fitting



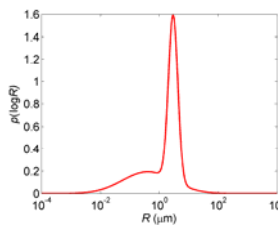
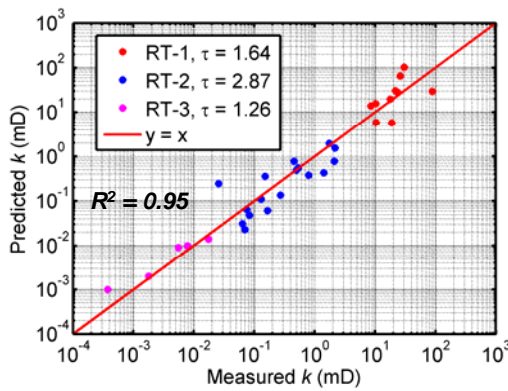
Rock-type specific fitting



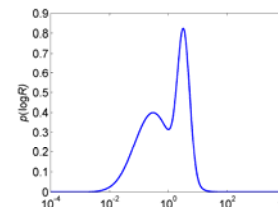
Hugoton Carbonate Gas Field

67

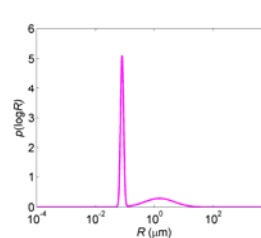
Quantifying Petrophysical Orthogonality or Dissimilarity



RT-1



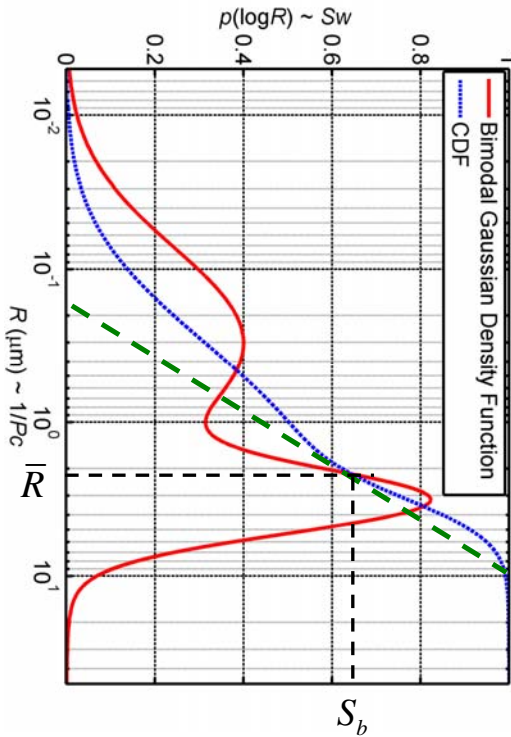
RT-2



RT-3

68

Comparison to Swanson's Model



$$K_w = \begin{cases} 431 & \left(\frac{S_b}{P_c} \right)_A \\ 2.109 & 4 \\ 290 & \left(\frac{S_b}{P_c} \right)_A \\ 1.901 & \\ 355 & \left(\frac{S_b}{P_c} \right)_A \\ 2.005 & \end{cases}, \quad \dots \dots \dots \quad (1)$$

S_b : volume fraction

P_c : pore-throat

Coefficient: tortuosity

$$k = \frac{\phi}{32\sqrt{\tau}} \left[\frac{\int_0^\infty f(\delta) \delta^4 d\delta}{\int_0^\infty f(\delta) \delta^2 d\delta} \right] = \boxed{\frac{\phi}{32\sqrt{\tau}}} \boxed{(R)}^3$$

69

Quantifying Petrophysical Orthogonality or Dissimilarity

$$k = \frac{\phi}{32\sqrt{\tau}} \left[\frac{\int_0^\infty f(\delta) \delta^4 d\delta}{\int_0^\infty f(\delta) \delta^2 d\delta} \right] = \frac{\phi}{32\sqrt{\tau}} (\bar{R})^2$$

Peters (2012)

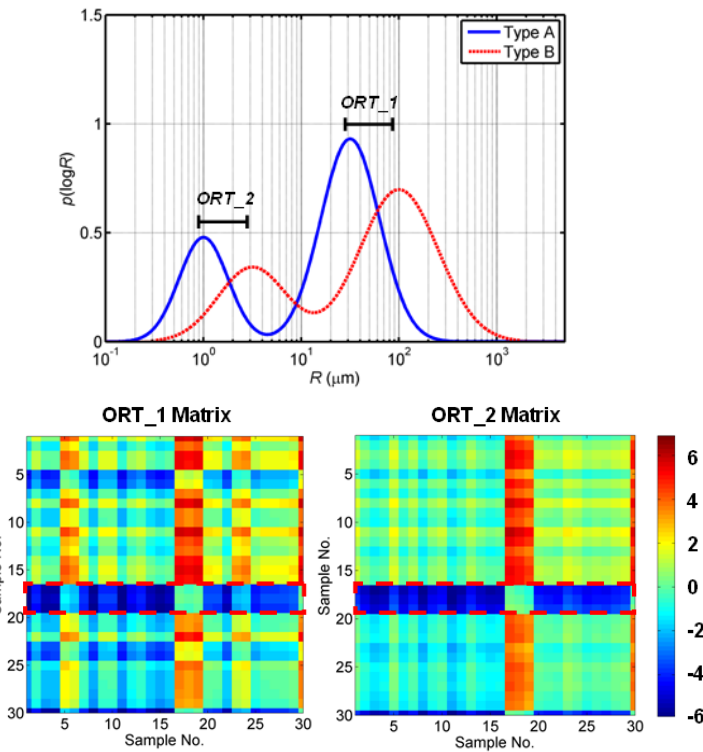
$$\log k = \log \phi + \log \overline{R}^2 + \log \frac{1}{\sqrt{\tau}} - 1.51$$

$$ORT_{1,2} = [\log \phi_1 - \log \phi_2] + [\log(\bar{R}_1^2) - \log(\bar{R}_2^2)] + [\log(\frac{1}{\sqrt{\sigma_1}}) - \log(\frac{1}{\sqrt{\sigma_2}})]$$

$$= \log\left(\frac{\phi_1}{\phi_2}\right) + 2\log\left(\frac{\overline{R}_1}{\overline{R}_2}\right) - 0.5\log\left(\frac{\sigma_1}{\sigma_2}\right)$$

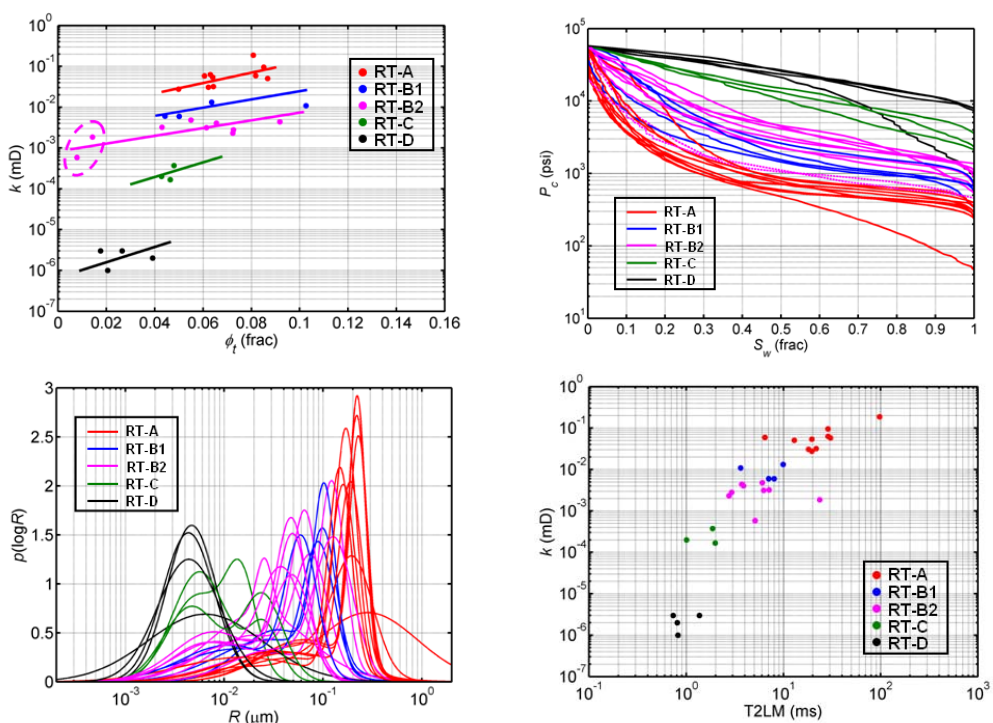
$$a \log\left(\frac{\phi_1}{\phi_2}\right) + b \log\left(\frac{\overline{R}_1}{\overline{R}_2}\right) + c \log\left(\frac{\sigma_1}{\sigma_2}\right) \quad \text{←} \quad a, b, \text{ and } c \text{ need calibration}$$

Petrophysical Orthogonality Matrix



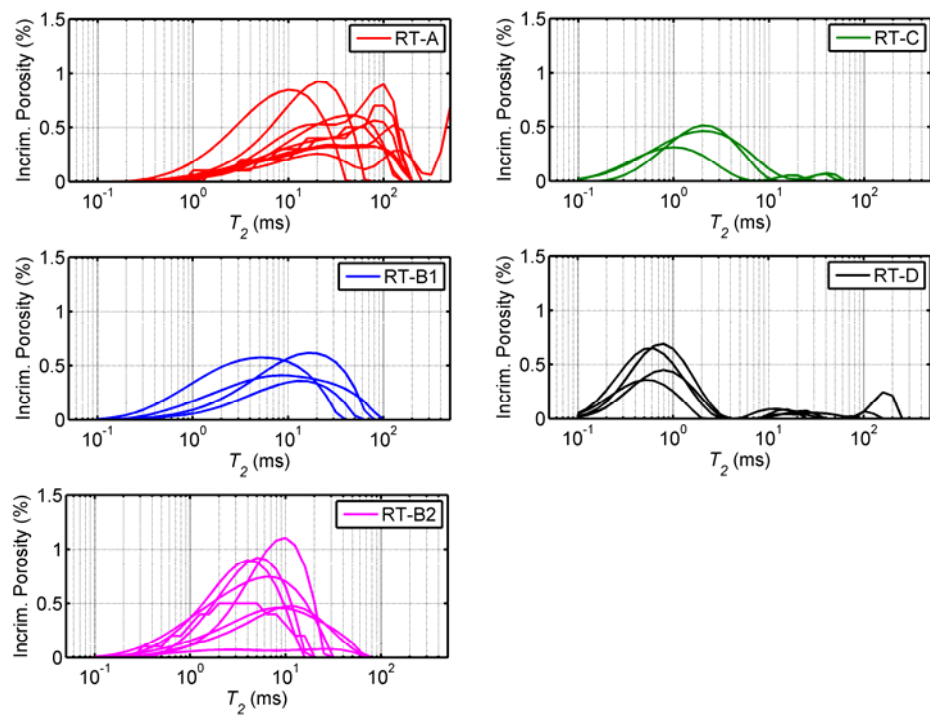
71

Field Application: Cotton Valley Tight-Gas Sands



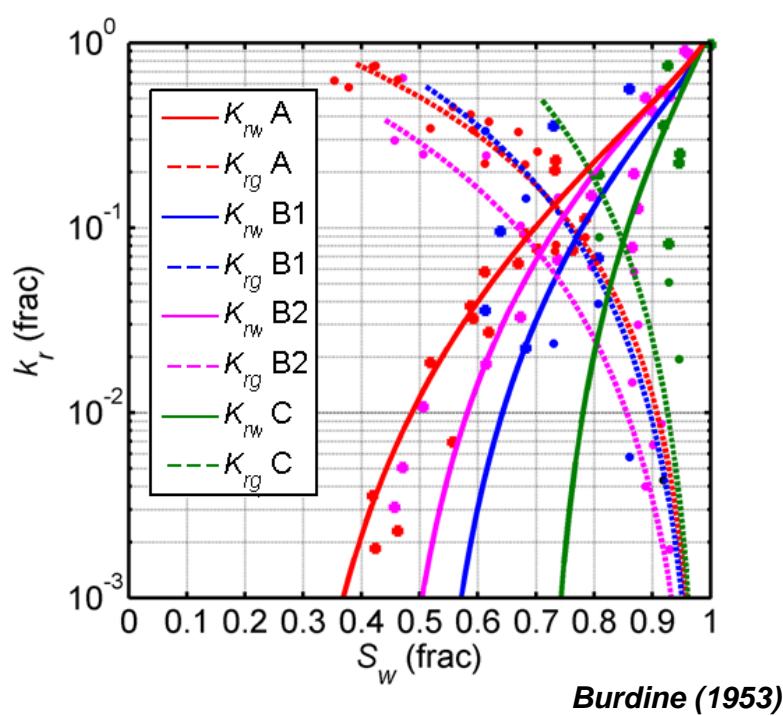
72

Field Application: Cotton Valley Tight-Gas Sands



73

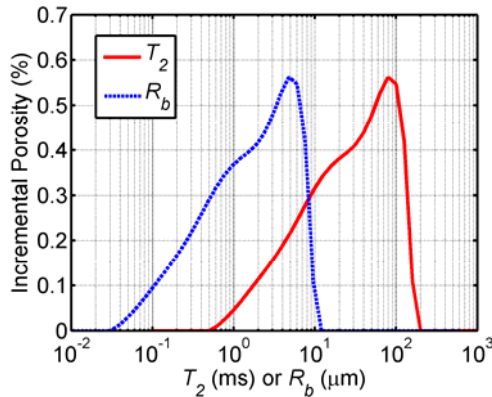
Field Application: Cotton Valley Tight-Gas Sands



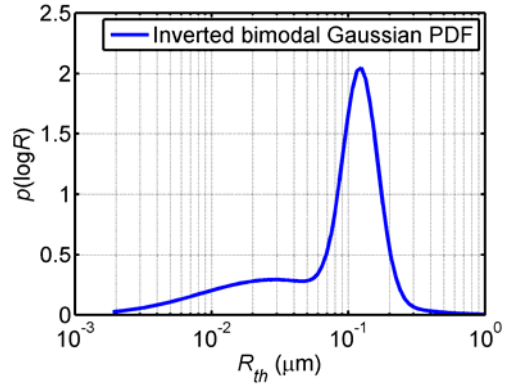
74

Burdine (1953)

Quantifying Fluid Distribution: NMR and MICP



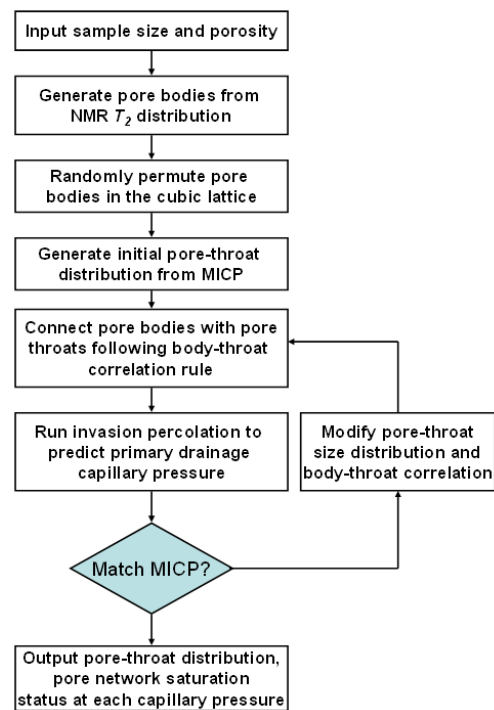
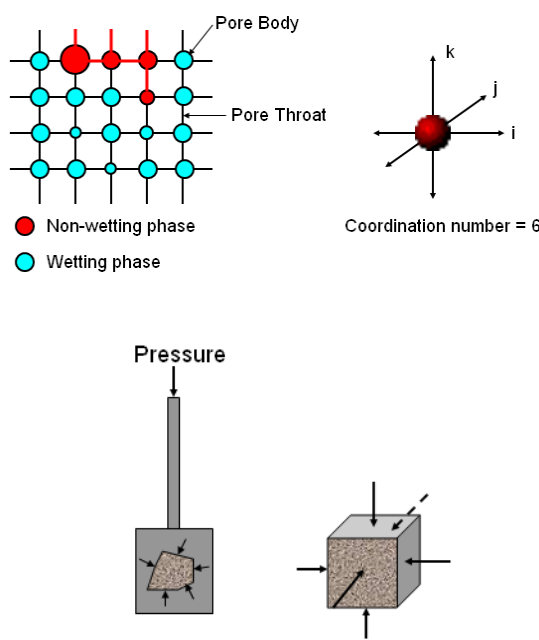
Pore Body Size Distribution



Pore Throat Size Distribution

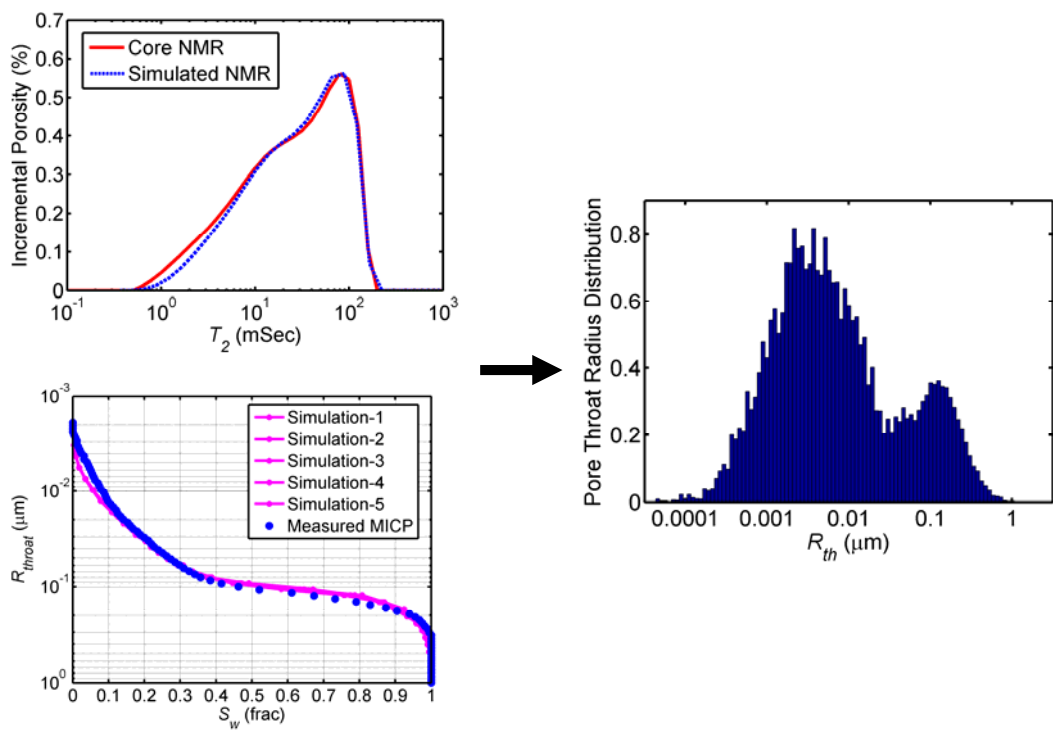
75

Quantifying Fluid Distribution: Pore Network Modeling



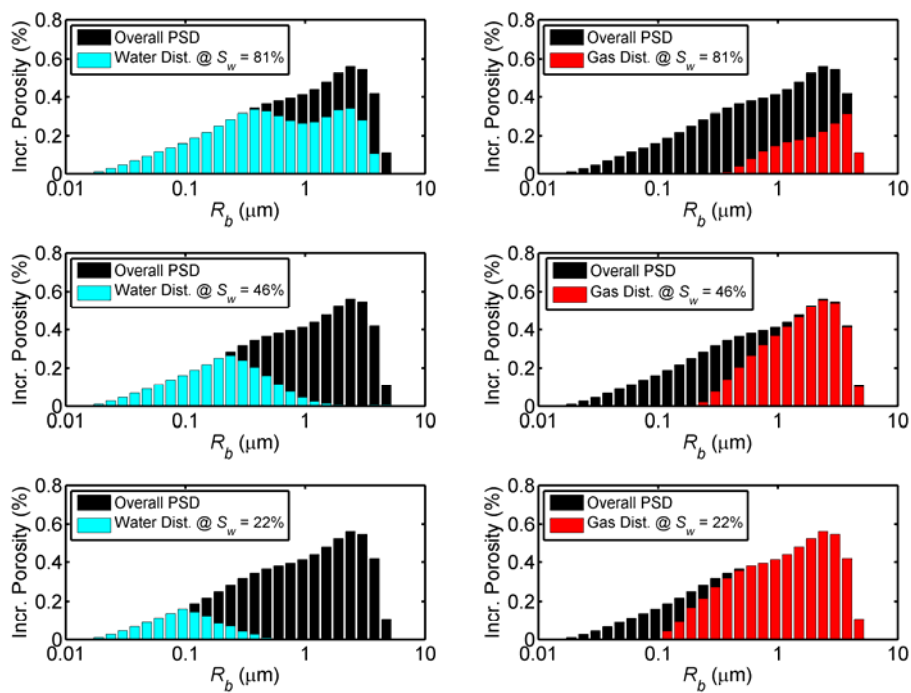
76

Quantifying Fluid Distribution: Model Validation



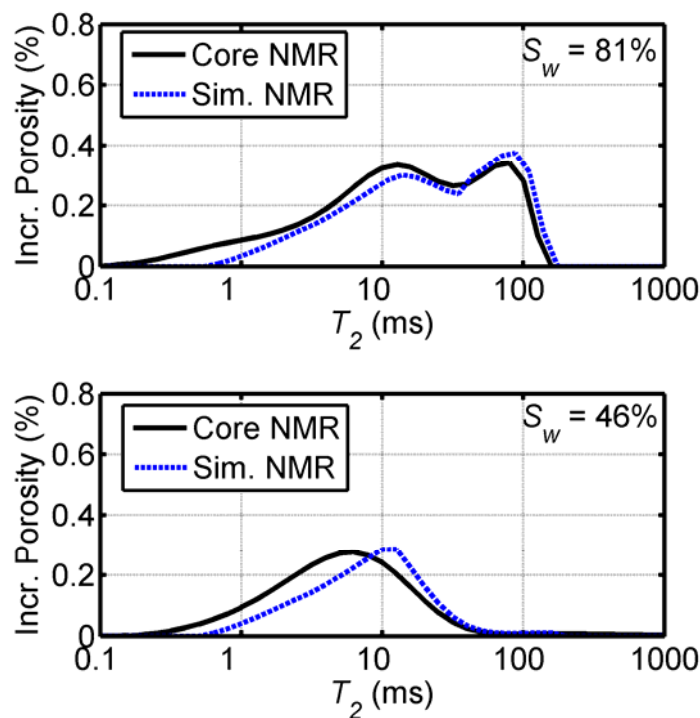
77

Quantifying Fluid Distribution: Desaturation/Drainage



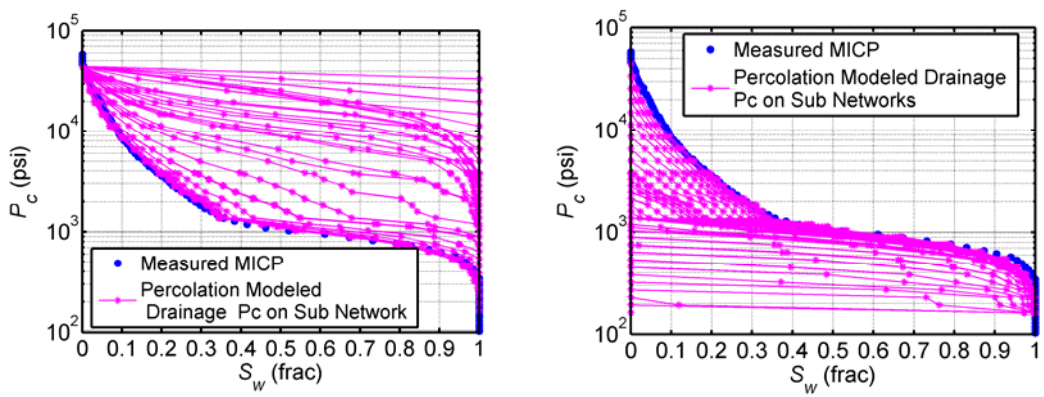
78

Quantifying Fluid Distribution: Validation



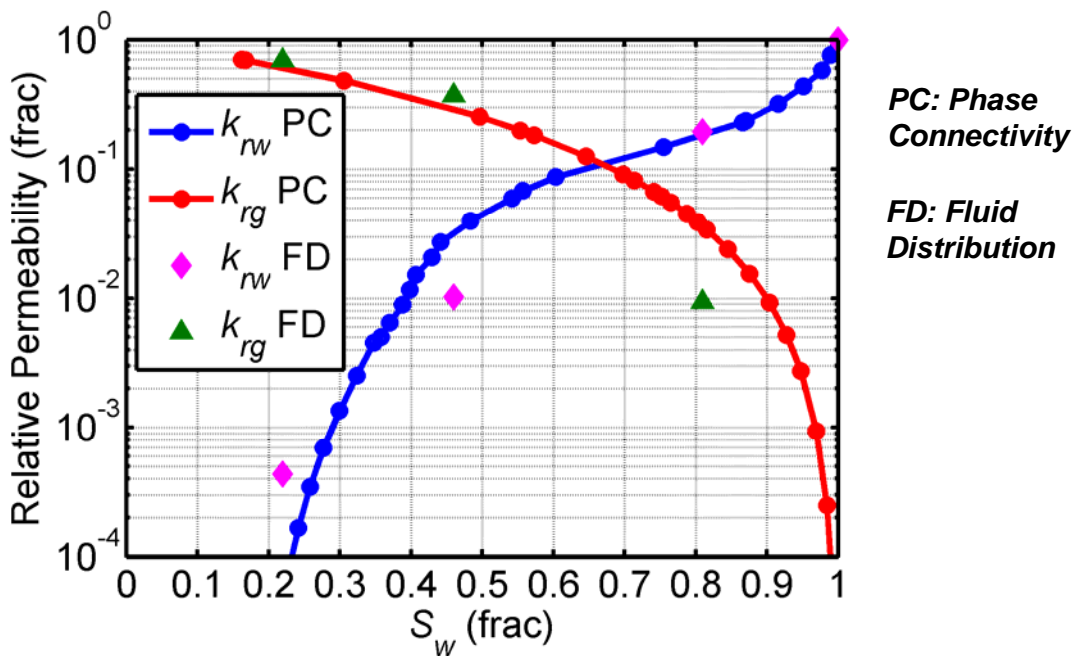
79

Quantifying Fluid Distribution: Effective Pore Network



80

Quantifying Fluid Distribution: Relative Permeability



81

Best Practices: Use of Mineralogy and Grain-Size

- Discriminate lithofacies.
- Correct hydration water effect on MICP.
- Understanding of cause-effect chain connecting deposition, pore geometry, fluid distribution, and physical measurements.

82

Best Practices: Use of Existing Methods

- RQI/R35/FZI are similar in both petrophysics and mathematical description.
- R35 formula needs to be calibrated using MICP.
- FZI trends are too steep in low-porosity end.
- RQI is the simplest method and does not need calibration.

83

Best Practices: Pore System Description

- Bimodal pore size distribution from MICP.
- Interpretable petrophysics:
 - Pore volume.
 - Pore connectivity.
 - Pore uniformity.
- Petrophysical orthogonality (dissimilarity).
- Fluid distribution: pore network modeling.

84

Rock Typing: from Core to Logs

- Petrophysics to physics: hydraulic vs. electrical.
- Surface to subsurface: capillary transition, mud-filtrate invasion.
- Inch scale to feet scale: shoulder-bed effects, heterogeneity, multiple tool resolutions.

85

Well-Log Sensitivity to Rock and Fluid

	<i>Composition</i>	<i>Texture</i>	<i>Structure</i>	<i>Fluid</i>
GR	High	Low	Low	Low
PEF	High	Low	Low	Low
Neutron	Medium	Sensing to volume	Low	High
Density	Medium	Sensing to volume	Low	High
Resistivity	Low	Medium	High	High
Sonic	High	Medium	Medium	High
NMR	Medium	High	Low	High

86

Apparent E-Facies

Electrofacies: the set of log responses that characterizes a sediment and permits the sediment to be distinguished from others. (Serra & Abbott, 1982)

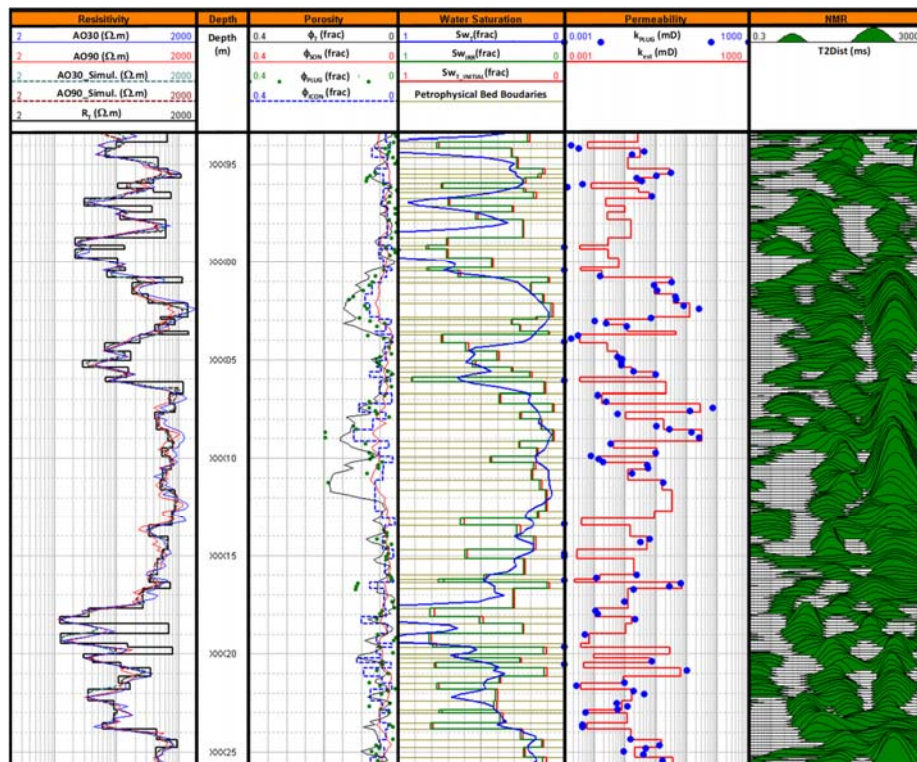
Q1: What type of rock type is defined by E-facies?

Q2: Are log responses truly representative of rock properties?

Q3: What logs are sensitive to pore geometry?

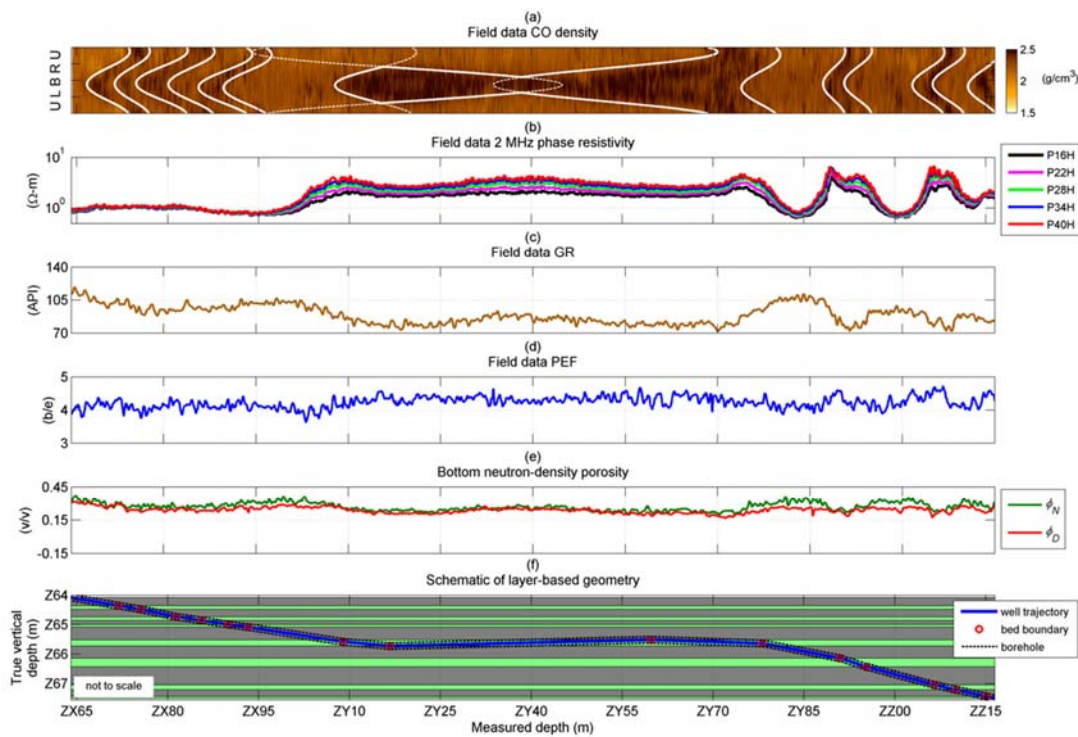
87

Example of Rock Formations at Irreducible Water Saturation



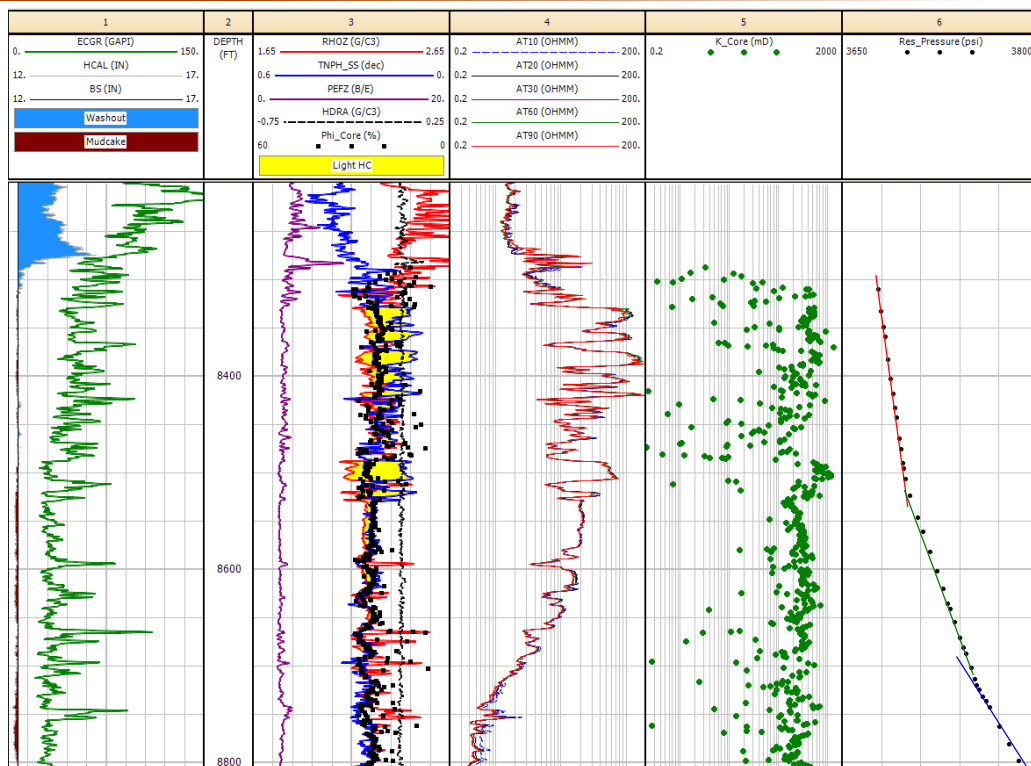
88

Abnormal Well Logs: Abnormal E-Facies



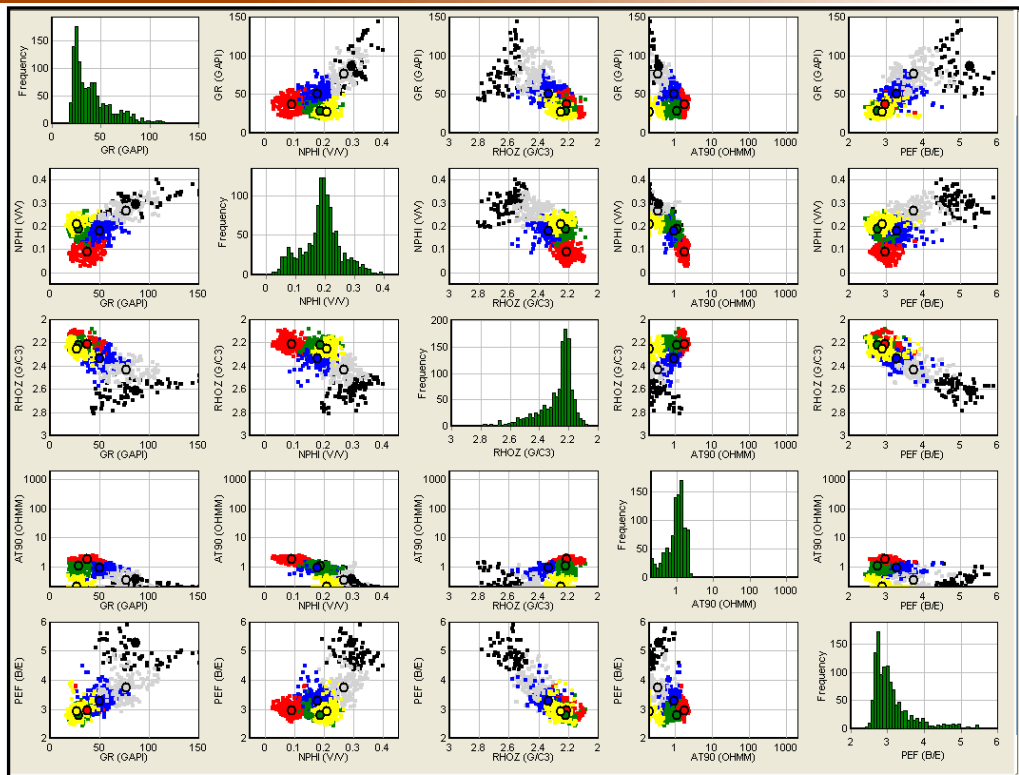
89

Field Example: North Sea



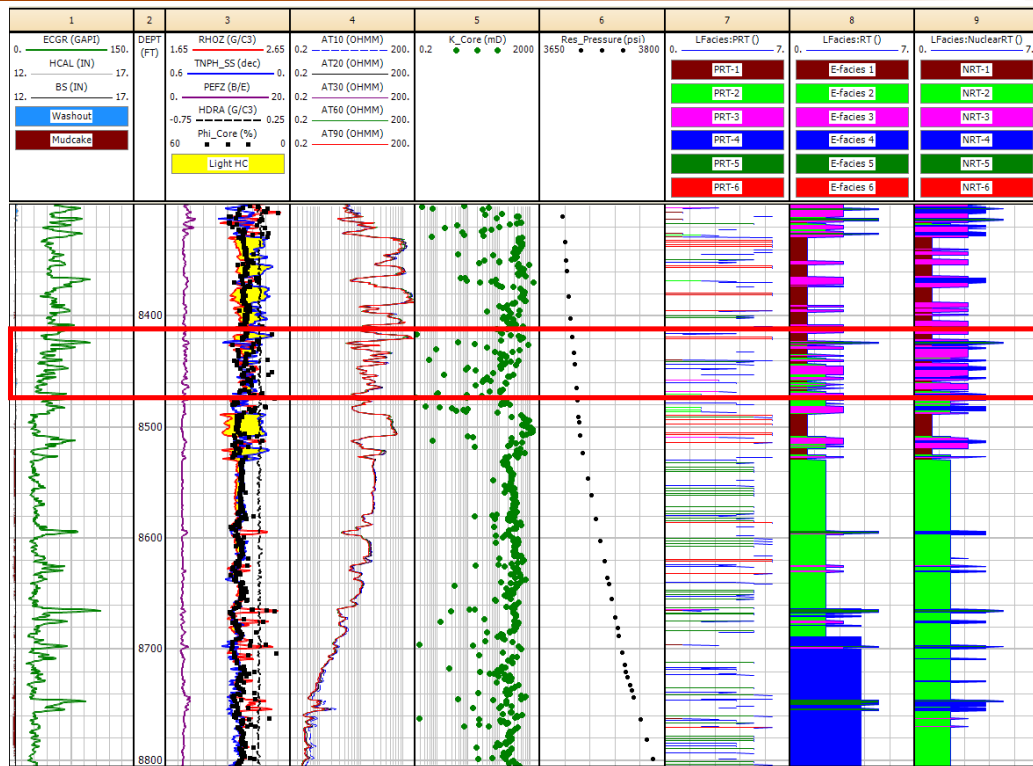
90

Field Example: Cluster E-facies



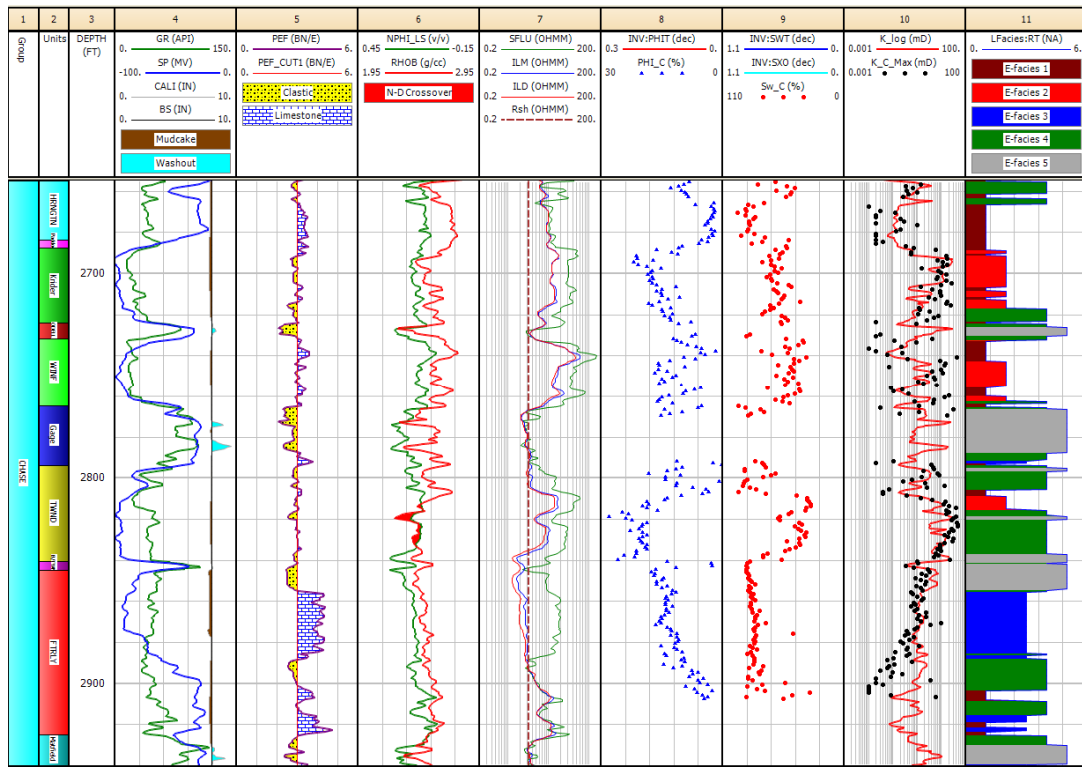
91

Field Example: Rock Type Comparison



92

Field Example: Hugoton Gas Field, Invasion



93

Field Example: Matters of Concern

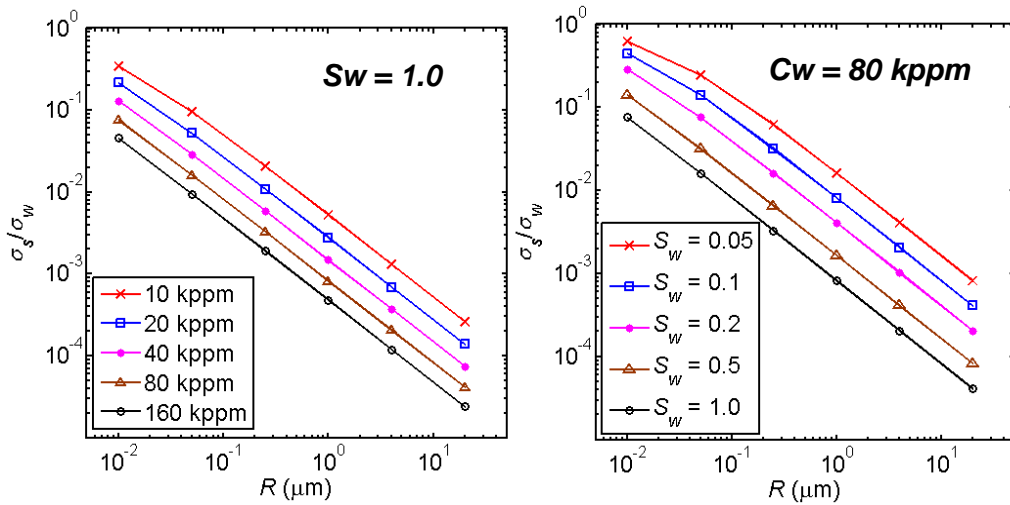
- Thinly bedded zone not explicitly identified and classified with well logs.
- Fluid content changing from gas to oil to water bias nuclear and density logs.
- Water saturation changing from irreducible water to transition zone to aquifer zone biases resistivity logs.
- Deep invasion affects resistivity logs.

94

Conductivity: Electrical vs. Hydraulic

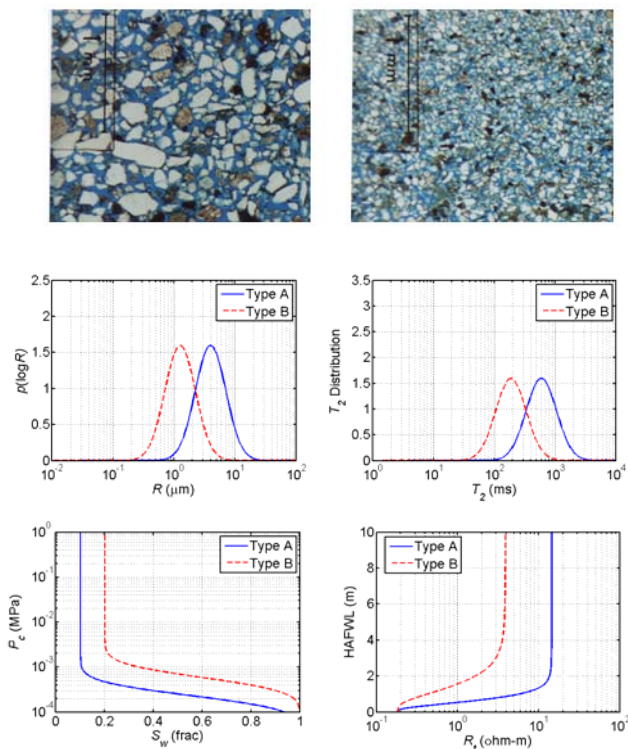
D. L. Johnson (1986)

$$\sigma_t = \frac{1}{FS_w^{-n}} [\sigma_w + \frac{2}{RS_w} \Sigma_s] \quad \text{while} \quad k = \frac{R^2}{8F}$$



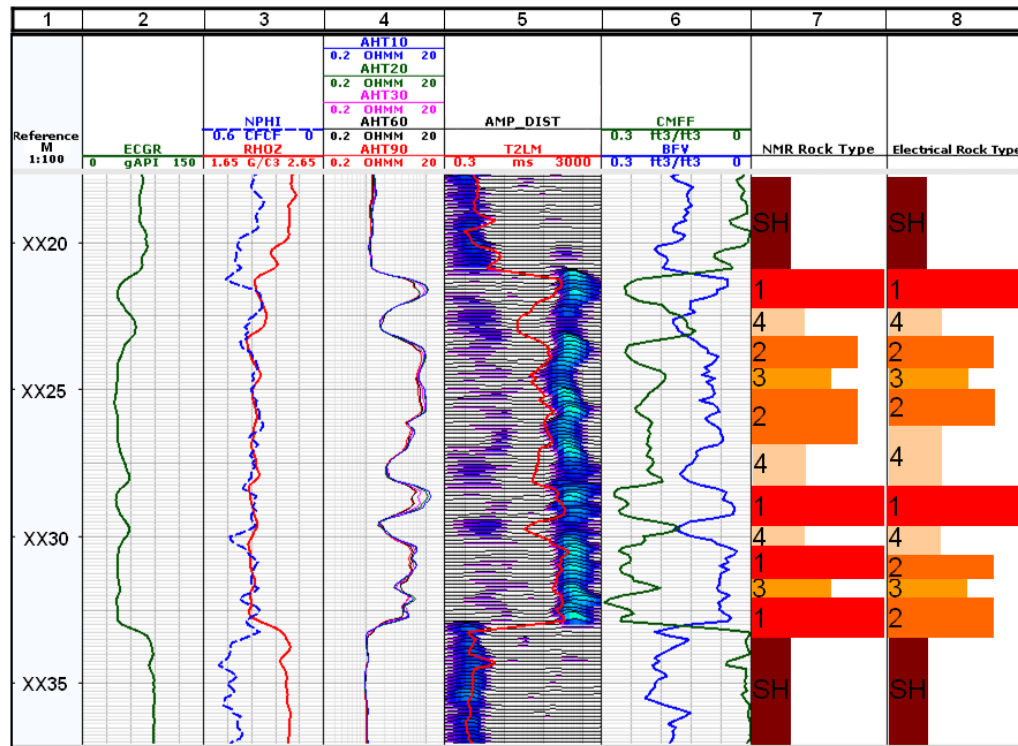
95

Grain Size → Pore Size → Irreducible Water



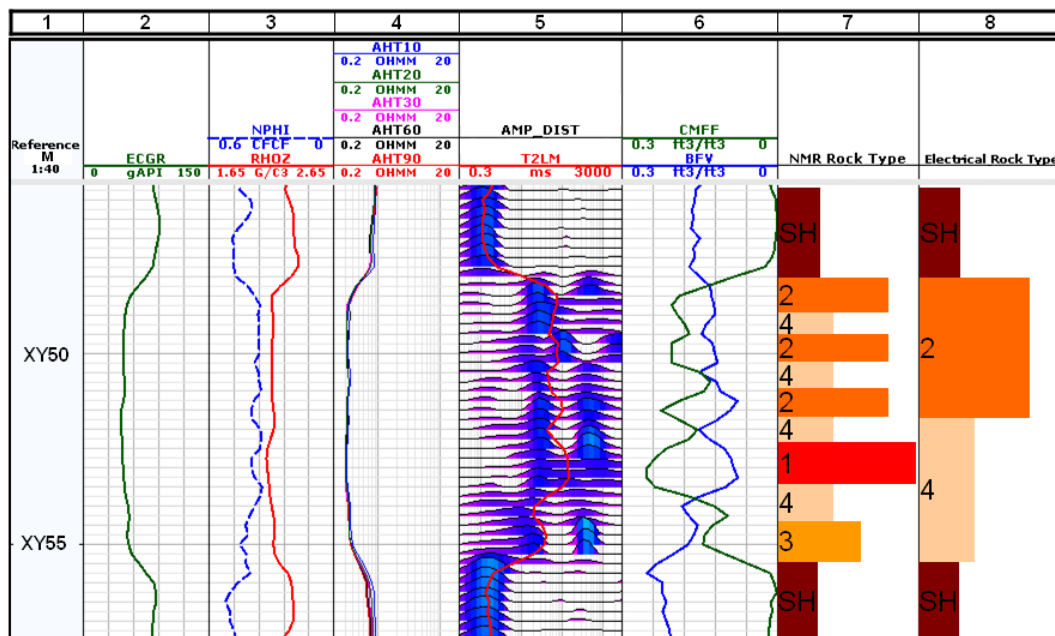
96

Field Applications: Gulf of Mexico, Oil Zone



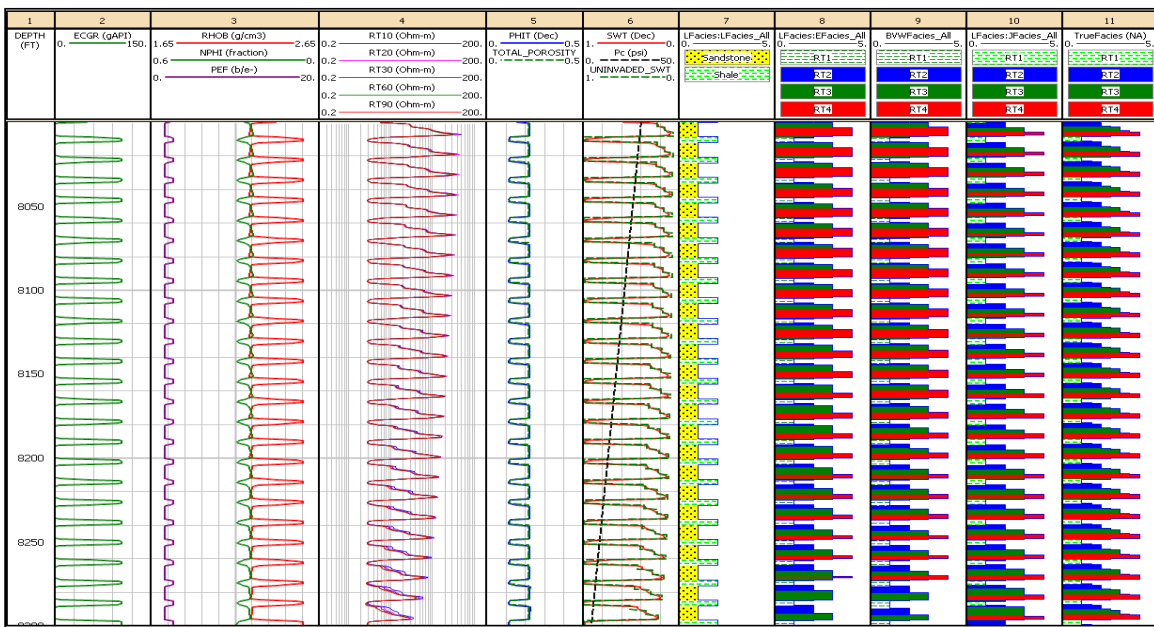
97

Field Applications: Gulf of Mexico, Water Zone



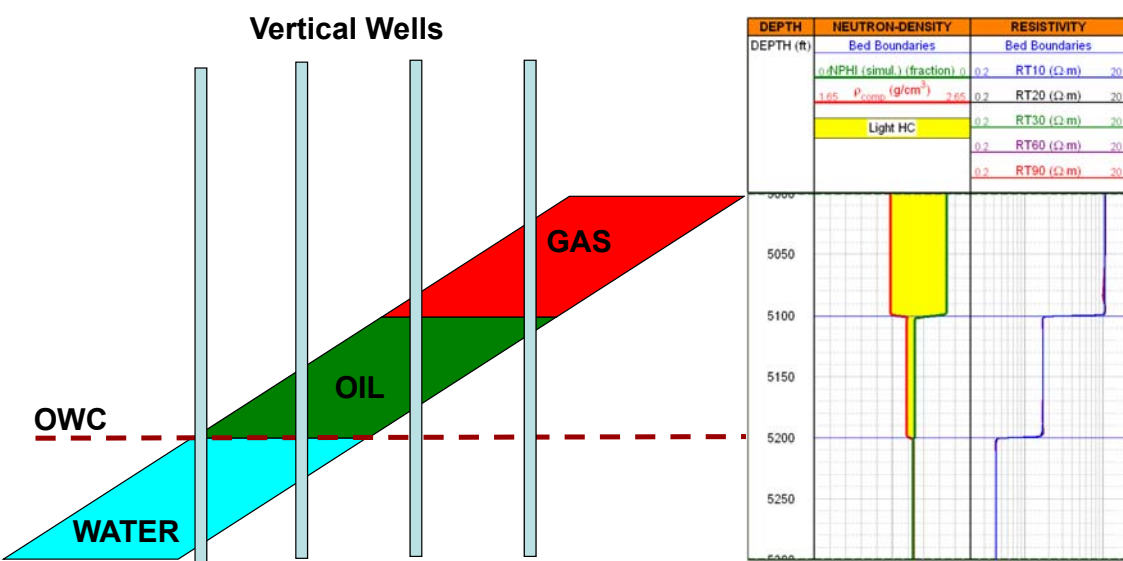
98

Synthetic Case: Transition Zone



99

Fluid Effect: Capillary Transition



Dipping Formation – Same Rock Type

100

Fluid Effect: Capillary Transition Correction

$$S_w = S_{wirr} + aJ^b \Rightarrow J(S_w) = \left(\frac{S_w - S_{wirr}}{a}\right)^{\frac{1}{b}}$$

↓

$$\sqrt{\frac{k}{\phi}} = \frac{J(S_w)}{P_c} \times \sigma \cos \vartheta = \left(\frac{S_w - S_{wirr}}{a}\right)^{\frac{1}{b}} \times \frac{\sigma \cos \vartheta}{P_c}$$

Reservoir QualitySaturationHeight

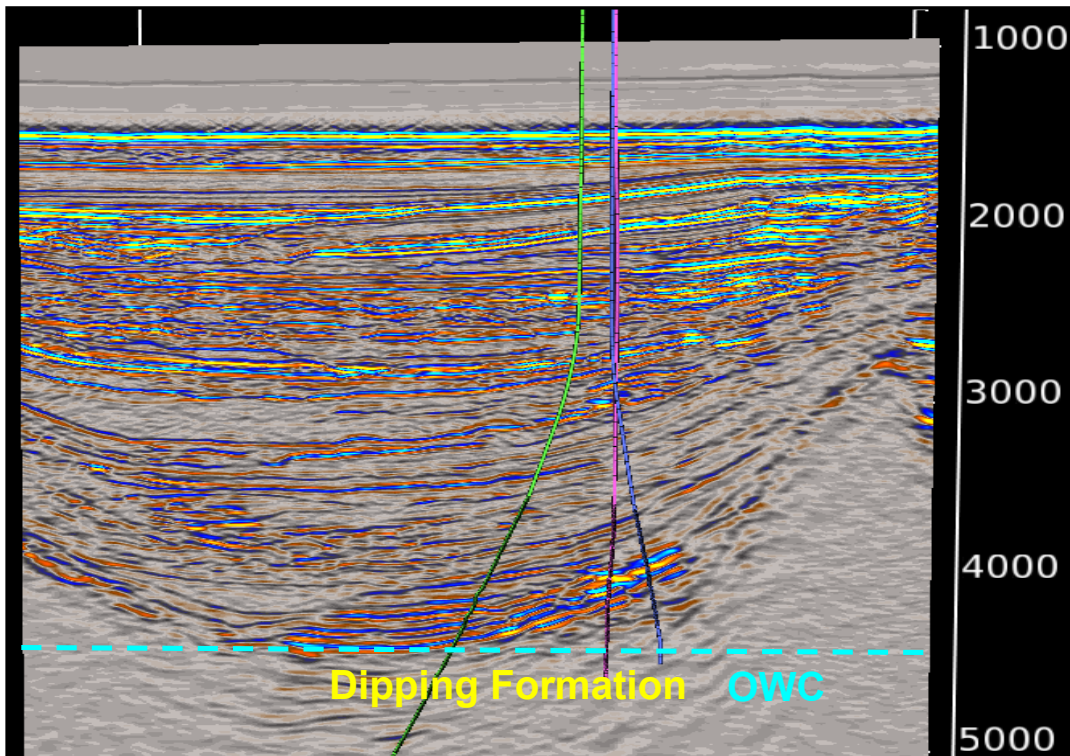
101

Field Case: Central GOM, US

- Deepwater Gulf of Mexico.
- Turbidite submarine fan depositional system.
- Unconsolidated shaly-sand sequence from amalgamated channels.
- OBM/WBM invading oil zone.
- Reservoir under capillary transition.

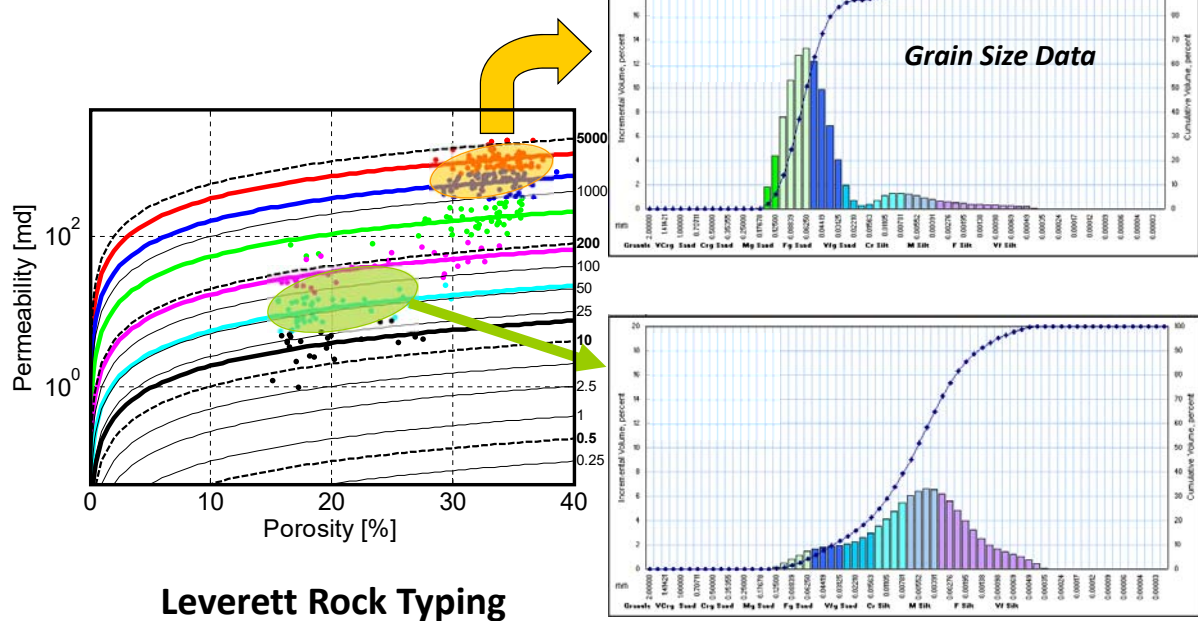
102

Well Location



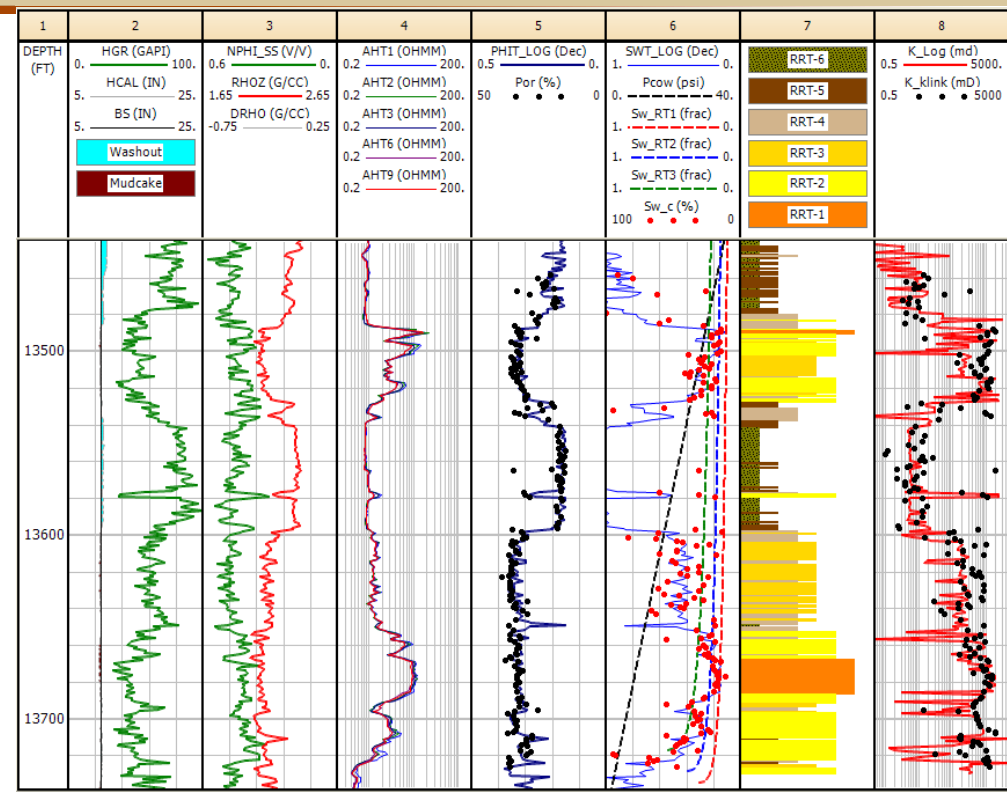
103

Core-Based Hydraulic Rock Typing

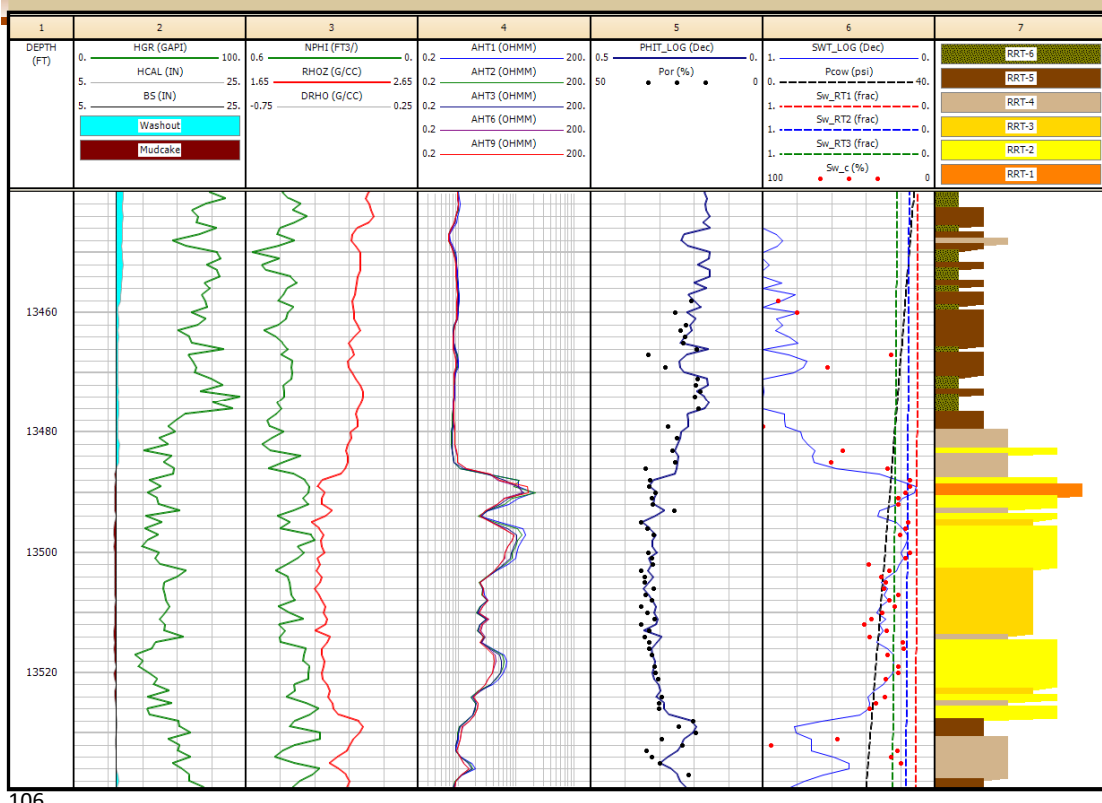


104

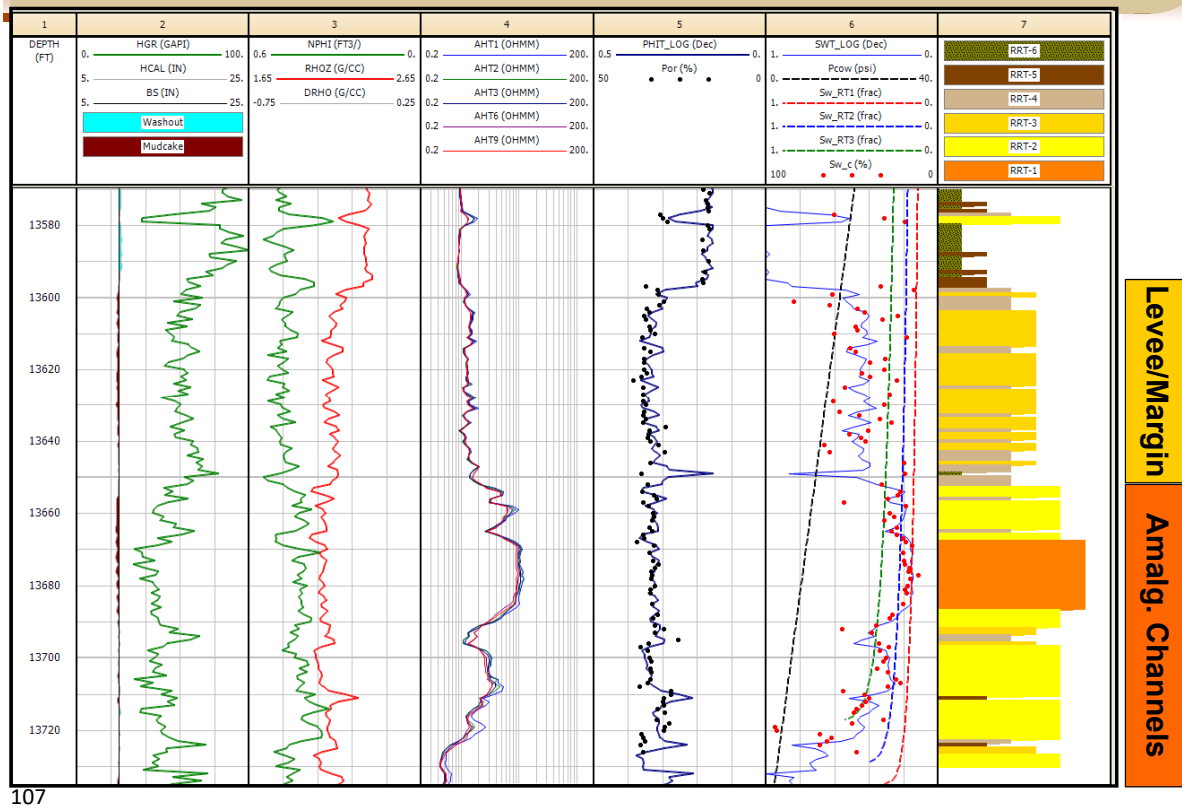
Key Well Application: Overview



Key Well Application: Detailed View (1)

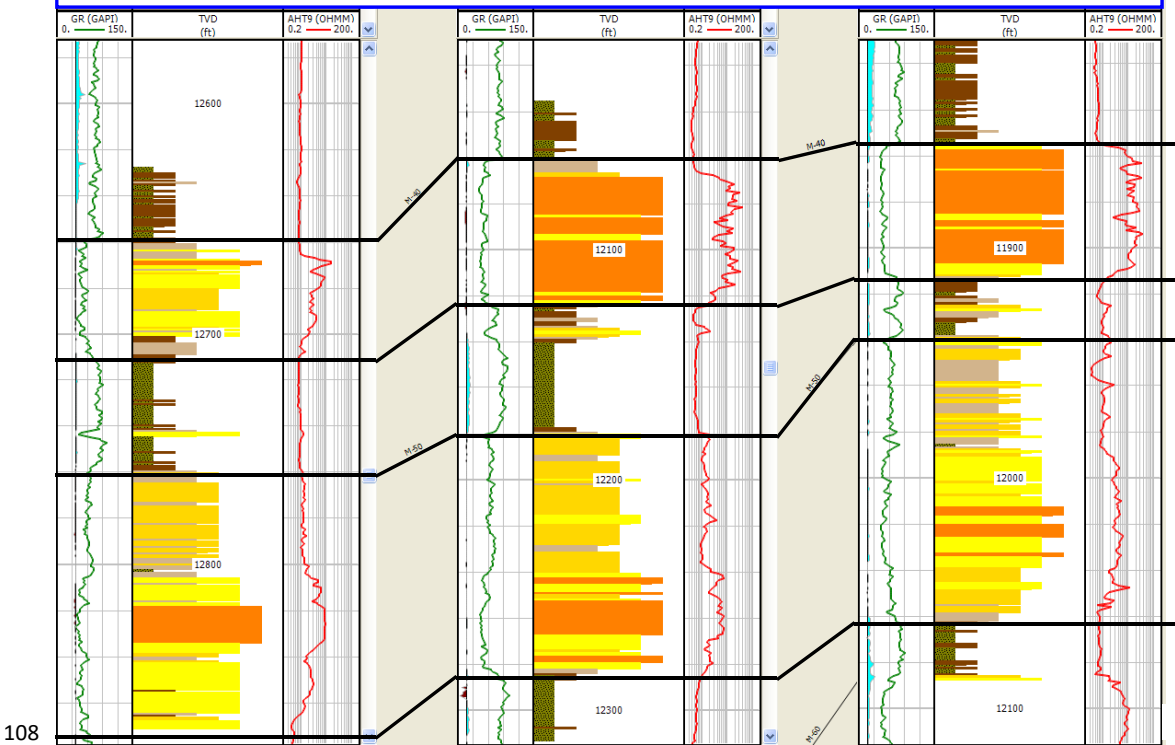


Key Well Application: Detailed View (2)

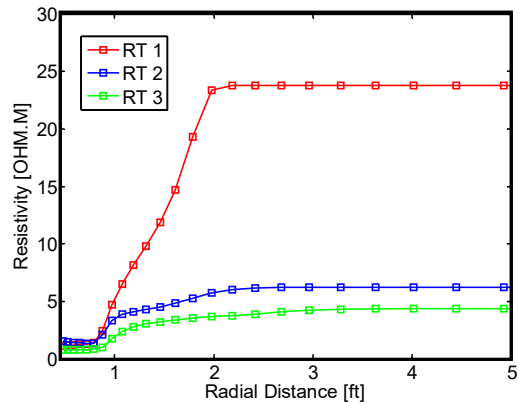
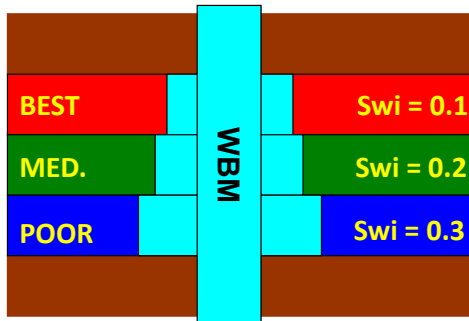


Multiple Well Application

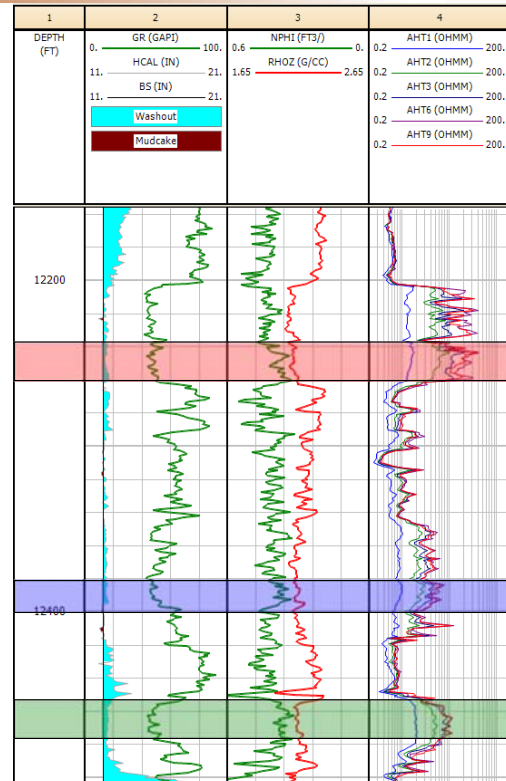
Prograding Fan System: Lateral Fining & Vertical Coarsening



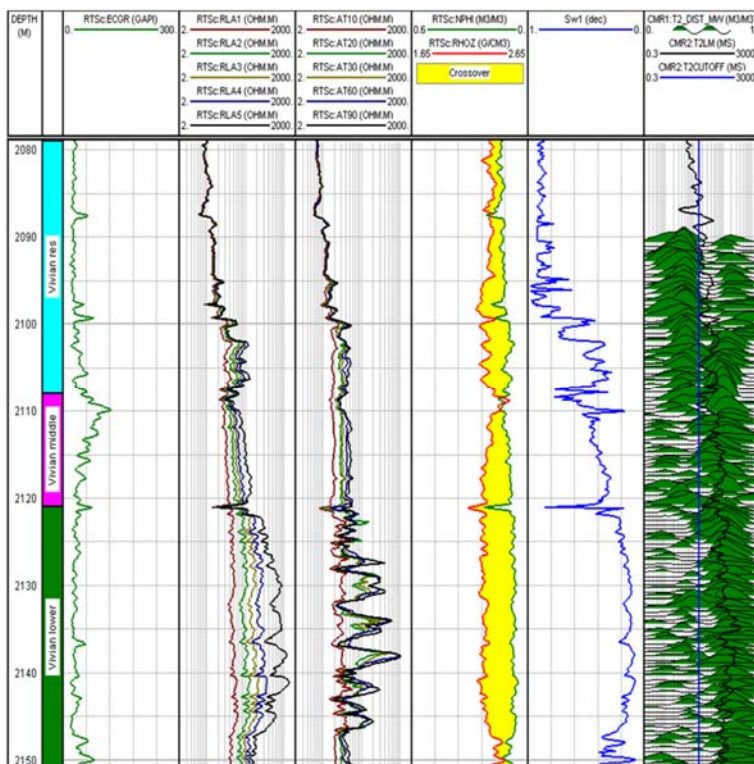
Fluid Effect: Mud-Filtrate Invasion



109



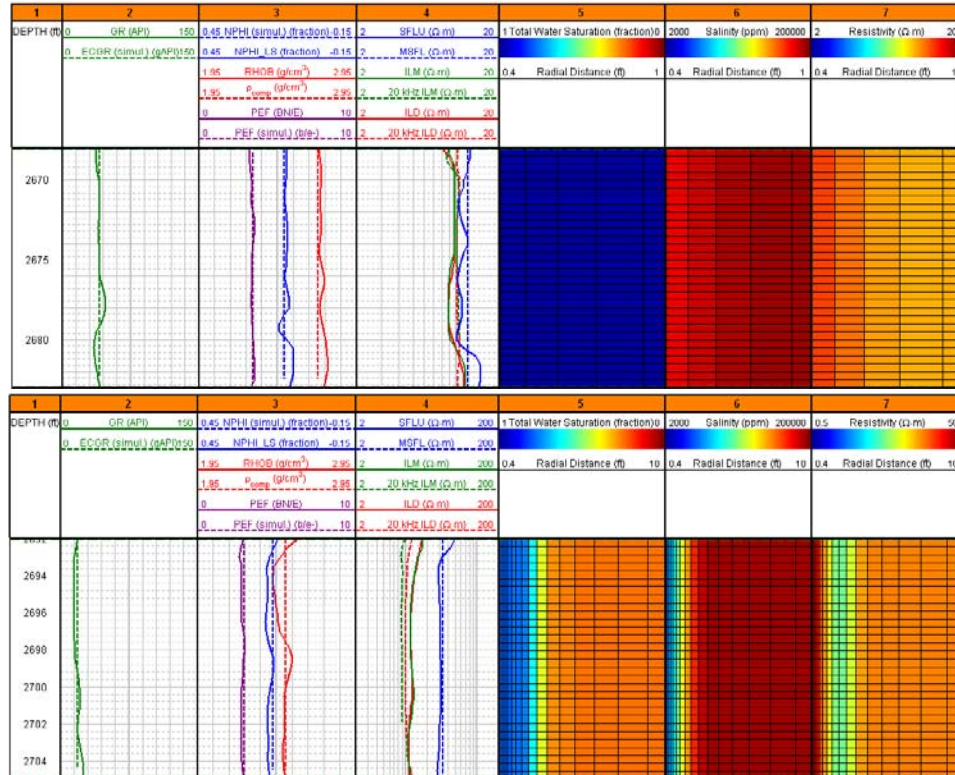
Example of Fluid Effect: Mud-Filtrate Invasion



110

Field Case: Hugoton Gas Field

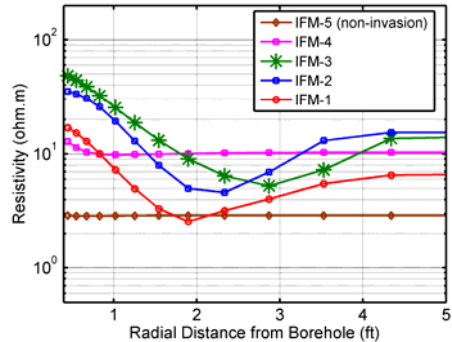
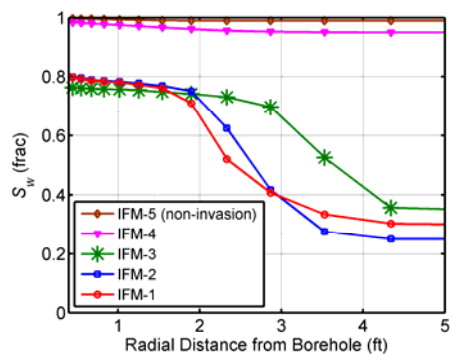
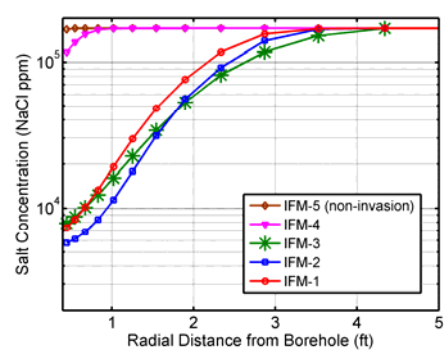
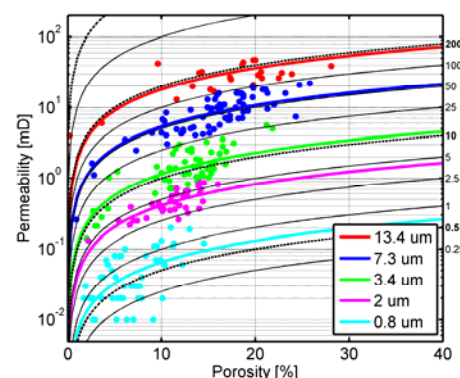
Wackestone



Packstone

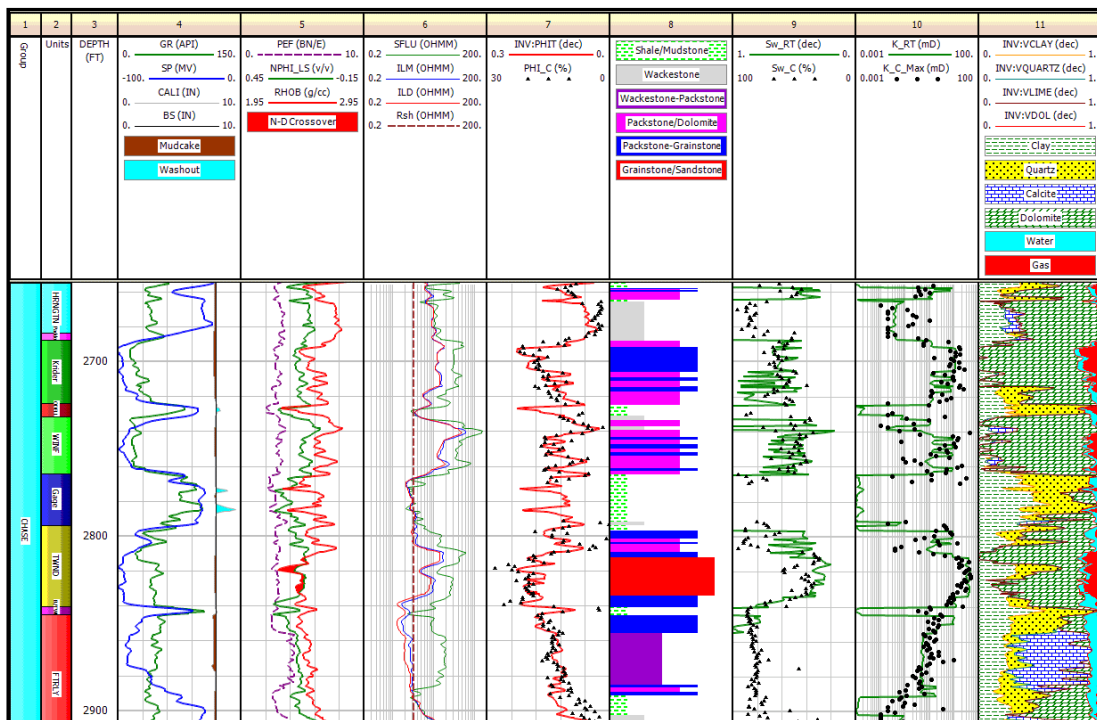
111

Field Case: Hugoton Gas Field



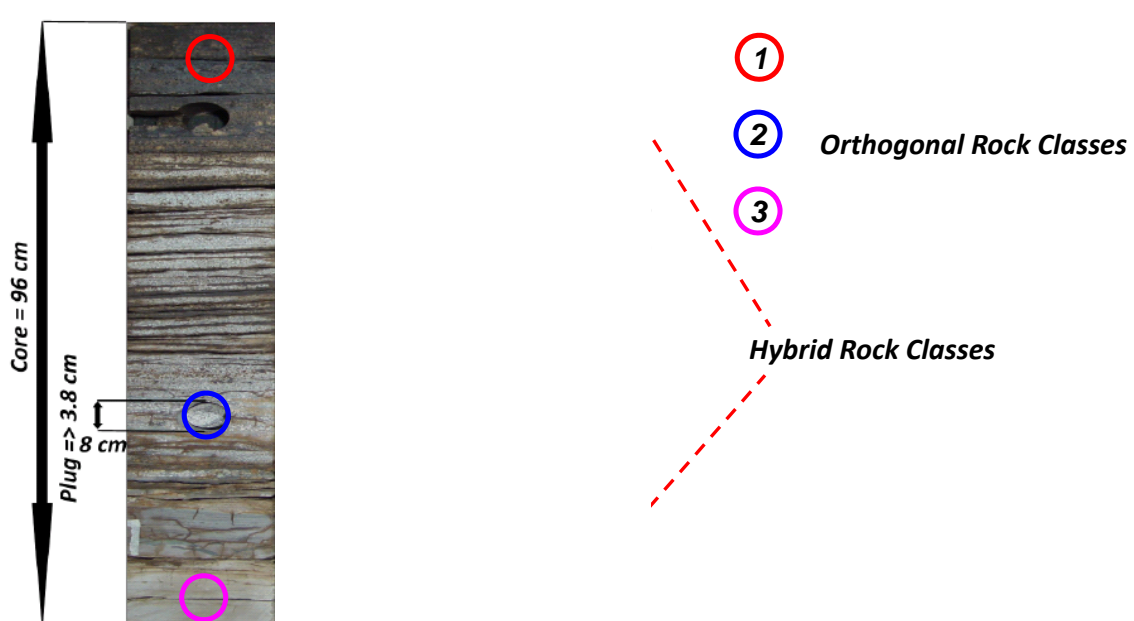
112

Field Case: Hugoton Gas Field



113

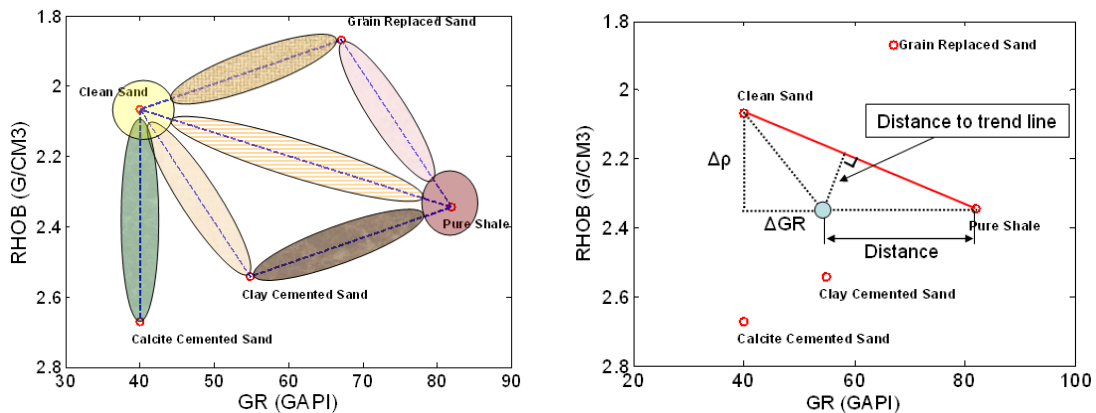
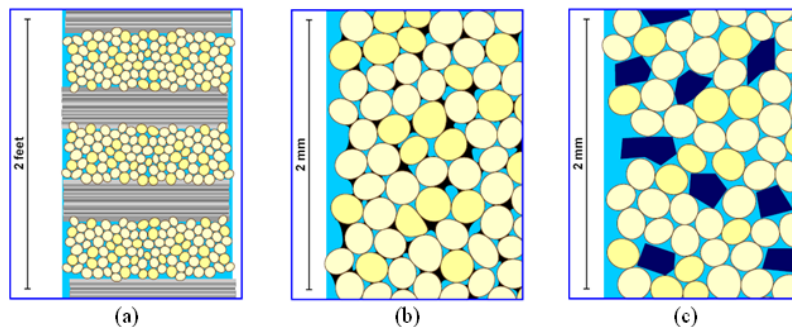
From Core to Logs: Thin beds and Laminations



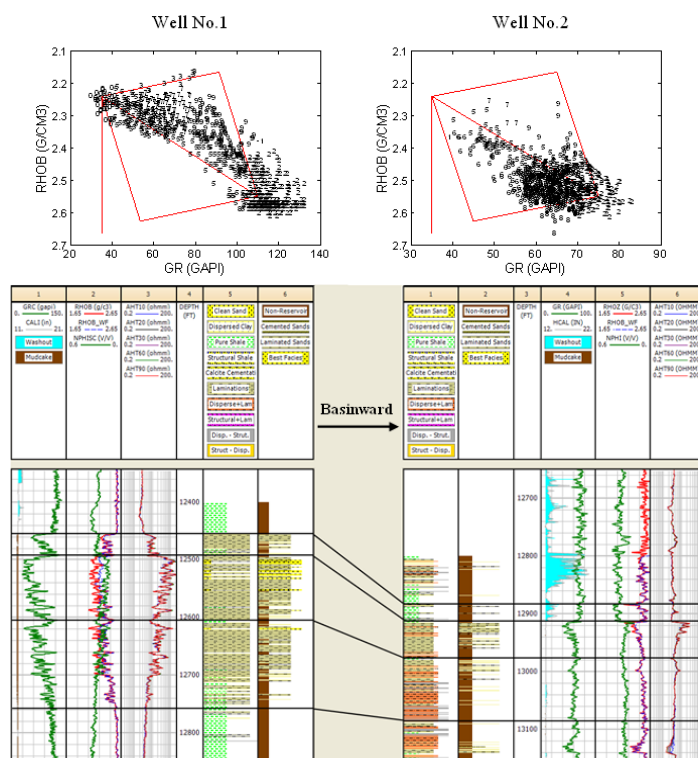
Diniz-Ferreira and Torres-Verdín, 2012 SPWLA

114

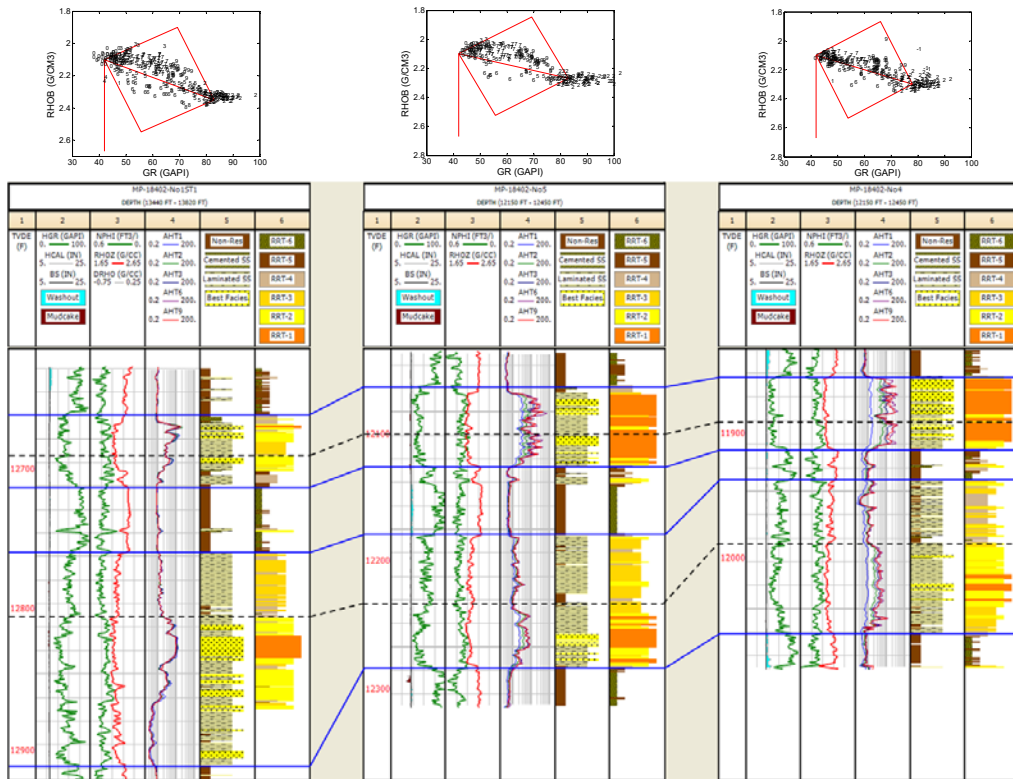
Thin-Bed Identification: Thomas-Stieber



Field Applications: Trinidad Gas Field

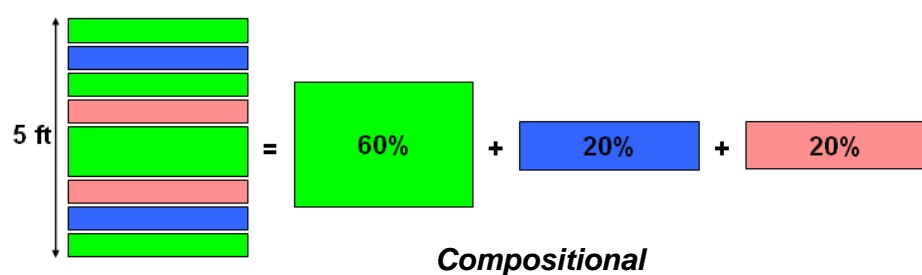
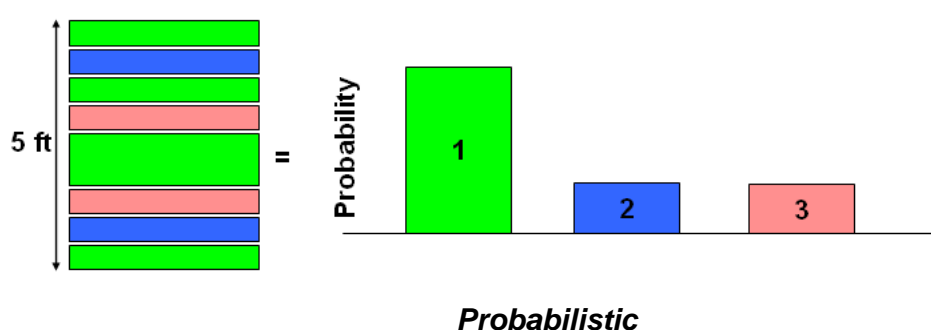


Field Applications: Gulf of Mexico



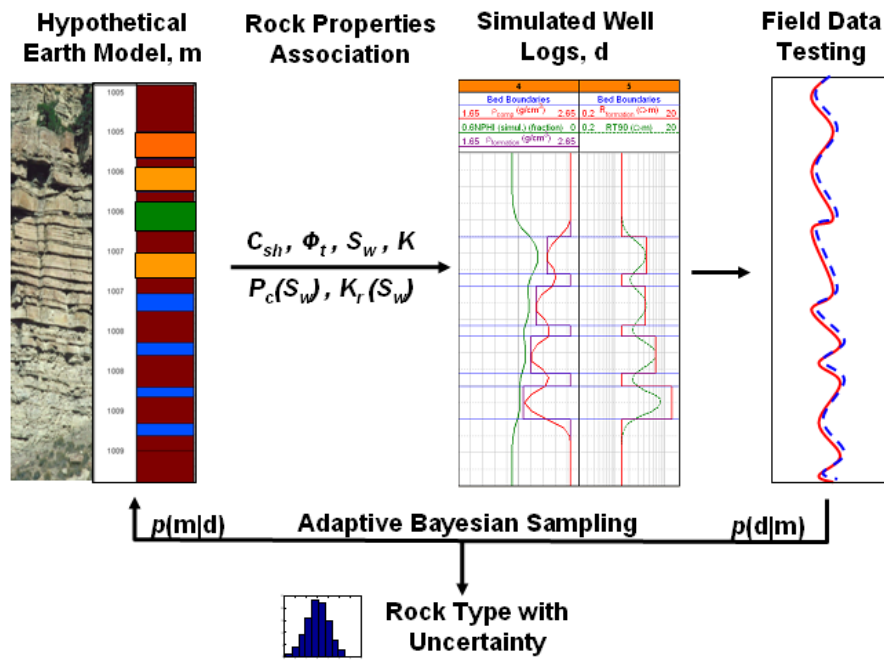
117

Description of Hybrid Rock Classes



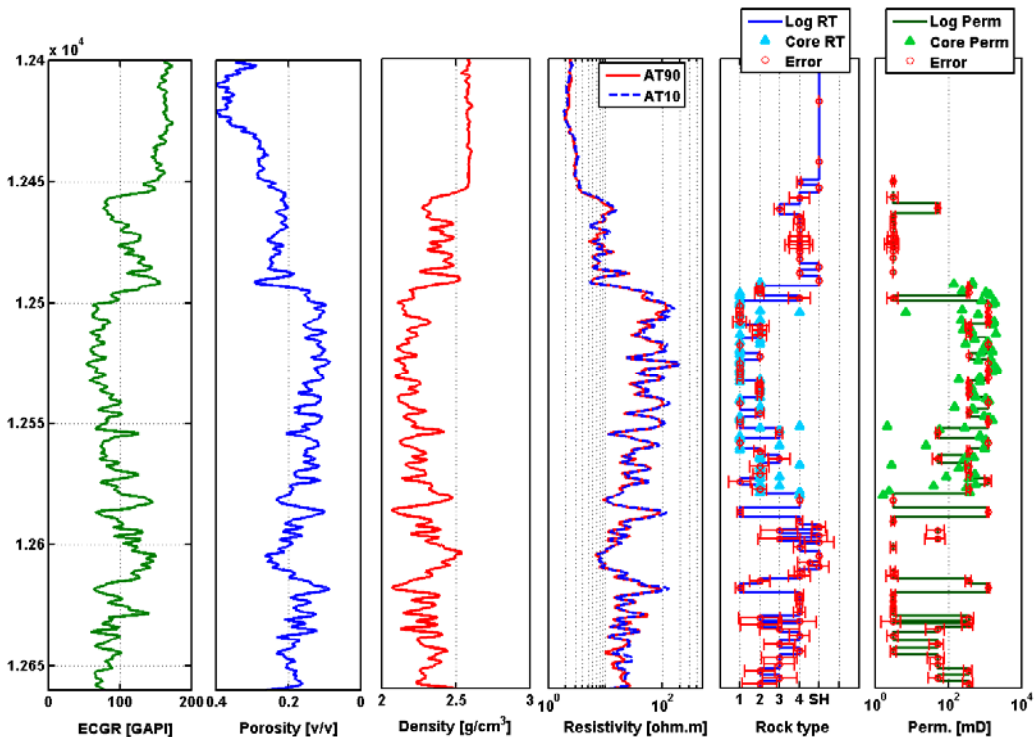
118

Bayesian Rock Typing



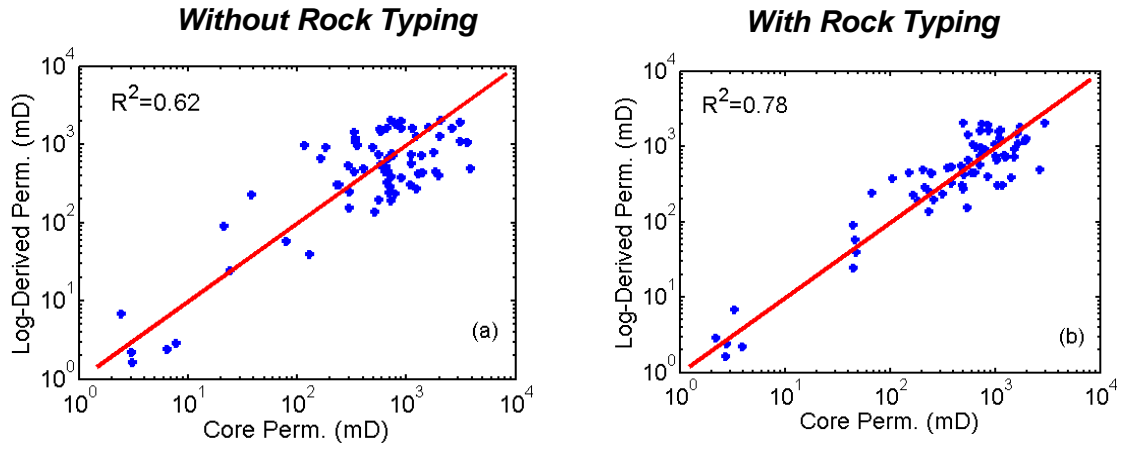
119

Field Application: Trinidad Gas Field



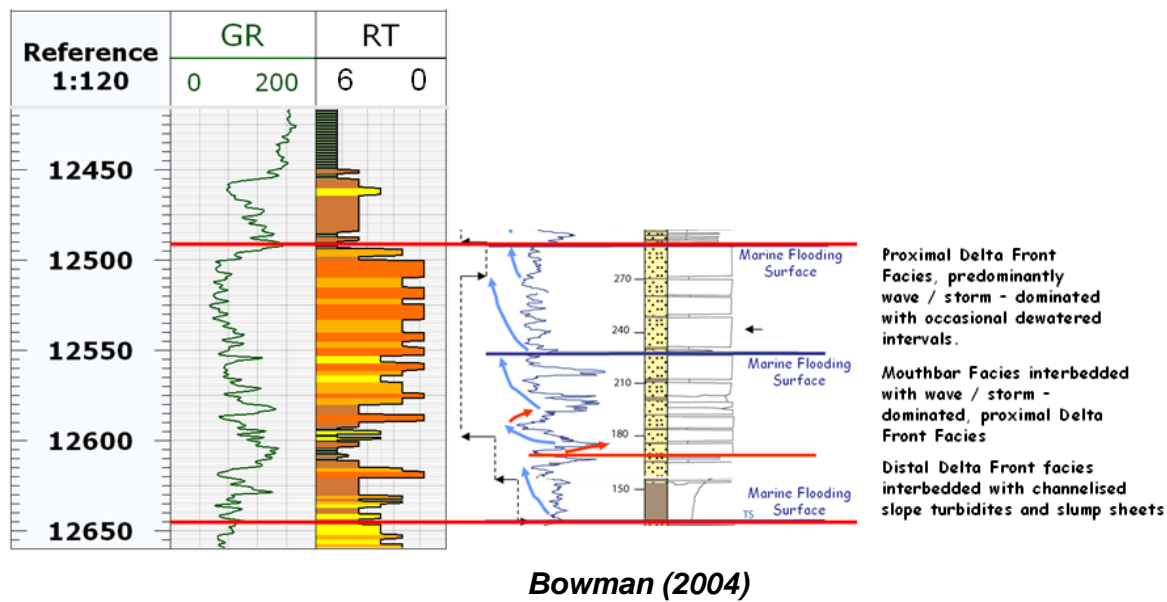
120

Field Application: Trinidad Gas Field



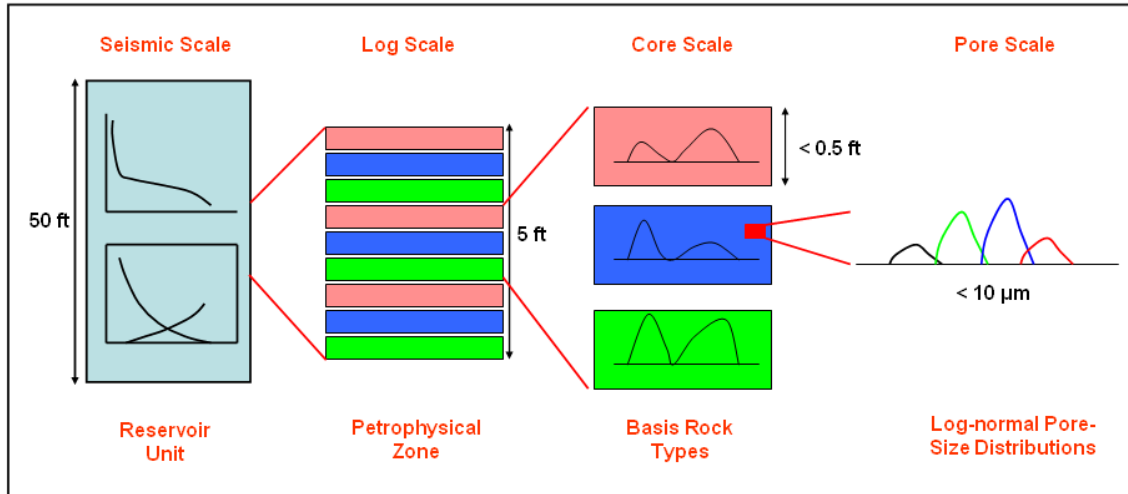
121

Field Application: Trinidad Gas Field



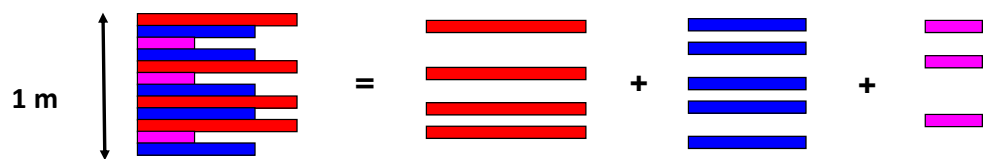
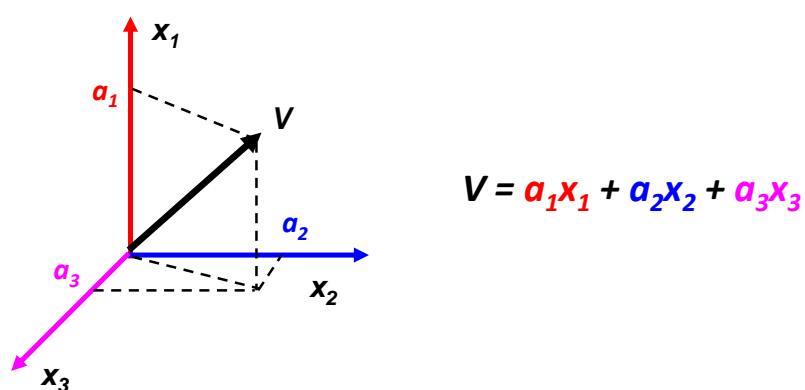
122

Decomposition of Orthogonal Rock Classes



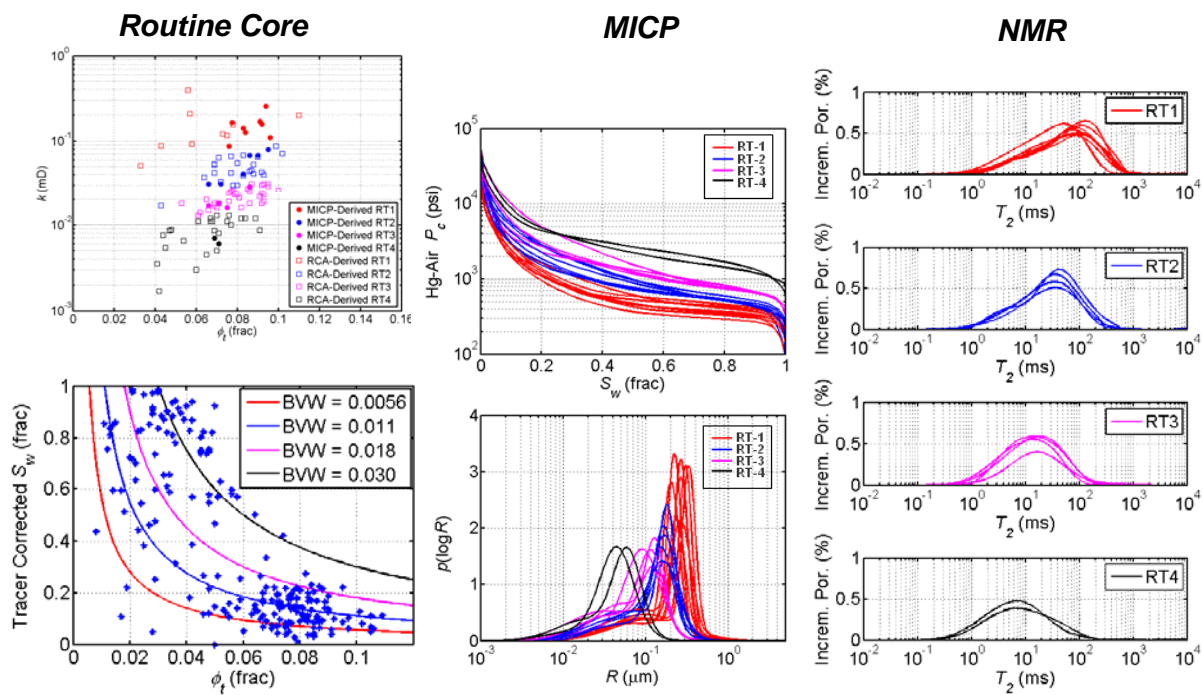
123

Decomposition of Orthogonal Rock Classes



124

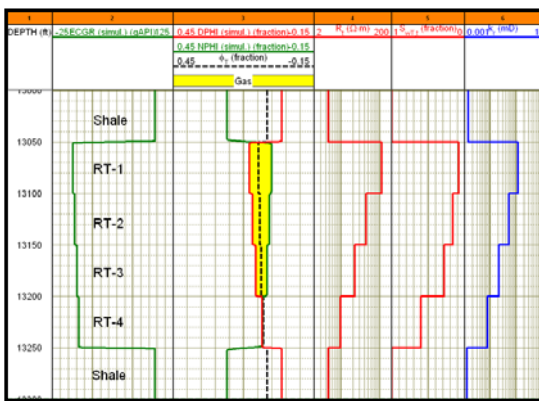
Field Application: Bossier Tight-Gas Sand



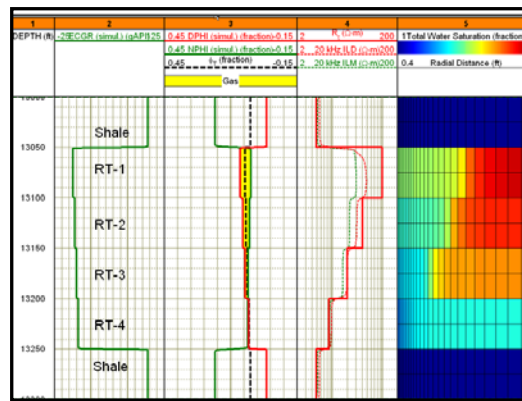
125

Field Application: Bossier Tight-Gas Sand

Pre-invasion

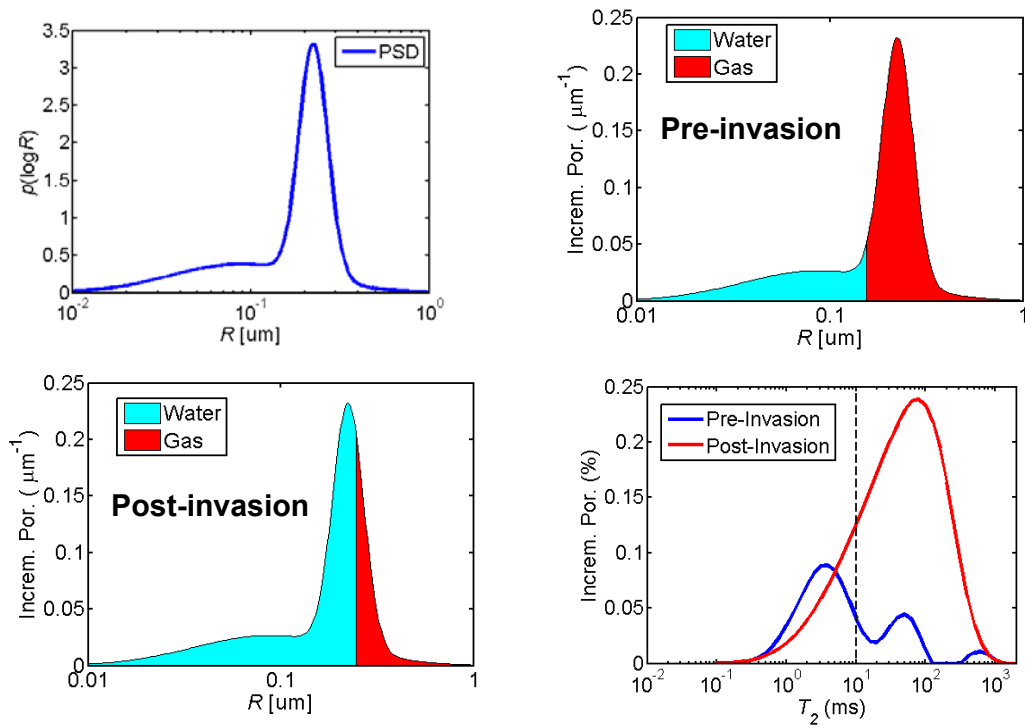


Post-invasion



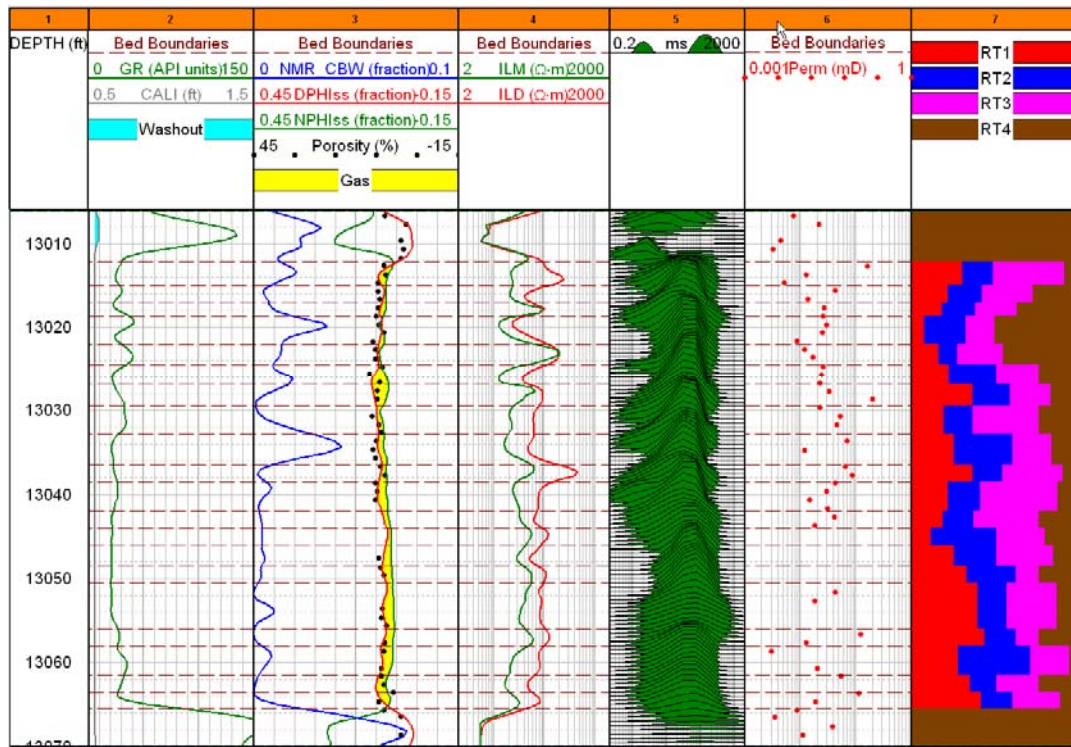
126

Field Application: Bossier Tight-Gas Sand



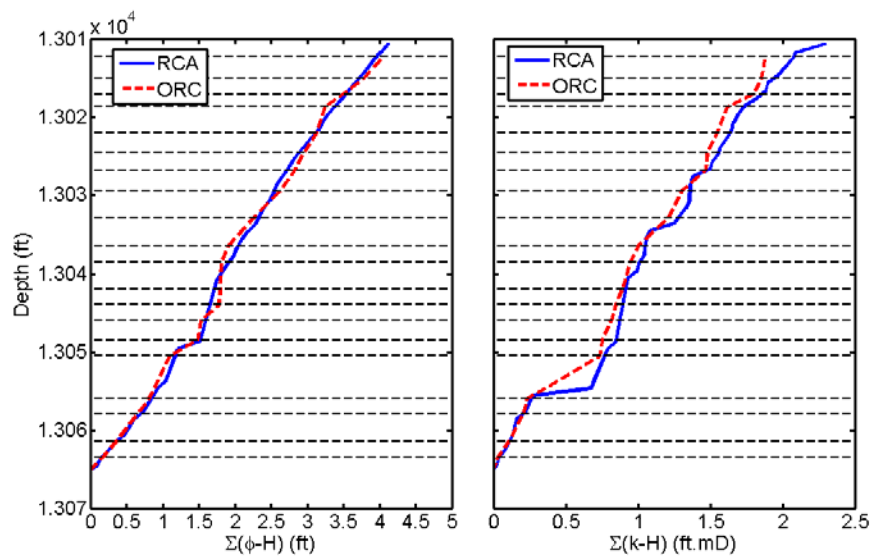
127

Field Application: Bossier Tight-Gas Sand



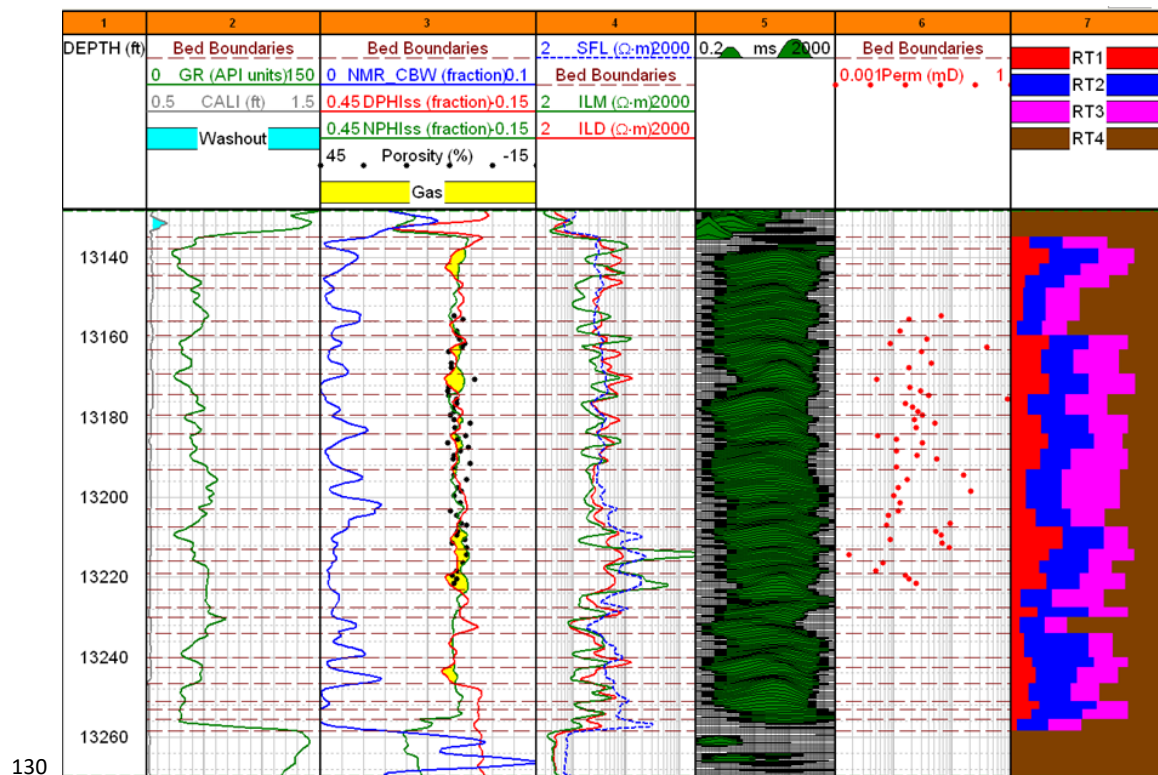
128

Field Application: Bossier Tight-Gas Sand

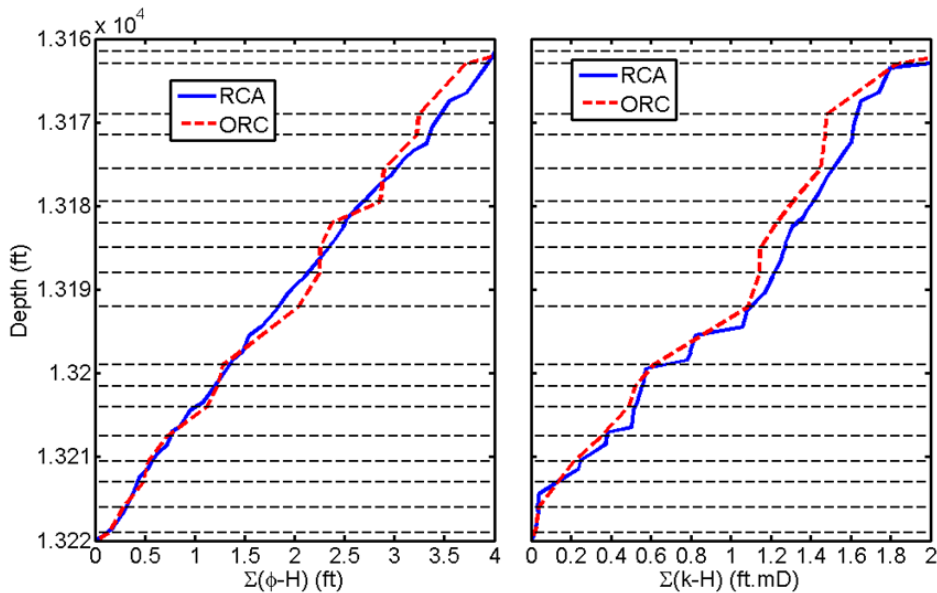


129

Field Application: Bossier Tight-Gas Sand



Field Application: Bossier Tight-Gas Sand



131

Summary: Log-Based Rock Typing

- Be cautious with apparent e-facies.
- Electrical conductivity correlates with hydraulic conductivity only at irreducible water saturation.
- Saturation-height relation reveals rock quality.
- Invasion profile indicates dynamic rock-fluid properties.
- Thin-bed or laminated zones should be identified and classified.
- Bayesian rock typing eliminates shoulder-bed effects and quantifies uncertainty.
- Orthogonal rock class decomposition describes heterogeneous formations.

132

Some Final Thoughts

- To classify or not to classify rocks?
- Variability of rock properties can be substantial.
- It is important to identify whether rock variability is within one or more rock classes.
- Mixing or rock classes is common in nature.
- The best rock classification is the one which diagnoses and quantifies orthogonal classes in terms of fluid storage and transport.
- Well logs are often inadequate for rock classification because of thin-bed, invasion, and fluid-saturation effects.
- Pore and throat structures are key for rock classification

133

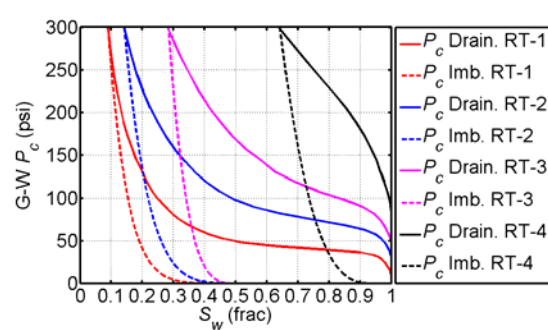
Acknowledgements



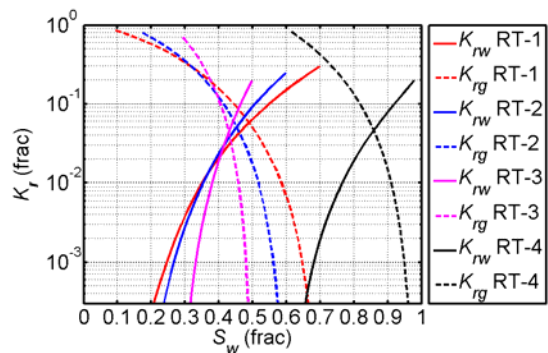
Backup Slides Follow

135

Dynamic Modeling



Capillary Pressure



Relative Permeability

136

Numerical results for cemented samples

Sample	Cement	Total porosity	Connected porosity				Permeability, mD				Tortuosity				Specific Surface, μm^{-1}
			x-dir	y-dir	z-dir	geom. average	x-dir	y-dir	z-dir	geom. average	x-dir	y-dir	z-dir	geom. average	
O	0.0%	0.207	0.207	0.207	0.207	0.207	1633	1769	1904	1765	1.53	1.51	1.48	1.51	0.0128
U1	7.2%	0.135	0.134	0.134	0.134	0.134	327.3	372.3	396.1	364.1	1.64	1.61	1.58	1.61	0.0102
U2	10.5%	0.102	0.100	0.100	0.100	0.100	92.99	109.7	116.4	105.9	1.72	1.68	1.65	1.68	0.0084
U3	11.9%	0.088	0.085	0.085	0.085	0.085	45.42	55.03	56.34	52.03	1.75	1.73	1.69	1.72	0.0075
U4	16.1%	0.046	0.021	0.022	0.021	0.021	0.27	0.45	1E-05	0.01	1.89	1.78	1.89	1.85	0.0042
T1	4.1%	0.166	0.164	0.164	0.164	0.164	511.9	597.0	632.0	578.0	1.66	1.63	1.61	1.63	0.0100
T2	7.5%	0.132	0.128	0.128	0.128	0.128	109.6	141.4	139.2	129.2	1.75	1.72	1.69	1.72	0.0082
T3	11.3%	0.093	0.043	0.046	0.046	0.045	2.56	3.49	1E-06	0.02	1.84	1.78	1.87	1.83	0.0059
B1	2.1%	0.186	0.186	0.186	0.186	0.186	1363	1478	1651	1493	1.55	1.54	1.48	1.52	0.0121
B2	5.1%	0.156	0.156	0.156	0.156	0.156	933.6	988.5	1182	1029	1.58	1.57	1.48	1.54	0.0111
B3	11.4%	0.092	0.092	0.092	0.092	0.092	293.4	297.5	392.3	324.7	1.66	1.64	1.51	1.60	0.0085